DIPLOMARBEIT

The determination of utmost accurate GNSS reference site velocities in the Asia-Pacific region

ausgeführt zum Zwecke der Erlangung des akademischen Grades eines Diplom-Ingenieur am

Department für Geodäsie und Geoinformation
Forschungsgruppe Höhere Geodäsie (E 120-4)

unter der Anleitung von

a.o.Prof. Dipl.-Ing. Dr.techn. Robert Weber
und Dipl.-Ing. Gregor Möller
als verantwortlich mitwirkenden Projektassistenten

präsentiert an der Technischen Universität Wien
Fakultät für Mathematik und Geoinformation

von

Bakk.techn. Hannes Maar

Baumstücklweg 10
A - 7162 Tadten
Matr.-Nr.: e0625330

Wien, Februar 2013

TECHNISCHE
UNIVERSITÄT
WIEN
Vienna University of Technology

DIPLOMA THESIS

The determination of utmost accurate GNSS reference site velocities in the Asia-Pacific region

carried out in order to obtain the academic degree Diplom-Ingenieur at the

Department of Geodesy and Geoinformation
Research Group Advanced Geodesy (E 120-4)

under the supervision of

a.o.Prof. Dipl.-Ing. Dr.techn. Robert Weber
and Dipl.-Ing. Gregor Möller
as responsible participating project assistant

presented at the Vienna University of Technology
Faculty of Mathematics and Geoinformation

by

B.Sc. Hannes Maar

Baumstücklweg 10
A - 7162 Tadten
Matr.-No.: e0625330

Vienna, February 2013

Supervisors

a.o.Prof. Dipl.-Ing. Dr. techn. Robert Weber

Department of Geodesy and Geoinformation

Research Group Advanced Geodesy (E120-4)

Faculty of Mathematics and Geoinformation

Vienna University of Technology

Vienna, Austria

Dr. Craig Roberts

&

Prof. Dr. Chris Rizos

School of Surveying and Geospatial Engineering

Faculty of Engineering

University of New South Wales

Sydney, Australia

Acknowledgments

I want to express my honest gratitude to my supervisor Robert Weber, who advised me on the interesting challenge of this thesis and whose expertise, calmness and patience carried and enriched me during my research.

In addition to his capable support, I am indebted to my friend and colleague Gregor Möller for his valuable advice and knowledge in GNSS data processing. His initial activity in the APREF project and the hours he spent in order to induct me into the use of the Bernese Software represent an important foundation for the achieved outcome of my work.

I esteem both the high commitment of Harald Schuh and the financial aid from the International Office of the Vienna University of Technology, without their help I would not have been able to participate the practicum exchange program and to gain memorable experiences in Australia.

It was a privilege and a great pleasure to meet my Australian supervisors Craig Roberts and Chris Rizos, who spared no effort to integrate me in their research group and offered me new perspectives on CORS networks. I would like to thank you for many inspiring discussions about geodetic datums and the chance to present my results in Canberra.

Regarding to the support from beyond university walls, I am much obliged to Joel Haasdyk for his adjuvant suggestions at the beginning of my work in order to establish a successful processing strategy. I am further grateful to John Dawson, Manoj Deo and Guorong Hu for welcoming me at Geoscience Australia and taking their time to review my progress.

Special thanks go to my parents Luise and Johann Maar, who gave me the opportunity to study and assisted me in every possible emotional and financial way, and to my sister Alexandra Maar for offering me a sympathetic ear in times of need.

Finally, I appreciate all my close friends, who remained steadfastly at my side and encouraged me in recent years.

Abstract

Today's demands for accuracy ask for a densification and homogenization of the geodetic infrastructure in some parts of the world in order to tap the full technological potential of modern positioning techniques. This task can be achieved by the increase of continuously operating GNSS reference sites, which deliver highly accurate and up-to-date station coordinates in a global and international terrestrial reference frame. The APREF project under the direction of Dr. John Dawson from Geoscience Australia pursues this objective by gathering and processing GNSS observations from a dense network of more than 400 stations in the Asia-Pacific region and provides final products on a regular and freely available basis.

This thesis covers the idea to use the raw data sets of a chosen regional subnetwork of 97 sites located in Australia, New Caledonia and New Zealand and to establish an appropriate post-processing strategy for the estimation of station coordinates and velocities in order to analyze the achieved accuracy in contrast to existing global solutions. A special focus lies on the strategy of the definition of the geodetic datum, whereat the results of different approaches reveal that a so-called minimum constraint solution using a no-net-translation and no-net-rotation condition leads to the best outcomes. Regarding to these constraints, the condition to avoid network translations is essential for the computation of accurate station coordinates and has a greater impact than the no-net-rotation condition. Therefore, the deliberate selection of datum defining sites and their corresponding a priori coordinates is an important aspect, because the network will be aligned to these coordinate sets.

Based on a processed time span of three years from October 2009 until September 2012, the strategy in use achieves mean velocity standard deviations of $1\,\mathrm{mm\,yr^{-1}}$ for the whole network and mean velocity differences of 2 - $3\,\mathrm{mm\,yr^{-1}}$ compared to the velocities of 17 sites from the IGS08/ITRF2008 reference frame. While all stations on the Australian continent display a consistent movement with an akin absolute value and azimuth, the varying velocities in New Zealand reflect the more complex geophysical activity on the predominant boundary between the Australian and the Pacific plate.

In contrast to these velocity estimations, the station coordinates reveal a slightly lower accuracy, in which the processed IGS sites show coordinate differences of up to 5 mm with respect to the weekly IGS solution. These uncertainties could be explained by the geometric limitation of the regional network compared to the IGS network, which represents a global and well distributed network of more than 250 IGS sites and allows a much more stable solution. Therefore, a global extension of the processed network and an increased set of datum defining IGS stations may improve the coordinate estimation and, furthermore, the resulting station velocities. Of course, the observed time span also plays a major role in the calculation of velocities. The longer the processed time period, the more reliable the achieved velocities, whereat significant coordinate jumps, which can be caused by geophysical events such as

earthquakes, have to be taken into account suitably.

Thus, it emerges that a regional network, which is processed in an appropriate time span of several years and includes as much datum defining reference sites with accurate a priori coordinates as possible, can reach mean accuracies in station velocity of a few $\mathrm{mm\,yr^{-1}}$ and hence can significantly support the geodetic reference frame of participating nations.

Kurzfassung

Heutige Genauigkeitsansprüche verlangen nach einer Verdichtung und Homogenisierung der bestehenden geodätischen Rahmenbedingungen in einigen Teilen der Welt, um das technologische Potential moderner Positionierungsverfahren größtmöglichst auszuschöpfen. Diese Aufgabe kann durch die Schaffung bzw. Ausweitung permanenter GNSS Referenzstationen erfüllt werden, durch die laufend hoch genaue Stationskoordinaten in einem globalen und internationalen terrestrischen Referenzrahmen bestimmt werden können. Das APREF Projekt unter der Leitung von Dr. John Dawson von Geoscience Australia verfolgt dieses Ziel indem es Rohdaten von mehr als 400 solcher Stationen unterschiedlicher Nationen vereint, daraus ein regionales Netzwerk im Asien-Pazifik-Raum errichtet und durch eine entsprechende Prozessierung finale Produkte in einer regelmäßigen und frei zugänglichen Form zur Verfügung stellt.

Diese Arbeit verwendet den Rohdatensatz eines APREF Teilnetzwerkes von 97 Referenzstationen in der Region um Australien, Neukaledonien und Neuseeland und integriert diesen in eine eigens gewählte Prozessierungs-Strategie, um dadurch präzise Stationskoordinaten und -geschwindigkeiten zu bestimmen. Durch die gewonnenen Ergebnisse sollen die erreichbaren Genauigkeiten untersucht und mit bestehenden Lösungen verglichen werden. Ein Schwerpunkt liegt in der Betrachtung unterschiedlicher Ansätze für die Realisierung des geodätischen Datums, wobei sich herausstellt, dass eine sogenannte Minimum Constraint Solution mit einer no-net-translation und no-net-rotation Bedingung die besten Resultate erzielt. Hinsichtlich dieser Festlegungen zeigt sich, dass die Vermeidung von Translationen einen größeren Einfluss auf die erfolgreiche Anbindung an einen globalen Referenzrahmen hat als die in geringem Maße auftretenden Rotationen des Netzwerks. Daher stellt die sorgfältige Auswahl von genauen a priori Koordinaten von datumsdefinierenden Stationen einen wichtigen Aspekt dar, da das gesamte Netzwerk an diese Koordinaten angeglichen wird.

Ausgehend von einer prozessierten Zeitspanne von drei Jahren, beginnend mit Oktober 2009 bis September 2012, werden in der vorliegenden Arbeit mittlere Standardabweichungen der Stationsgeschwindigkeiten von etwa $1\,\mathrm{mm\,yr^{-1}}$ für das gesamte Netzwerk und mittlere Geschwindigkeitsdifferenzen von 2 - $3\,\mathrm{mm\,yr^{-1}}$ verglichen mit den bestehenden Daten von 17 Stationen aus dem IGS08/ITRF2008 Referenzrahmen erzielt. Während alle Beobachtungen des australischen Festlandes eine einheitliche Bewegung in Bezug auf Größe und Azimut der Geschwindigkeitsvektoren zeigen, spiegeln die variierenden Ergebnisse in Neuseeland die komplexere geophysikalische Aktivität an der vorherrschenden Grenze zwischen australischer und pazifischer Platte wider.

Im Gegensatz zu den Geschwindigkeitsabschätzungen zeigen die resultierenden Stationskoordinaten eine etwas geringere Genauigkeit, die sich durch Positionsdifferenzen von bis zu 5 mm gegenüber der wöchentlichen IGS Lösungen darstellen. Diese Unsicherheiten kön-

nen durch die geometrische Begrenzung meines regionalen Netzwerkes erklärt werden, während das zu Vergleichszwecken herangezogene IGS Netzwerk eine global verteilte Anzahl von mehr als 250 IGS Stationen repräsentiert und dadurch zu einer stabileren Lösung führt. Aus diesem Grund würde eine globale Ausweitung des Netzwerkes und eine größere Menge an datumsdefinierenden IGS Stationen mit hoher Wahrscheinlichkeit eine weitere Verbesserung der Bestimmung von Stationskoordinaten und -geschwindigkeiten mit sich bringen. Natürlich geht die Dauer der untersuchten Zeitspanne stark in die Geschwindigkeitsberechnung mit ein, wobei eine längere Beobachtungsperiode eine zuverlässigere Abschätzung von Geschwindigkeiten zur Folge hat. Auftretende, signifikante Koordinatensprünge, die beispielsweise durch geophysikalische Ereignisse wie Erdbeben entstehen, müssen in der Berechnung entsprechend berücksichtigt werden.

Demnach zeichnet sich ab, dass ein regionales Netzwerk, das für eine ausreichend lange Zeitspanne von mehreren Jahren ausgewertet wurde und möglichst viele datumsdefinierende Referenzstationen mit verlässlichen a priori Koordinaten enthält, mittlere Genauigkeiten von wenigen $\mathrm{mm\,yr^{-1}}$ der Stationsgeschwindigkeiten erreichen und somit den geodätische Referenzrahmen teilnehmender Nationen erheblich verbessern kann.

Contents

Chapter 1

Motivation

The lithosphere, Earth's rigid outer face, is not a stationary body but it is moving. Since the discovery of plate tectonics, it is an accepted fact that the crust consists of more than a dozen major tectonic plates, which are floating on the deeper ductile asthenosphere with different directions and velocities. Although the permanent movement describes only several centimeters per year, its impacts show global and partly disastrous dimensions. Transform, normal and reverse faults are responsible for today's unique shape of the Earth's surface, but also cause volcanic activity and earthquakes and pose a major challenge for geodesists, which try to measure these temporal changes not only for scientific applications but in order to establish a reference framework close to reality, which serves as a foundation for regional and global Earth observations.

The first plate velocity model, named Northwestern University Velocity model 1 (NUVEL-1), was realized through geophysical methods such as the determination of spreading rates by dating the ridge's magnetic interference fringes and the analysis of transform fault azimuths and earthquake slip directions. Both, the application of a no-net-rotation (NNR) condition, which set the total angular momentum of all plates to zero, and the correction of dating errors yield to the successor named NNR-NUVEL-1A, which is one of today's international standard models (Jin & Zhu, 2004).

Whereas the mentioned geophysical approaches represent a sight of the geological past (in terms of million years), the rise of several space-geodetic techniques enabled the observation of instantaneous crustal deformations on a global and continuous way. The combination of observations from VLBI, SLR, TRANSIT, DORIS and GPS led to the establishment of a global Earth-fixed reference frame called the International Terrestrial Reference Frame (ITRF, see Chapter 3), which was aligned to the geophysical NNR-NUVEL-1A velocity model, but also included these modern geodetic methods to characterize the present plate motion (Altamimi *et al.*, 2012).

The currently realized ITRF2008 velocity field (Figure 1.1) is based on a global CORS (Continuously Operating Reference Station) network of about 580 sites, at which only 117 sites are located on the southern hemisphere. This imbalance leads to a lack of available ITRF

coordinate and velocity information in the southern regions and therefore causes a weakness in the characterization of local or regional dynamics, whose description is essential to create a proper link between national datums and the global reference frame, and results in an accuracy below today's technological capabilities.

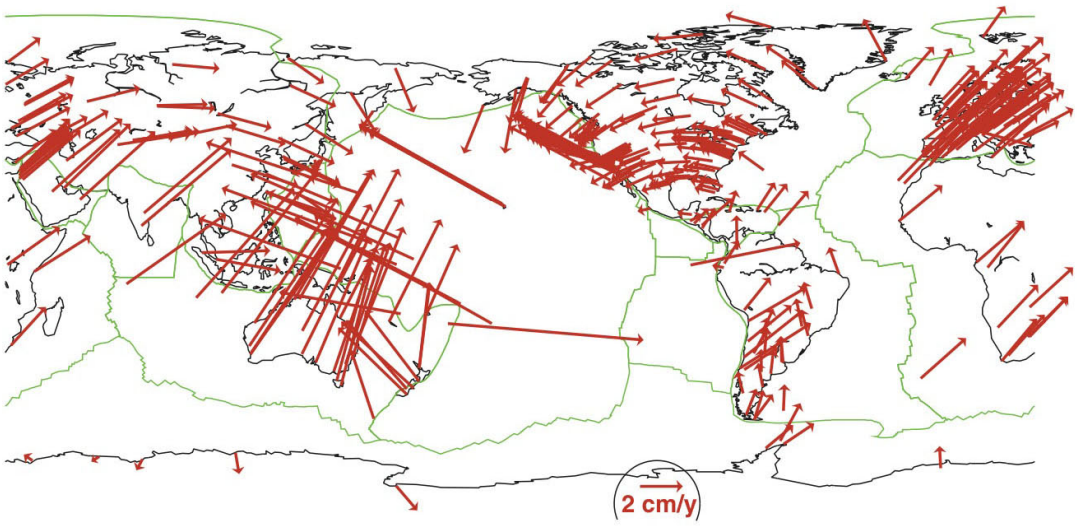

Figure 1.1: ITRF2008 horizontal velocities, major plate boundaries are displayed in green (Altamimi *et al.*, 2011)

This thesis examines the attempt of estimating ground motions in the oceanic region using GNSS observations on a highly accurate basis (see Chapter 2), in which the area of interest is represented by a regional network of almost 100 reference sites in Australia, New Zealand and New Caledonia. The densification of the emerging velocity field is enabled through the APREF project, which tries to establish a more accurate and homogeneous geodetic infrastructure in the Asia-Pacific region and therefore provides access to a large number of national GNSS reference site data sets (see Chapter 4). The applied processing strategy is circumstantially described in Chapter 5 and results in several approaches of the definition of the geodetic datum, mainly based on the adoption of different conditions in a minimum constraint solution. Hereupon, the corresponding coordinate solutions are used for the estimation of station velocities, whereat the final conclusion focuses on following key aspects:

- the achieved accuracy of the overall regional network with respect to station positions and velocities
- the impact of different approaches of the datum definition
- the comparison with existing geodetic and geophysical velocity models
- a closer look at the plate boundaries in New Zealand
- the achieved tropospheric estimates compared to a standard model

Chapter 2

Introduction to GNSS

2.1 Origins and applications

Though the beginnings of satellite navigation go back to 1973, where the foundation for NAVSTAR GPS (*NAV*igation *S*ystem with *T*ime *A*nd *R*anging *G*lobal *P*ositioning *S*ystem), in short *GPS*, was laid, its significance highly increased during the mid-1980s, when the technology became accessible to the civilian community. The change of the audience has enabled a wide range of geospatial applications, whose major goal is to provide a precise three-dimensional position, navigation and time information. GPS met these requirements in a world-wide basis by providing data independent of meteorological conditions and by being continuously available. The first civilian users in that time were geodesists, who began to use this system as an additional method in order to observe and maintain geodetic control networks, which are the basis for all national coordinate systems as well as for the international terrestrial reference frame, to determine variations in the Earth's rotation and to monitor crustal displacements caused by e.g. geophysical events. Soon it was recognized that with the help of relative positioning, where most of the correlated biases can be eliminated, the potential of GPS may reach a dimension, in which cm-level accuracy could be achieved so that it would fill the gap in capabilities between the terrestrial surveying tools and the already existing space geodetic techniques, such as SLR and VLBI.

As a result of the technological progress, the gap was closed and high accurate positioning via GPS found its way into the non-scientific, commercial usage such as cadastral surveying, civil engineering and geographic information systems. Selective Availability (SA) was formerly a technique to deny the navigation accuracy to potential antagonists by dithering the satellite clocks and corrupting the ephemerides, but was deactivated in 2000. Although it was possible to eliminate the effect of SA in the relative positioning of receivers, the shutdown improved the accuracy of stand-alone receivers by the factor of ten. Professionals were able to use this technology in order to carry out land surveys, set up the infrastructure for construction sites or to control agricultural vehicles and finally implemented GPS to the mass market, where the possibilities rose from car navigation to recreation applications and outdoor location based

services (LBS) using smartphone-integrated GPS antennas. Its benefits also had an impact on the non-navigational applications so that it was possible to use GNSS signals not only for positioning but also for monitoring atmospheric variations or to provide a highly accurate time and frequency standard.

At the moment (February, 2013), NAVSTAR GPS and its Russian counterpart GLONASS, both being primarily under military control, are the two operational satellite-based navigation systems, but they will soon be complemented by other systems, like the European Galileo and the Chinese Beidou. An important output beside the increase of accuracy is to provide and ensure integrity, availability and continuity of service. For navigational purposes, integrity is defined as the "ability of a system to provide timely warnings to users, when the system should not be used" (Brown, 1989). Although the integrity message was a desired achievement at the beginning of the Galileo project, it is now shown that this service will not be realized in the near future. Both existing and upcoming operations are now covered under the name Global Navigation Satellite Systems (GNSS).

2.2 Methods of positioning

All satellite-based positioning systems are based on a similar fundamental observation technique, namely on the signal propagation between the available GNSS-Satellites in space and one or more receivers on or near the ground using code and carrier phase measurements. Therefore, errors in the observations range from ground-based influences such as receiver clock errors and tidal effects to atmospheric delays and inaccurate orbit information. Most of the acting biases are highly correlated with distance or time, where the latter can be coped with synchronized or nearly simultaneous observations. Due to the fact that ephemeris and atmospheric propagation errors are nearly the same for neighboring stations, they disappear while forming baselines between at least two receivers (stations) and make the relative positioning much more accurate than the absolute determination of station coordinates. By measuring baselines, which are in fact coordinate differences, two strategies can be distinguished represented by the relative positioning in post-processing mode and the differential positioning, which provides solutions in real-time. This leads to four basic methods, where the following names reflect today's common notations, at which the term GPS is still more often in use than the nowadays more adequate name GNSS (Seeber, 2003):

1. Ordinary Differential GPS (DGPS): use of pseudorange corrections provided by code observations at a nearby reference station in real-time

2. Precise DGPS (PDGPS), or also Real-Time Kinematic (RTK) GPS: use of corrections provided by code-range and carrier-phase data at a nearby reference station in real-time

3. Network RTK, or also Local-area DGPS: use of data from the nearest stations of a network of reference sites for pseudorange and phase corrections in real-time

4. Relative positioning in post-processing: uses long-term observations of stationary antennas, mostly in the form of a set of reference stations

Tectonic plate movements range in velocities of several centimeters per year, which means that the daily or weekly position of reference stations does not change more than a few millimeters in series, unless equipment changes or geophysical events, such as earthquakes, occur. Therefore, it is necessary to use the most accurate observation technique, which is the relative positioning in post-processing, in order to detect minimal displacements of a subset of reference stations so that finally the determination of accurate velocities can be achieved. Figure 2.1 illustrates the corresponding accuracy of different methods of GNSS positioning.

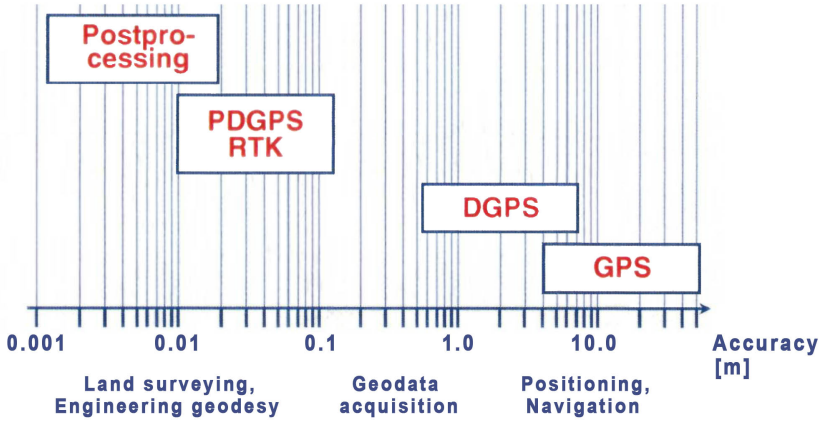

Figure 2.1: Methods of positioning and their accuracy (Scherer, 1998)

2.3 Observables

Basically, GNSS observables are so-called pseudoranges, which are derived from time or phase information based on the comparison between the transmitted signal from the satellite and a reference signal generated in the receiver. As the signal propagation from the satellite to the receiver is a one-way transmission where two clocks are involved, satellite and receiver clock errors occur during the data acquisition. These and other disturbing errors, like tropospheric delays and uncertainties in the satellite orbits lead to the case where the uncleaned observations are named pseudoranges (*PR*). In practice, two fundamental observables are in use and separated as following:

- code phases: pseudoranges from code observations
- carrier phases: pseudoranges from carrier observations

The main difference between these two observables lies in the signal structure, which will now be shortly described for the GPS system only.

Each GPS satellite transmits signals on several carrier frequencies, located in the L-Band. The first civil frequencies were called L1 and L2, where the launch of the first GPS Block IIF in 2010 introduced the third civil signal L5. This new carrier is chosen for safety of life applications, especially in aviation, and will become fully operational in about 2020. All carriers are generated from a fundamental frequency f_0 of 10.23 MHz. The transmitted signals can be grouped into the navigation message and the codes. The message data contains general information about the satellite's ephemerides and its clock behavior, whereat the codes are responsible for the actual range measurement. The first established C/A- and P-codes are binary modulations on the carrier frequencies, called pseudo random noise (PRN) sequences. Each GPS satellite has a unique PRN signature so that a clear identification is possible, though all satellites are operating on the same frequency. The P-code has a much smaller wavelength than the C/A-code and is available on L1 and L2, whereas the C/A-code is only transmitting on L1. This yields to two advantages of the P-code, which are a higher resolution due to the smaller wavelength and the elimination of dispersive influences in the ionosphere by using two carrier frequencies. Anti-Spoofing (AS) is an intentional limitation and controls the access to this benefits by encrypting the P-code for non-authorized users. Its general aim is to avoid a volitional deception of a receiver by imitating ("spoofing") the P-code. Next to the C/A- and P-code, the already established L2C and the prospective L1C code, both signals which are not encrypted, will enhance accuracy and reliability in the future. Carrier and code characteristics are given in Table 2.1, values in brackets describe the planned year of availability.

Table 2.1: Signal characteristics of civil GPS code- and carrier phases (Hofmann-Wellenhof *et al.*, 2008)

Description		Factor ($\cdot f_0$)	Frequency / Code rate	Wave-length	Band-width
f_0			10.23 MHz		
Carriers					
	L1	154	1575.42 MHz	19.0 cm	
	L2	120	1227.60 MHz	24.4 cm	
	L5	115	1176.45 MHz	25.5 cm	
Codes					
	C/A		1.023 Mcps	293.1 m	2.046 MHz
	P		10.23 Mcps	29.3 m	20.46 MHz
	L2C		1.023 Mcps	293.1 m	2.046 MHz
	L1C (2015)		1.023 Mcps	293.1 m	4.092 MHz

Table 2.2 summarizes the notation for the following mathematical annotations and represents a slightly adapted form as from Seeber (2003). To simplify the equations the speed of light c is used as expected signal propagation velocity, although the atmospheric delays represent an effect of the actual velocity variation due to the characteristics of the ionosphere and troposphere.

Table 2.2: Denotation of the basic mathematical quantities in use

Variable	Description
PR_{CD}	pseudorange from code phases
PR_{CR}	pseudorange from carrier phases
φ_m	carrier phase observables
φ_{CR}	transmitted carrier phase
Φ_0	reference carrier phase
c	speed of light
f_0	fundamental frequency of GPS satellites
f_{CR}	carrier frequency
t_r	moment of reception
T_t	moment of emission
R	slant range
dt_u	receiver clock error
dt_a	atmospheric delay
dt_s	satellite clock error
N	integer ambiguity term
ϵ_R	relativistic effects, multipath effects and observation noise

Particular error sources which influence pseudorange measurements can be separated into orbit and clock errors, atmospheric delays and residual errors such as relativistic effects, multipath effects, observation noise and antenna phase centre variations at the receiver. The combined effect of these errors is called User Equivalent Range Error (UERE). In addition, the geometric configuration of the satellites in use affects the impact of the mentioned errors on the resulting accuracy of positioning and is named Dilution of Precision (DOP).

2.3.1 Code phases

Code phases are measured by tracing the correlation between observed and generated code segments on ground. Once the satellite's binary PRN sequences have reached the receiver, the reference signal is shifted bit by bit against the transmitted code, until maximum correlation is achieved. At that time, the measured phase-shift represents the time difference between the moment of transmission from the satellite and arrival at the ground antenna, considering that two time systems are involved. The signal emission time T_t is included in the broadcasted message and therefore in the satellite clock frame, whereas the reception time t_r is measured in the receiver clock system. Assuming that the signal propagates with approximately the speed of light, the measured phase-shift (t_r -T_t) leads to the observation equation for code phases including its major disturbing influences respectively errors (Seeber, 2003):

$$PR_{CD} = c \cdot (t_r - T_t) = R + c \cdot dt_u + c \cdot dt_a + c \cdot dt_s + \epsilon_R \tag{2.1}$$

2.3.2 Carrier phases

Carrier phase measurements do not use the code segments, but the carriers L1 and L2 itself. Observables are phase differences $\varphi_m(t_r)$ between the carrier phase $\varphi_{CR}(T_t)$, transmitted from the satellite, and the reference phase $\Phi_0(t_r)$ which is generated in the receiver:

$$\varphi_m(t_r) = \varphi_{CR}(T_t) - \Phi_0(t_r) = \varphi_{CR}(T_t) - t_r \cdot f_0 \tag{2.2}$$

Note that the transmitted signal is Doppler-shifted due to the relative velocity between satellite and receiver and therefore has a different frequency than the reference signal. By using the carrier signals, which operate in much higher ranges of frequency (1.23 GHz and 1.58 GHz), the accuracy of this method exceeds the one of code observations by far. A main problem of measuring phase differences between harmonic functions is that the observables are only relative phase-shifts with values not bigger than 360° (or 2π). Hence, it is not possible to measure the total number of complete cycles the transmitted signal passed through before it reached the receiver. This number, also called integer ambiguity N, is introduced as a new unknown parameter and its estimation is a non-trivial issue, which will be discussed later. Using the observables in Equation (2.2) and the integer ambiguity N, the carrier signal state $\Phi_{CR}(T_t)$ at the moment of emission T_t can be described as

$$\Phi_{CR}(T_t) = N \cdot 360^\circ + \varphi_{CR}(T_t). \tag{2.3}$$

By introducing the carrier frequency f_{CR}, Equation (2.3) yields to the moment of emission in the satellite time frame

$$T_t = \frac{\Phi_{CR}(T_t)}{f_{CR}} = \frac{\varphi_{CR}(T_t) + N}{f_{CR}} = \bar{T}_t + \frac{N}{f_{CR}}, \tag{2.4}$$

whereat the first term $\bar{T}_t$ contains the observed phase and therefore will be introduced in the simplified equation for the pseudorange from carrier phase measurements

$$PR_{CR} = c \cdot (t_r - \bar{T}_t) \tag{2.5}$$

The ambiguity term $N \,/\, f_{CR}$ is a new unknown parameter, which will be added in the more detailed observation equation for carrier phases (Seeber, 2003):

$$\begin{aligned} PR_{CR} &= R + c \cdot dt_u + c \cdot dt_a + c \cdot dt_s + c \cdot \frac{N}{f_{CR}} + \epsilon_R \\ &= R + c \cdot dt_u + c \cdot dt_a + c \cdot dt_s + \lambda_{CR} \cdot N + \epsilon_R \end{aligned} \tag{2.6}$$

2.4 Parameter estimation

The subsequent statements are condensed in order to give a review and follow the considerations and notations of Hofmann-Wellenhof *et al.* (2008) and Seeber (2003)[1].

2.4.1 Linear combinations

As shown in Section 2.3, pseudoranges can be obtained from code and carrier phases. A common procedure in relative positioning is to form derived observables out of different combinations of all available measurements. In the differenced observations a reduced set of correlated errors, as described in Equations (2.1) or (2.6), remains and leads to an easier performance in the parameter estimation. Combinations can be separated in using observations from different stations, satellites or epochs, where in the case of stations and satellites, the data acquisition has to be done simultaneously. According to the notation of Wells (1986), the following operators are used in order to distinguish between the different combinations:

- differences between receivers: $\Delta(\ldots) = (\ldots)_{\text{receiver } j} - (\ldots)_{\text{receiver } i}$
- differences between satellites: $\nabla(\ldots) = (\ldots)^{\text{satellite } q} - (\ldots)^{\text{satellite } p}$
- differences between epochs: $\delta(\ldots) = (\ldots)_{\text{epoch 2}} - (\ldots)_{\text{epoche 1}}$
- spectral combinations

The subsequent explanations refer to carrier phase differences, because their solutions are much more accurate than results from code phases and therefore commonly in use by a various number of post-processing software.

2.4.1.1 Single differences

Single differences can be formed by combining data from either two satellites, two receivers or two epochs. A conventional case is to create a single difference between two stations i and j, whereat both measure to one satellite. Carrier phase observations measured at station i are simply subtracted from simultaneous carrier phase measurements at station j, which leads to the pseudorange difference

$$\begin{aligned} \Delta PR_{CR_{ij}} = \Delta R_{ij} + c \cdot (dt_{u_j} - dt_{u_i}) + c \cdot (dt_{a_j} - dt_{a_i}) \\ + c \cdot (dt_s - dt_s) + \lambda_{CR} \cdot (N_j - N_i) + \epsilon_{\Delta CR} \end{aligned} \tag{2.7}$$

or in short

$$\Delta PR_{CR} = \Delta R_{ij} + c \cdot \Delta dt_{u_{ij}} + c \cdot \Delta dt_{a_{ij}} + \lambda_{CR} \cdot \Delta N_{ij} + \epsilon_{\Delta CR}. \tag{2.8}$$

[1] A more detailed description can be found in the mentioned publications as well as in Teunissen & Kleusberg (1998)

The simplified form of the single difference equation, where the atmospheric effect $c \cdot dt_{a_{ij}}$ is split in the tropospheric and ionospheric path delay, finally reads

$$\Delta PR_{CR} = \Delta R + c \cdot \Delta dt_u - \Delta d_{ion} + \Delta d_{trop} + \lambda \cdot \Delta N + \epsilon_{\Delta CR}. \tag{2.9}$$

It is obvious that the satellite clock error dt_s was eliminated and the remaining atmospheric delay $dt_{a_{ij}}$ becomes a differenced error and therefore much smaller than the absolute atmospheric bias, especially for nearby stations.

The opposite case of measuring from one station to two satellites may be used for the determination of satellite orbits and is not relevant for this work.

2.4.1.2 Double differences

Double differences represent a subtraction of two simultaneously observed single differences, which means at minimum two receivers and two satellites are involved. Baselines between stations i and j are observed from both satellites p and q. The two single differences form

$$\begin{aligned} \Delta PR^p_{CR} &= \Delta R^p_{ij} + c \cdot \Delta dt_{u_{ij}} + c \cdot \Delta dt_{a^p_{ij}} + \lambda_{CR} \cdot \Delta N^p_{ij} + \epsilon_{\Delta CR} \\ \Delta PR^q_{CR} &= \Delta R^q_{ij} + c \cdot \Delta dt_{u_{ij}} + c \cdot \Delta dt_{a^q_{ij}} + \lambda_{CR} \cdot \Delta N^q_{ij} + \epsilon_{\Delta CR} \end{aligned} \tag{2.10}$$

and their subtraction leads to the equation of double differences

$$\begin{aligned} \nabla\Delta PR_{CR} = (\Delta R^p_{ij} - \Delta R^q_{ij}) + c \cdot (\Delta dt_{u_{ij}} - \Delta dt_{u_{ij}}) \\ + c \cdot (\Delta dt_{a^p_{ij}} - \Delta dt_{a^q_{ij}}) + \lambda_{CR} \cdot (\Delta N^p_{ij} - \Delta N^q_{ij}) + \epsilon_{\nabla\Delta CR} \end{aligned} \tag{2.11}$$

or in the simplified notation

$$\nabla\Delta PR_{CR} = \nabla\Delta R - \nabla\Delta d_{ion} + \nabla\Delta d_{trop} + \lambda \cdot \nabla\Delta N + \epsilon_{\nabla\Delta CR}. \tag{2.12}$$

Due to the use of more than one satellite, the receiver clock error disappears. Therefore, the observations from double differences are free from clock errors. The remaining biases are reduced atmospheric delays and orbit errors, unknown ambiguities and residual errors such as relativistic effects, multipath effects and observation noise.

Double differences are the basic input data for many adjustment methods in relative positioning using GNSS, including the detection of cycle slips and the resolution of integer ambiguities. Cycle slips arise when a loss of the signal lock leads to an abrupt jump of the phase measurement so that the number of full cycles, which ran through during this observation break, will be introduced as a new unknown parameter.

2.4.1.3 Triple differences

A further step is to go from double to triple differences, which use an additional combination method, namely the observations from different epochs t_1 and t_2. The subtraction of two time shifted double differences leads to

$$\begin{aligned}\delta\nabla\Delta PR_{CR} = (\nabla\Delta R_{ij}(t_2) - \nabla\Delta R_{ij}(t_1)) + c \cdot (\nabla\Delta dt_{a_{ij}}(t_2) - \\ \nabla\Delta dt_{a_{ij}}(t_1)) + \lambda_{CR} \cdot (\nabla\Delta N_{ij} - \nabla\Delta N_{ij}) + \epsilon_{\delta\nabla\Delta CR}.\end{aligned} \tag{2.13}$$

Since the integer ambiguity parameter is an initial value and therefore time-independent, N_{ij} vanishes for the same baseline constellation of receivers and satellites and the simplified equation for triple differences remains as

$$\delta\nabla\Delta PR_{CR} = \delta\nabla\Delta R + \delta\nabla\Delta d_{ion} + \delta\nabla\Delta d_{trop} + \epsilon_{\delta\nabla\Delta CR}. \tag{2.14}$$

A big disadvantage of triple differences is the mathematical correlation. In contrast to zero or single differences, which are linearly independent and uncorrelated, the covariance matrix of a set of double or triple differences differs from a diagonal matrix and hence shows a correlation of the unknown parameters. The degree of correlation increases with the level of differentiation, which leads to the fact that small measurement errors may affect the whole system of equations, especially when using triple differences. Therefore, modern GNSS processing software avoid the use of triple differences and focus on zero or double differences.

2.4.1.4 Spectral combinations

Both code and carrier phase measurements operate on the carrier frequencies L1 and L2 and hence can be observed on both if the receiver equipment has the ability to access the P-code by applying correlation techniques or can measure carrier phases. If dual-frequency observations are available, it is possible to create a linear combination by introducing arbitrary coefficients n and m both for carrier and code phase measurements. The resulting signal can be described as

$$f_{n,m} = n \cdot f_1 + m \cdot f_2 \tag{2.15}$$

or in terms of wavelength

$$\lambda_{n,m} = \frac{c}{n \cdot f_1 + m \cdot f_2}. \tag{2.16}$$

The main advantage of this method is the elimination of ionospheric path delays. Due to the dispersive characteristic of the ionosphere, delays in the signal propagation depend on their frequency and thus can be determined respectively cancelled by forming a linear combination of observations which are founded on a different spectral range.

As seen in Equations (2.15) and (2.16), the chosen set of coefficients influences the resulting frequency $f_{n,m}$ and so its wavelength $\lambda_{n,m}$. By applying the law of error propagation, the observation noise for the linear combination can be written as

$$\sigma_{\lambda_{n,m}} = \frac{n \cdot f_1^2 \cdot \sigma_{\lambda_1} + m \cdot f_2^2 \cdot \sigma_{\lambda_2}}{(n \cdot f_1 + m \cdot f_2)^2}. \tag{2.17}$$

Based on the Interface Specification IS-GPS-200F (GPS-IS, 2011), "the phase noise spectral density of the unmodulated carrier shall be such that a phase locked loop of 10 Hz one-sided noise bandwidth shall be able to track the carrier to an accuracy of 0.1 radians RMS." Therefore, the maximum observation noise of a single carrier i is defined as

$$\sigma_{\lambda_i} = \frac{\lambda_i}{2\pi} \cdot 0.1 rad \tag{2.18}$$

and can be calculated for L1, L2 and furthermore for all their combinations. Well known and also the simplest linear combinations of the two carrier signals are their summation (narrow lane, NL) and subtraction (wide lane, WL), as shown in Equations (2.19) and (2.20). Their characteristics are illustrated in Table 2.3, whereat the given σ_{λ_i} describe upper bounds and hence may perform better in practice.

$$L_\Sigma = \frac{f_1 \cdot L_1 + f_2 \cdot L_2}{f_1 + f_2} \tag{2.19}$$

$$L_\Delta = \frac{f_1 \cdot L_1 - f_2 \cdot L_2}{f_1 - f_2} \tag{2.20}$$

Table 2.3: Characteristic of simple linear combinations

Name	n	m	λ	σ
Original carriers:				
L1	1	0	19.0 cm	3.0 mm
L2	0	1	24.4 cm	3.9 mm
Linear combinations:				
L_Σ (narrow lane)	1	1	10.7 cm	1.7 mm
L_Δ (wide lane)	1	-1	86.2 cm	13.7 mm

Though the wide lane combination has the highest observation noise, its large wavelength shows a capability to resolve ambiguities or to fix cycle slips. An advantage of the narrow lane combination is the small noise ratio. More complex linear combinations are the so-called "ionosphere-free" linear combination L_3 for carrier and code measurements and the

Melbourne-Wübbena linear combination L_{MW}, described as

$$L_3 = \frac{1}{f_1^2 - f_2^2} \cdot (f_1^2 \cdot L_1 - f_2^2 \cdot L_2) \tag{2.21}$$

and

$$L_{MW} = \frac{1}{f_1 - f_2} \cdot (f_1 \cdot L_1 - f_2 \cdot L_2) - \frac{1}{f_1 + f_2} \cdot (f_1 \cdot PR_{CD_1} + f_2 \cdot PR_{CD_2}). \tag{2.22}$$

Due to approximations in the derivation of Equation (2.21), ionospheric biases are not completely eliminated in L_3, but rigorously reduced. The Melbourne-Wübbena linear combination L_{MW} actually is a subtraction between the wide lane combination of the carrier phases and the narrow lane combination of the code phases. Its large wavelength of 86.2 cm and reduced noise ration ($\sigma_{MW} = 2.4$ mm) makes it appropriate for wide lane ambiguity resolution (referring to Melbourne (1985) and Wübbena (1985)).

2.4.2 Adjustment method

The main method of positioning via GNSS is based on the observation equations (2.1) and (2.6), respectively their corresponding differentiations, and uses the standard least-squares adjustment strategy. Known input quantities are the satellite coordinates $X^q(T_t)$, $Y^q(T_t)$ and $Z^q(T_t)$, which are given in the conventional terrestrial reference system and the individual satellite time frame T_t. The primary unknown parameters in the processing of carrier phase measurements are

- a set of three station antenna coordinates X_u, Y_u and Z_u (included in the term R of Equation (2.1) resp. (2.6))
- the clock sychronization dt_u between receiver clock and GNSS system time
- the ambiguity parameter N_u^s of each pseudorange measurement between receiver u and satellite s

and can be summarized in the parameter vector

$$\mathbf{X} = \begin{pmatrix} X_u \\ Y_u \\ Z_u \\ dt_u \\ N_u^s \end{pmatrix}. \tag{2.23}$$

N_u^s is an initial value and can be solved for each pseudorange by the adjustment of continuous phase measurements, but due to the fourth temporal variable dt_u, it is necessary

to observe at least four satellites simultaneously in order to be able to solve the system of equations. Additional terms of Equation (2.1) respectively (2.6) which can influence the pseudorange measurement are represented by

- 6 orbital biases per satellite
- 1 clock bias per satellite
- 1 ionospheric parameter per station and epoch (e.g. every 2 h)
- 1 tropospheric parameter per station and epoch (e.g. every 1 h)

The satellite's orbital and clock biases are provided by the International GNSS Service (IGS) in form of real-time or highly accurate post-processing products and therefore do not need to be estimated, unless the special aim is to compute precise satellite orbits, which would ask for a global network of reference stations. Tropospheric and ionospheric parameters have to be introduced as unknown parameters and can be reduced by the use of e.g. tropospheric models or linear combinations.

All unknown quantities are combined in the parameter vector $\mathbf{X}$, where the observed pseudorange measurements are represented by the vector $\mathbf{PR}$. By introducing an approximation of the parameter vector $\mathbf{X_0}$, the linearized observation equation can be read as

$$\mathbf{l} = \mathbf{PR} - \mathbf{PR}(\mathbf{X_0}), \tag{2.24}$$

at which the discrepancy between $\mathbf{X_0}$ and the unknown vector $\mathbf{X}$ is given by

$$\mathbf{x} = \mathbf{X} - \mathbf{X_0}. \tag{2.25}$$

This leads to the the functional model of the reduced observations

$$\mathbf{l} = \mathbf{A} \cdot \mathbf{x}, \tag{2.26}$$

where $\mathbf{A}$ describes the design matrix, which contains the partial derivations of the observations $\mathbf{PR}$ with respect to the unknowns $\mathbf{X}$. Equation (2.26) yields to the solution of the reduced parameter vector

$$\mathbf{x} = \mathbf{A}^{-1} \cdot \mathbf{l}. \tag{2.27}$$

A higher number of independent observations than unknowns creates redundancy and hence causes an overdetermined problem. The least-squares estimation technique solves this problem by assuming a Gaussian normal distribution of the observation noise with a mean value of zero:

$$\mathbf{v} = N(\mathbf{0}, \mathbf{\Sigma_v}) \tag{2.28}$$

$\mathbf{v}$ indicates the residual vector of the reduced observations, where $\mathbf{\Sigma_v}$ stands for its variance-covariance matrix. The resulting extension of the function model is written as

$$\mathbf{l} = \mathbf{A} \cdot \mathbf{x} + \mathbf{v}. \tag{2.29}$$

This generalized Gauß-Markov model leads to the correlation between the expected covariance matrix of the observations $\mathbf{\Sigma_l}$ and the cofactor matrix $\mathbf{Q_l}$, where σ_0^2 represents the a priori variance of the unit weight,

$$\mathbf{\Sigma_l} = \sigma_0^2 \cdot \mathbf{Q_l} \tag{2.30}$$

and to the weight matrix

$$\mathbf{P} = \mathbf{Q_l^{-1}}. \tag{2.31}$$

The aim of the least-squares adjustment is to determine the minimal sum of the squares of the residuals using following criteria

$$\mathbf{v^T} \cdot \mathbf{P} \cdot \mathbf{v} = (\mathbf{l} - \mathbf{A} \cdot \mathbf{x})^T \cdot \mathbf{P} \cdot (\mathbf{l} - \mathbf{A} \cdot \mathbf{x}) = \text{minimum!}, \tag{2.32}$$

which finally leads to the equation of the estimated parameter vector

$$\hat{\mathbf{x}} = (\mathbf{A^T} \cdot \mathbf{P} \cdot \mathbf{A})^{-1} \cdot \mathbf{A^T} \cdot \mathbf{P} \cdot \mathbf{l}. \tag{2.33}$$

As mentioned above, the method of the least-squares adjustment expects unbiased, normally distributed stochastic elements. Therefore, any outliers should be eliminated prior to the adjustment.

In accordance with Section 2.4.1, linear combinations eliminate some errors and therefore simplify the system of equations for an easier adjustment. Influences like clock biases can be completely eliminated, whereat other parameters, e.g. the ambiguity resolution, need a more sophisticated approach. By the use of linear combinations as input equations for the parameter estimation, most biases can be determined very precisely. On the other hand, differenced observations create unwanted correlations between the parameters, can cause problems in the fixing of integer ambiguities, lead to baseline solutions and to the problem that this relative network has to be placed appropriately into an absolute coordinate system. In the case of a local network with a small number of receivers, the network can simply be fixed to a stable reference station. With respect to this thesis, in which the regional network consists of about 100 stations, the used subset of underlying reference stations has to be considered in order to perform a network adjustment including specific constraint conditions.

The purpose and differences of modern datums and their realization will be described in the following Chapter 3.

Chapter 3

Geodetic reference systems

The major role of reference systems is not only restricted to satellite-based observation techniques, but concerns the whole field of geodesy. In the following, its background and purpose will be shortly discussed, focussing on modern reference systems related to GNSS observations and local realizations in the area of interest, namely the Australian region.

3.1 Fundamentals

Today's scientific application fields of GNSS range from the detection of variations in the Earth's rotation to the formation of plate velocity models, as mentioned in Section 2.1. Like in other space geodetic techniques, every single GNSS implementation is based on the existence of a well defined reference system, in which all observations can be correctly embedded. Therefore, the conventional *reference system* describes an idealized model and defines the physical and mathematical foundation, whereat its realization, named *reference frame*, is built through (defective) geodetic observations. The term "conventional" indicates a base of clearly specified mathematical elements, models and algorithms. Following systems can be distinguished, which are both used in GNSS:

- space-fixed: (conventional) *celestial reference systems* (CRS) respectively *frames* (CRF)
- Earth-fixed: (conventional) *terrestrial reference systems* (TRS) respectively *frames* (TRF)

The celestial reference system is realized by the measurements to extraterrestrial stars and quasars and is appropriate for the description of the motion of celestial bodies, like planets or satellites. Newton's laws of motion can be used to express the satellite's movements in a terrestrial system, but due to the Earth's underlying acceleration and rotation, it is much more easier to describe the satellite motion in an inertial or in other words *celestial* system, where no fictitious forces act.

Observations related to the Earth surface and the determination of its changes in time require an Earth-fixed model and hence are represented in the *terrestrial* reference system.

It is realized by a large set of globally distributed and stable reference stations on Earth and shows the characteristics of a cartesian coordinate system. By conventions, the origin is set to the geocenter, the equatorial x-axis intersects the Greenwich meridian and the z-axis is located very close to the mean rotational axis.

It should be mentioned that due to the satellite clocks, which stay in different levels of the Earth potential field, relativistic effects in the signal propagation have to be taken into account for the later processing.

Pseudorange measurements between satellite and ground station and its formulation in Sections 2.3 and 2.4 require a uniform coordinate system. Therefore, the relations between celestial and terrestrial system should be determined in a way so that the transformation process does not cause more noise than the code or phase measurement itself.

Regarding to the dynamic characteristics of the Earth, the transformation from the (geocentric) celestial to the terrestrial frame can be described by means of rotations and is defined as

$$\mathbf{x_{TRF}} = \mathbf{W(t)} \cdot \mathbf{R(t)} \cdot \mathbf{N(t)} \cdot \mathbf{P(t)} \cdot \mathbf{x_{CRF}}. \tag{3.1}$$

The Earth orientation parameters (EOPs) represent these rotations in terms of precession $\mathbf{P(t)}$, nutation $\mathbf{N(t)}$, rotation of the Earth $\mathbf{R(t)}$ around the Celestial Ephemeris Pole (CEP) axis (proportional to Greenwich sidereal time) and polar motion (wobble) matrix $\mathbf{W(t)}$ (Kaplan, 2005).

3.2 Terrestrial realizations

3.2.1 ITRF2008

Since its establishment in 1988, the International Terrestrial Reference System (ITRS) defines the basic concept in order to create a global reference frame of mm-level accuracy. It is today's most used reference system for scientific and practical applications and is constructed on four conditions, imposed by the International Union of Geodesy and Geophysics (IUGG) (Petit & Luzum, 2010)[1]:

- it is geocentric with respect to the center of mass of the Earth (including oceans and atmosphere)
- the SI-metre is the unit of length and is in context with the relativistic theory of gravity
- its orientation is defined by the BIH[2] orientation at epoch 1984.0
- a no-net-rotation condition ensures the time evolution of the orientation

[1] More details to the ITRS and its realization are given in Petit & Luzum (2010) and Altamimi *et al.* (2011)
[2] Bureau International de l'Heure

Its latest realization, the International Terrestrial Reference Frame 2008 (ITRF2008), is defined by coordinate and velocity estimations of a set of 580 sites, which are observed with a combination of the four modern space geodetic techniques VLBI, SLR, GPS and DORIS (Figure 3.1). The ITRF2008 shows the characteristics of a dynamic datum, which considers actual coordinate drifts caused by plate tectonics and allows accurate models of long-term site displacements. Time series beginning from epoch 1980.0 until 2009.0 were used to compute mean station velocities, where the reference epoch of station coordinates is set to the January 1st, 2005.

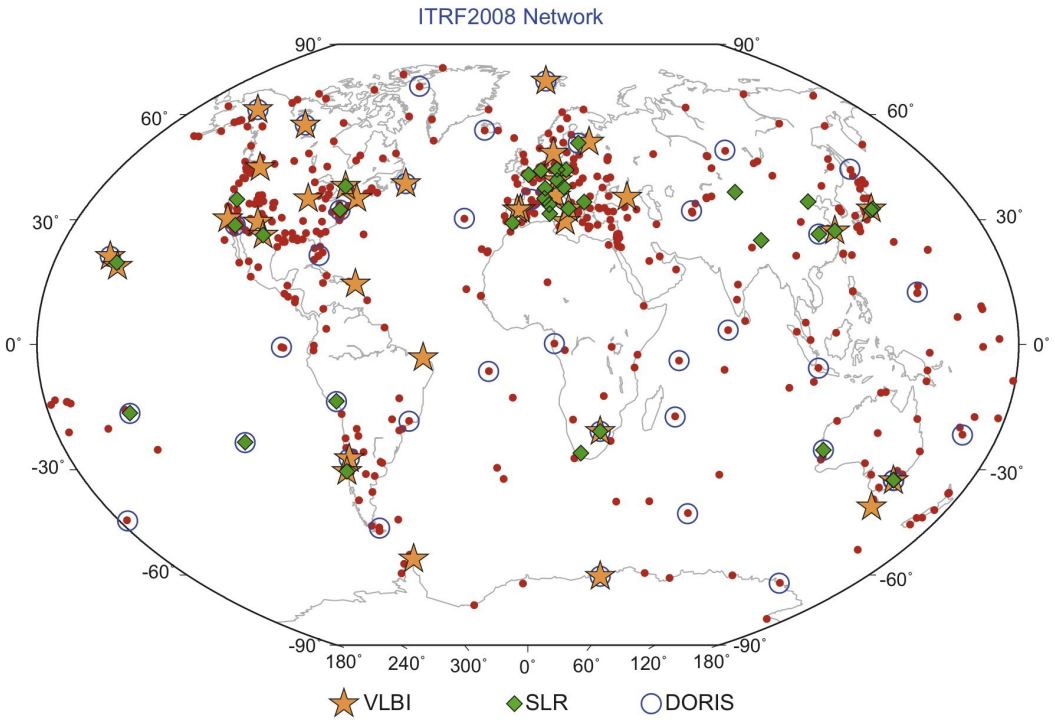

Figure 3.1: ITRF2008 network of GPS sites (black dots) co-located with VLBI, SLR and DORIS (Altamimi *et al.*, 2011)

3.2.2 IGS08

The IGS has adopted an own reference frame which is based on GNSS observations only. Its newest realization is called IGS08 and is closely related to ITRF2008. In fact, both frames are based on the same underlying datum, for which reason the global Helmert transformation from ITRF2008 to IGS08 should be considered as close to zero. Small deviations are caused by a different set of underlying reference stations. The whole network includes coordinates and velocities of 262 stations, taken from the ITRF2008, whereat only a subset of up to 91 stations is used for the realization of the frame. The main selection criteria of this so-called core network (Figure 3.2) are the global distribution and station stability in terms of RMS of

residual time series, number of observations, monumentation and level of discontinuity. Small differences in some station coordinates occur as a result of two different antenna calibration models in use. ISG08 is consistent with the updated model igs08.atx, where ITRF2008 is still based on igs05.atx (Rebischung *et al.*, 2011). IGS08, such as ITRF2008, represents a dynamic datum and defines the January 1st, 2005 as a reference epoch for its network coordinates.

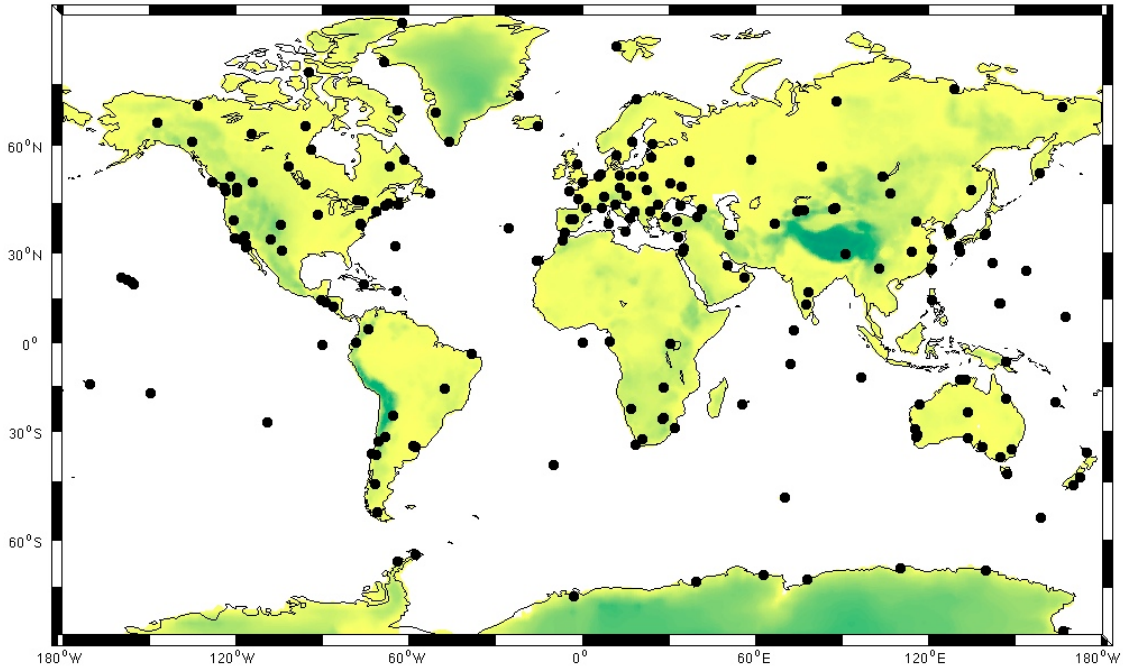

Figure 3.2: IGS08 core network of reference stations (Dow *et al.*, 2009)

3.2.3 WGS 84 and PZ 90

Each of the two fully developed global navigation satellite systems (GPS and GLONASS) operates with its own terrestrial reference system.

GPS uses the World Geodetic System 1984, in short WGS 84. It was initially established by the use of TRANSIT observations and later revised so that an accuracy of cm-level was reached. The latest realization of WGS84 is based on GPS data and called WGS84 (G1150). The term in brackets refers to the GPS week when the system was adopted and aligned with ITRF2000. This WGS84 realization shows a coincidence with ITRF at a range of a few cm.

The GLONASS terrestrial reference system is named Parametri Zemli 90 (PZ 90), and was realized by the establishment of 26 ground stations using Doppler measurements, laser ranging and satellite altimetry. Today's realization, introduced back in 2007, is called PZ 90.02 and agrees with ITRF in cm - dm level. (Ziebart & Bahrami, 2012).

Both underlying reference ellipsoids can be described by (1) the semimajor axis a and (2) the flattening f of the ellipsoid, (3) the angular velocity of the Earth ω and (4) the Earth's

gravitational constant $G \cdot M$, as given in Table 3.1.

Table 3.1: Parameters of the WGS 84 and PZ 90 ellipsoid (Hofmann-Wellenhof *et al.*, 2008)

Parameter	WGS 84 (GPS)	PZ 90 (GLONASS)
a	6 378 137.0 m	6 378 136.0 m
f	1 / 298.257 223 563	1 / 298.257 839 303
ω	$7\,292\,115 \cdot 10^{-11}$ rad s^{-1}	$7\,292\,115 \cdot 10^{-11}$ rad s^{-1}
$G \cdot M$	$3\,986\,004.418 \cdot 10^{8}$ m^3 s^{-2}	$3\,986\,004.400 \cdot 10^{8}$ m^3 s^{-2}

3.2.4 GDA94

The Geocentric Datum of Australia 1994 (GDA94) is Australia's nowadays used reference frame and represents a local static datum. It is based on a fiducial network of several stable Australian GNSS sites, taken from the former ITRF1992 (Boucher *et al.*, 1993). In 1994, measurements of around 70 well distributed stations were combined to a single regional GPS solution with respect to ITRF1992 and initialized at the reference epoch of the January 1st, 1994. At that time both frames, GDA94 and ITRF1992, were coincident. The projection of geodetic coordinates of these first-order bench marks is performed through the UTM projection and uses the GRS80 ellipsoid. Due to regional tectonic movements of around 7 cm yr^{-1}, today (February, 2013) GDA94 and ITRF diverge by more than 1 m. Since its introduction, Geoscience Australia evaluates and provides parameters for the transformation between GDA94 and the most common ITRF realizations, but the resulting RMS errors of several cm led to considerations, whether the Australian reference frame should be modernized or even converted into a dynamic datum (Dawson & Woods, 2010).

Chapter 4

The APREF project

4.1 Initiation and aims

Chapter 3 already highlighted the needs of a precise geodetic reference frame. Until 2009, the Asia-Pacific region consisted of a large number of local national reference systems based on different underlying datums and was therefore hard to access and to combine. Multinational projects and higher requirements in accuracy increased the demand for a consistent reference frame covering the Asia-Pacific region in its entirety. By then, national governments exclusively ran their own local reference frames, where transformation approaches and the sparse distribution of reference sites led to significant losses in accuracy. Many applications such as engineering geodesy, mining, hazard assessment and furthermore scientific tasks like the determination of crustal deformation or sea level rise exceed the quality of national geodetic systems and moreover require a very accurate reference frame at mm-cm level.

Huisman *et al.* (2011) called the presently Asia-Pacific geodetic reference frame "a patchwork of national and regional datums, ... below the standard that is now available, ... comparatively sparse, inhomogeneous in accuracy, infrequently realized (and) often difficult to access ...". Therefore, the needs were given to improve the Asia-Pacific infrastructure by the establishment of the Asia-Pacific Reference Frame (APREF) in order to satisfy today's geodetic demands and to afford a competitive environment compared to other existing permanent networks, such as EUREF in Europe, the CORS network in the United States and SIRGAS in South America.

Since its foundation in 2009, the purpose of the APREF project is to meet these demands by the creation of a precise regional network, which can be easily linked to international frames such as the ITRF, including its maintenance and with a view to expand the number of participating agencies and reference stations. The objectives of APREF can be split into a short term and long term perspective (GA, 2012). In short terms, the project pursues a strategy to

- make GNSS raw data from regional CORS freely available
- provide an authoritative and open access to final products, represented by station coor-

dinates and velocities.

The long term view includes challenges for the following years and can be described as follows:

- the development and maintenance of the APREF Permanent CORS network in cooperation with IGS
- to encourage the participation of other agencies in order to increase the number of reference stations and to densify and improve the geodetic infrastructure
- to enable an involvement of APREF stations to the realization of the ITRF
- the preparation of a dense velocity field model for the Asia-Pacific region
- the scheduling and accomplishing of APREF-related workshops and symposia

The organizational structure of APREF follows an honorary and non-commercial thought. Participating agencies allocate sources of raw data from their local station network to so-called Local Analysis Centres (LACs). These centres collect data from an assigned subnetwork of APREF, compute daily and weekly solutions in an automated post-processing step and provide them to the Central Bureau, APREF's coordinating body. There, the individual LAC solutions are going to be analyzed, validated and combined to a final solution covering the whole APREF network in ITRF coordinates. The Central Bureau is also responsible for the regular publication of final products, not only for participating organizations, but for the entire geodetic community. John Dawson from Geoscience Australia (GA) is the initiator of the APREF concept and the current chair of its steering committee. Hence, he is the official representative and contact person of APREF and leads the Central Bureau, located within GA in Canberra.

4.2 Today's APREF network

At the moment (February, 2013) the entire APREF network counts around 500 reference stations, including about 100 globally distributed IGS stations. Participating countries which either provide raw data from their GNSS network or act as local analysis centres are shown in Figure 4.1, including Alaska (USA), Brunei and numerous small insular states in the area of Polynesia, Micronesia and Melanesia. Though the APREF network includes globally distributed IGS stations, the development of a dense field of Asia-Pacific reference sites is clearly visible, especially in Australia and New Zealand.

Table 4.1 describes the contributing agencies which act as local analysis centres, where VIC has stopped its processing in July 2011 after a period of around 1.5 years.

Currently, Geoscience Australia (AUS) and Curtin University of Technology (CUT) represent the two operational LACs and provide processing solutions of their assigned subnetwork regularly to the Central Bureau of APREF. Figure 4.2 illustrates the dimensions of all existing

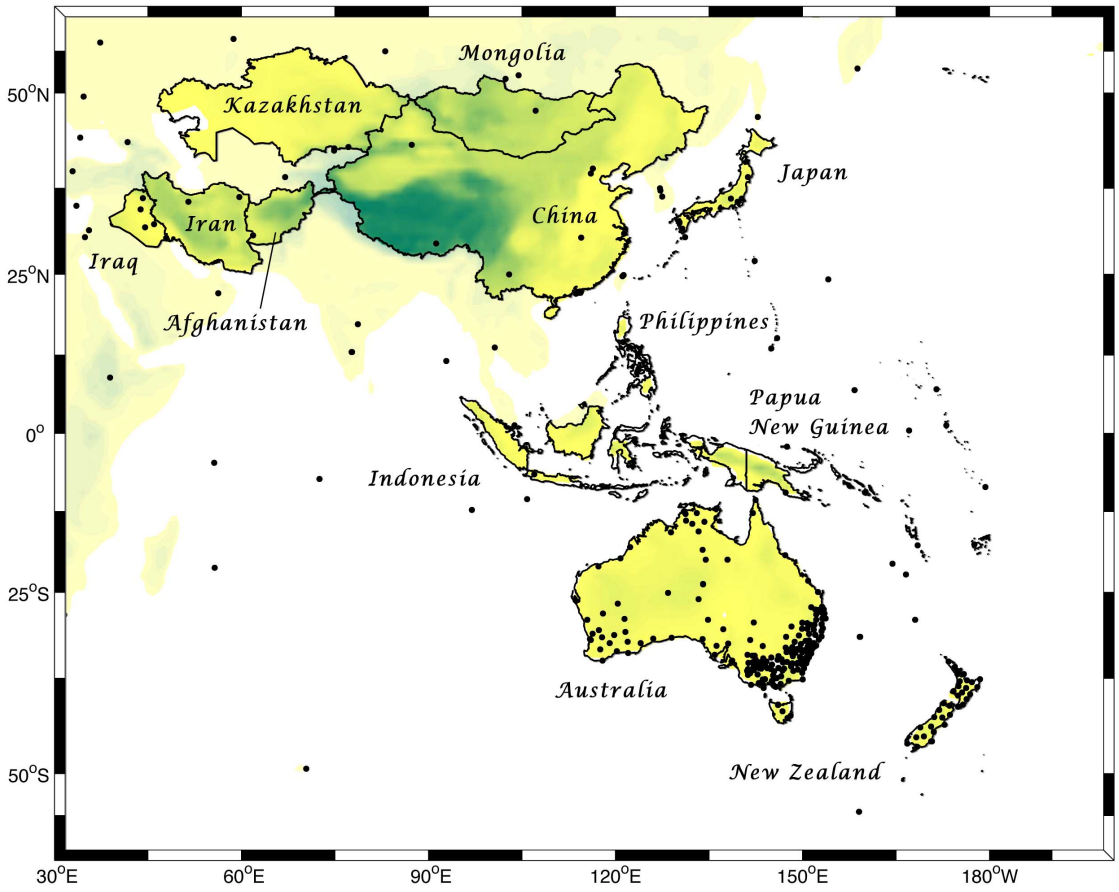

Figure 4.1: Participating countries of APREF (GA (2012), as from February, 2012)

Table 4.1: LAC members of APREF, status February, 2013 (GA, 2012)

Group	Description	operational
AUS	Geoscience Australia, Canberra, Australia	online
CUT	GNSS Research Group, Curtin University of Technology, Perth, Australia	online
VIC	Geodetic Survey, Office of Surveyor - General Department of Sustainability and Environment, Victoria, Australia	offline since July 2011

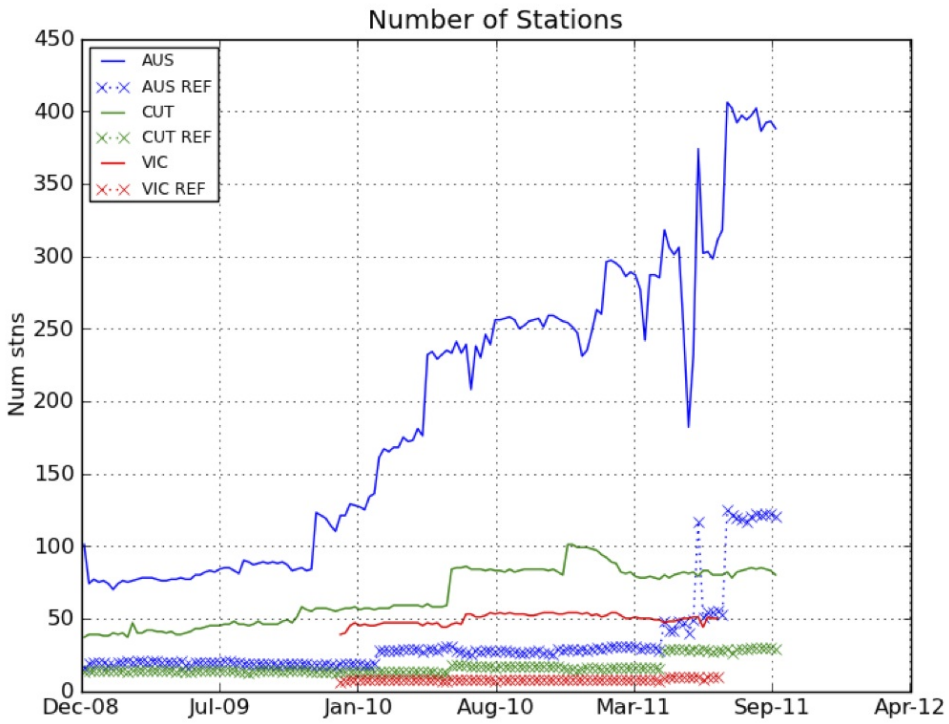

Figure 4.2: Dimensions of contributing LAC networks (Dawson, 2012)

LAC networks (including VIC) and the number of datum determinant fiducial sites during a three year time span.

All solutions are computed independently, where CUT's and VIC's stations lie in the region of Oceania and therefore within AUS's global network. GA continues to encourage participating organizations to become local analysis centres[1] in order to increase the number of individual solutions and with it the accuracy and stability of the final products, which can be described as:

- weekly station coordinates in a solution independent exchange format (SINEX, using IGS final products such as precise orbits, etc.) with a latency of about 4 - 6 weeks

- weekly station performance in terms of repeatability

- access to time series plots of all APREF stations, including accumulated coordinate and velocity solutions along with potential station discontinuities[2]

[1] More details to the standards in becoming an analysis centres or a station operator are given in the guidelines GA (2011a), GA (2011b) and at the official APREF website of GA (2012)

[2] Available at http://192.104.43.25/status/solutions/analysis.html

4.3 SAGE's contribution to APREF

This section describes the endeavor of raising a new local analysis centre and represents the link between APREF and the objectives of this thesis.

Shortly after GA established the APREF network, Prof. Chris Rizos' School of Surveying and Geospatial Engineering (SAGE), formerly known as School of Surveying and Spatial Information Systems (SSIS), located at the University of New South Wales (UNSW) in Sydney, Australia, started to work on an automatic processing table which fulfills the requirements of GA in order to become a local analysis centre. Unfortunately, SAGE's efforts were retarded due to a deficit of human resources. As a consequence of the preparations for the author's practicum at UNSW, it was recognized that an involvement in the APREF project could reveal potential benefits both for SAGE and the author. The creation of a stable and automated processing table would be a major step in the establishment of an additional (third) operational LAC. Furthermore the generation of an own processing strategy, which ranges from the automatic acquisition of GNSS raw data to the final estimation of daily and weekly station coordinates, would serve as a cornerstone in this thesis.

Because of SAGE's research interests in the area of New South Wales and in order to include a zone of tectonic faults and analyze different directions of ground motion for the sake of this thesis, the region around Australia, New Zealand and New Caledonia was defined as the investigative APREF subnetwork. Due to GA's three-character LAC notation, the proposed network will be called *NSW* (New South Wales). NSW consists of a total number of 97 reference stations, located in the countries mentioned above and illustrated in Figure 4.3 (Miller projection). IGS respectively ITRF stations are marked blue and will be used as potential fiducial sites for the datum definition (later described in Sections 5.2 and 5.3), the others represent new APREF stations.

The next chapter explicitly deals with the particular processing steps which are necessary for the accurate and consistent estimation of daily and weekly solutions of network NSW.

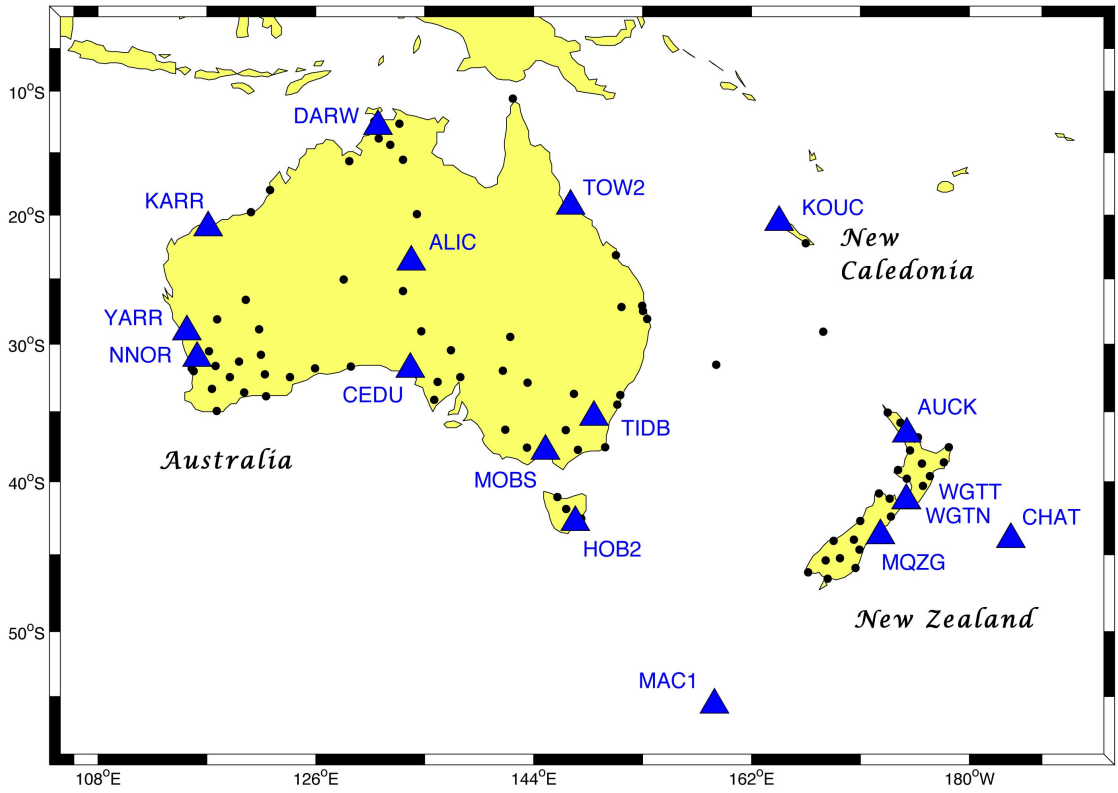

Figure 4.3: IGS/ITRF sites (blue triangles) and APREF stations (black dots) of network NSW

Chapter 5

Applied parameter estimation

The procedure of computing final CORS network solutions based on different types of input data sets includes several preparation steps and intricate adjustments of model parameters. Software packages which can handle these tasks and hence are appropriate for highly accurate GNSS post-processing applications, are e.g. BERNESE, EPOS.P.V2, GAMIT/GLOBK, GINS/DYNAMO, GIPSY-OASIS II and NAPEOS. In this thesis the focus lies on the use of the Bernese GPS Software (Version 5.0), developed and maintained at the Astronomical Institute of the University of Bern (AIUB).

The following Section 5.1 provides a short insight into Bernese and passes on to the individual processing scripts and parameters (see Section 5.2), which were chosen in order to receive final APREF products, such as

- daily solutions in terms of normal equations, station coordinates and estimates of the troposphere
- weekly solutions in terms of SINEX files, station coordinates and weekly summary files showing single and total repeatability

Section 5.3 takes a separated look at the non-trivial problem of the datum definition, whereas the last Section 5.4 highlights the computation of final station velocities out of weekly solutions.

5.1 The Bernese GPS Software

Bernese fulfills highest accuracy requirements for multi-GNSS data analysis and is well suited for an automated processing of local, regional or global permanent networks, including the combination of different receiver types, GPS and GLONASS observations, the ambiguity resolution on baselines longer than 2000 km, the generation of minimum constraint network solutions and ionosphere and troposphere monitoring (Dach, 2012). Moreover, its capability is not restricted to network solutions or atmospheric analysis, but also provides strategies for

orbit determination, estimation of Earth orientation parameters and is accordant to the IERS 2010 conventions and IGS standards.

Bernese is composed of a multitude of single processing scripts, each responsible for a particular task, written in the script language PERL and allocated through a graphical user interface in order to simplify changes in the processing parameters. However, its input and output data sets are restricted to the format of text files respectively binary extensions (Haasdyk, 2009). Hence, the graphical visualization of obtained results has to be performed by another software if demanded[1]. The individual Bernese scripts can be assembled in a so-called Process Control File (PCF), which describes the sequential arrangement of the specific processing strategy and commits parameters (global variables) to the contained scripts. Beside the standard Bernese scripts, represented e.g. by CODSPP (responsible for the receiver clock synchronization) or COOVEL (responsible for the epoch-specific extrapolation of reference coordinates), it is possible to create own PERL scripts and include them in the PCF. Thereby, it is possible to automate specific preparation tasks, such as the download of input data sets from an FTP server.

The PCF can be executed via the Bernese Processing Engine (BPE), which allows an automated, multi-session data processing of a large campaign within several hundred GNSS sites over a user-defined time span. The established process control file NSW.PCF, named after the proposed APREF subnetwork (see Section 4.3), contains the whole processing strategy and represents an adopted version of Bernese's example RNX2SNX.PCF (Dach *et al.*, 2007).

5.2 Implemented processing strategy

All processing steps, beginning with the acquisition of raw data to the point of determining weekly solutions, can be grouped into three general aspects:

- preparation
- preprocessing
- final processing

In the following, the focus lies on the successful execution of each step and its underlying number of single processing scripts.

5.2.1 Preparation

Prior to the estimation of GNSS-related errors and model parameters, all required data sets have to be collected from the different sources, partially converted, renamed and allocated to

[1] e.g. by The MathWorks™ MATLAB®

the specific directories of the Bernese campaign (called NSW). Furthermore, a priori coordinate files need to be created and pole, orbit and clock information has to be prepared. Figure 5.1 illustrates the corresponding part of the PCF and its individual scripts. Green names represent Bernese-internal scripts, red names stand for scripts which are developed by the author.

```
# ============================================================================
# NSW.PCF
# Modified from RNX2SNX.PCF
# Modified by Hannes Maar for APREF implementation at UNSW, Sydney
# ============================================================================
#
…
#
PID SCRIPT   OPT_DIR  CAMPAIGN CPU      P WAIT FOR....
3** 8******* 8******* 8******* 8******* 1 3** 3** 3** 3** 3** 3** 3** 3**
#
# Copy required files
# -------------------
001 FTP_RNX  UNSW_GEN          ANY      1
002 FTP_ORB  UNSW_GEN          ANY      1 001
003 FTP_ION  UNSW_GEN          ANY      1 002
004 FTP_STA  UNSW_GEN          ANY      1 003
005 FTP_IGS  UNSW_GEN          ANY      1 004
006 SNX2NQ0  UNSW_GEN          ANY      1 005
007 FTP_GEN  UNSW_GEN          ANY      1 006
#
# Create a priori CRD file and fiducial site file
# -----------------------------------------------
010 COOVEL   UNSW_GEN          ANY      1 007
011 CRDMERGE UNSW_GEN          ANY      1 010
020 REF_STA  UNSW_GEN          ANY      1 011
#
# Prepare pole, orbit, and clock information
# ------------------------------------------
101 POLUPD   UNSW_GEN          ANY      1 020
111 PRETAB   UNSW_GEN          ANY      1 101
112 ORBGEN   UNSW_GEN          ANY      1 111
```

Figure 5.1: Preparation scripts of NSW.PCF

5.2.1.1 Required data sets and their acquisition

The required input data can be split into primary and secondary data sets, which have to be acquired from different kinds of sources.

Primary input data sets are of course the particular code and carrier observations from each reference station of the network. These measurements are given in the form of daily receiver independent exchange format (RINEX) files (Table 5.1). Basic observables in the RINEX files are

- the epochs of observations expressed in the receiver time frames
- carrier phase observations
- pseudorange code observations

Table 5.1: Characteristics of station-based raw data

Format	Period of observations	Sample interval	Latency
RINEX	24h	30s	1 day

Sources of these data sets are several freely accessible FTP servers. IGS stations provide their raw data through a couple of IGS-related servers, where RINEX files of new APREF sites are gathered on a single server hosted by GA (Table 5.2).

Table 5.2: Sources of RINEX files (IGS and APREF Server), status February, 2013

Station type	Provider	Location	Host address
IGS	CDDIS	Greenbelt, USA	ftp://cddis.gsfc.nasa.gov/
	SOPAC	San Diego, USA	ftp://garner.ucsd.edu/
	IGN	Paris, France	ftp://igs.ensg.ign.fr/
APREF	GA	Canberra, Australia	ftp://ftp.ga.gov.au/

The network to be analyzed is defined by the cluster file named NSW.CLU, which includes a list of all involved reference stations and an arrangement in clusters. Figure 5.2 illustrates the first lines of this file and its format. Perl script FTP_RNX is responsible for the acquisition of the RINEX raw data files and performs the following tasks on a daily basis

- extraction of the individual station names from cluster file NSW_CLU
- download of the corresponding compact RINEX files from the data sources, given in Table 5.2, into the subdirectory of the specific campaign
- unpack the gathered files
- execution of a Hatanaka transformation to convert the compact RINEX files into ordinary RINEX files
- generation of a text file containing all stations which could not be found

Secondary data sets are necessary to establish a link to space-fixed satellite positions, to model disturbing influences in a highly accurate way and to allow a wise selection of datum-defining fiducial sites. Some of them are stored within the Bernese software and do not need to be updated regularly (such as the planetary ephemeris file DE200.EPH). Other data sets, which need to be acquired respectively updated on a continuous basis or represent network-specific pieces of information, are described as:

```
NSW station cluster file                                        01-Jun-12 10:45
-------------------------------------------------------------------------------

STATION NAME      CLU
****************  ***
AUCK 50209M001      1
CHAT 50207M001      1
MAC1 50135M001      1
WGTN 50208M003      1
WGTT 50208S004      1
KTIA 50241M001      1
WHNG 50218M001      1
GISB 50223M001      1
TAUP 50217M001      1
HAMT 50222M001      1
...
```

Figure 5.2: Network determinant cluster file NSW.CLU

- precise orbit and Earth rotation parameter (ERP) files
- ionospheric models
- a station information file
- a priori station coordinates
- ocean loading effects
- general Bernese files

The precise orbit file is part of the final IGS products and given in the international format for exchanging precise orbit information, known as SP3c. This file contains satellite positions and clock information, given in an Earth-fixed, geocentric system for a certain time span using equidistant intervals of 15 min. In order to use these pieces of information, the satellite's coordinates have to be transformed in a space-fixed reference frame using a set of Earth Rotation Parameters (ERP). This ERP (pole) file includes a three-parameter subset of the EOP, which are represented by time series of polar motion coordinates (x_p, y_p), length of day (respectively UT1), nutation offsets and their respective sigmas (Dach *et al.*, 2007). Both the precise orbit file and the pole file can be acquired form several IGS servers (Table 5.2).

Global ionosphere models can be provided daily and include sets of total electron content (TEC), using coefficients of spherical harmonics of a maximum degree and order 15 and their RMS. Although linear combinations (as described in Section 2.4.1) can eliminate the influence of ionospheric propagation delays, these pieces of information have to be taken into account for the later ambiguity resolution.

Station- respectively receiver-specific information is given in a so-called station information file (STA file). It contains valid station names, information about the technical equipment such as receiver/antenna type and antenna eccentricities, and specifies if single stations cause problems for a particular epoch and hence have to be excluded from the processing. It is also

possible to apply relative coordinate and velocity constraints between two nearby stations in order to estimate one and the same velocity for two different stations (Dach *et al.*, 2007). Bernese uses the STA file for several processing steps, beginning from the import of RINEX files (RXOBV3) to the main parameter estimation script (GPSEST), and can e.g. reveal inconsistencies in the RINEX headers and, in such a case, act appropriately. This information has to be kept up-to-date in order to consider changes in the station equipment and therefore should be refreshed regularly. GA provides access to a station information file called AUS.STA, which contains current information of all APREF stations, updated on a daily basis. So it is suitable to be used by local analysis centres respectively APREF subnetworks such as ours.

The strategy of creating adequate a priori station coordinates is described in detail in the next Section 5.2.1.2. In order to execute this task and to distinguish between new APREF stations and datum-defining fiducial sites, it is necessary to collect three types of data sets:

- predicted coordinates of IGS stations, represented in the datum-defining IGS08 reference frame
- weekly IGS solutions, in order to check the consistency of the predicted IGS08 coordinates
- approximate coordinates of new APREF stations

The former predicted data sets are extrapolated through a set of IGS08 coordinates, given in the reference epoch January 1st, 2005, and its corresponding velocity file. Therefore, these IGS08 data sets and the approximate APREF coordinates have to be gathered only once, where the regularly processed IGS solutions are provided on a weekly basis. Depending on whether a station is an IGS station and therefore a potential fiducial site, it adopts the more precise IGS08 coordinates. Otherwise, less accurate APREF coordinates are applied.

Ocean loading tidal effects produce horizontal and vertical site displacements due to the changing mass distribution caused by ocean tides. There are numerous ocean loading models, which can be applied on a set of stations using Chalmers' online platform[1]. The compiled ocean loading file contains station specific coefficients regarding the amplitude and phase shift of the most important constituents. It only has to be generated once, but it is required that all sets of coefficients are consistent, which implies that all corrections rely on the same ocean tidal model. The chosen ocean tide model for network NSW is called GOT00.2. It is a long waveform adjustment of the former ocean tide model FES94.1, which describes a global and pure hydrodynamic tide model. GOT00.2 uses additional TOPEX/Poseidon data and is given on a 0.5 by 0.5 degree grid (OSO, 2012).

General Bernese files describe Bernese-formatted data sets which contain constants and correction parameters, as seen in Table 5.3. These files have to be refreshed from time to time,

[1]More details to the creation of ocean loading corrections are given at the website provided by Chalmers University of Technology, OSO (2012)

e.g. every week, and can be obtained from the AIUB data server, illustrated in Table 5.4.

Table 5.3: Fundamental general Bernese files

File name	Describtion
DATUM.	includes geodetic constants defining the parameters of different conventional datums
RECEIVER.	the receiver information file
PHAS_COD.I08	the antenna phase centre file
SATELLIT.I08	the satellite information file
SAT_2012.CRX	characterizes satellite problems, e.g. maneuvers or bad observation intervals
GPSUTC.	contains information of occurrent leap seconds

Table 5.4: Source of general Bernese files, status February, 2013

Provider	Location	Host address
AIUB	Bern, Switzerland	ftp://ftp.unibe.ch/

Table 5.5 summarizes the mentioned primary and secondary data sets, which are required for the later processing, and their acquisition. It can be seen that the latency of some data sets leads to the case that the network processing can be executed at the earliest date of approximately 2 - 3 weeks after the time of observation.

5.2.1.2 Creation of an a priori coordinate file

The main processing strategy is based on relative positioning using double differences, which means that the calculated network has to be transformed into an superior reference frame using a certain datum definition. This important task is realized through a well defined set of fiducial sites and their a priori coordinates. Therefore, it is essential that these stations have highly accurate coordinates. As already mentioned, three sources of coordinate data sets are in use. A first step is to distinguish between IGS and APREF stations.

IGS stations represent stable and well-performing reference stations of the current IGS08 reference frame and feature accurate coordinates and velocities based on long-term GNSS observations over several years. 15 IGS and two ITRF stations (WGTN and WGTT) will be used as potential datum-defining fiducial sites in network NSW (blue triangles in Figure 4.3). Their coordinates are calculated by the Bernese script COOVEL, which extrapolates the reference coordinates, given in the coordinate file NSW.CRD (Figure 5.3), to the certain epoch using the corresponding velocity information, given in the velocity file NSW.VEL.

The remaining APREF stations do not demand such accurate a priori coordinates, since they are not used for the datum definition. It is adequate to use a priori coordinates with an

Table 5.5: Types of required data sets and their acquisition

Type of data set	Provider	Latency	Download interval	Executive script
RINEX files	GA	1 day	daily	FTP_RNX
Precise orbit Information	IGS	12 - 18 days	daily	FTP_ORB
Earth Rotation Parameters	IGS	11 - 17 days	weekly	FTP_ORB
Ionosphere models	AIUB	∼ 14 days	daily	FTP_ION
Station information file	GA	1 day	daily	FTP_STA
A priori coordinates				
- predicted	AIUB	-	(singular)	-
- weekly IGS	IGS	11 - 17 days	weekly	FTP_IGS
- APREF	GA	-	(singular)	-
Ocean loading file	Chalmers	-	(singular)	-
General Bernese files	AIUB	1 day	daily	FTP_GEN

```
APREF COORDINATES (UNSW SUBNETWORK)                              1-Jun-2012
------------------------------------------------------------------------------
LOCAL GEODETIC DATUM: IGS08             EPOCH: 2005-01-01 00:00:00

NUM  STATION NAME           X (M)          Y (M)          Z (M)     FLAG

  1  AUCK 50209M001    -5105681.1754    461564.0313  -3782181.4818   IGS08
  2  CHAT 50207M001    -4590671.1092   -275482.6825  -4404596.5757   IGS08
  3  MAC1 50135M001    -3464038.6094   1334172.9184  -5169224.1736   IGS08
  4  WGTN 50208M003    -4777269.4835    434270.2089  -4189484.4102   ITR08
  5  WGTT 50208S004    -4779508.0540    436517.4510  -4186741.0400   ITR08
  6  KTIA 50241M001    -5190163.3614    612173.6114  -3644201.5304   P
  7  WHNG 50218M001    -5153430.6911    513057.5109  -3710655.7946   P
  8  GISB 50223M001    -4985376.2500    184022.2155  -3960829.9802   P
...

Meaning of flags:
-----------------
IGS08 : IGS08
ITR08 : ITRF2008
P     : Approximate APREF Coordinates (cm level)
```

Figure 5.3: Format of reference coordinate file NSW.CRD

accuracy in m-level, as the performed network solution improves the relative baseline accuracy to a few mm. A priori APREF coordinates are gathered from GA prior to the processing start. Instead of APREF station velocities, another way will be used in order to perpetuate the station movement and to keep the a priori coordinates accurate enough. Script CRDMERGE reads the APREF stations in the reference coordinate file and replaces their coordinates with more accurate results from a former processed solution. This coordinate merge affects APREF sites only. IGS (respectively ITRF) station coordinates remain, as they were already extrapolated through their velocity information.

The third coordinate data set represents the weekly IGS solutions and is required in the next section.

5.2.1.3 Creation of a fiducial site file

For the later definition of the datum, it is necessary to define a fiducial site file, which contains all datum-definitive stations. The specifically developed mini-script REF_STA generates such a fiducial site file for each session (day). It is based on two selection criteria:

- the station has to be an IGS or ITRF station
- the station should not exceed a specified threshold between a priori coordinates and weekly IGS solution

Therefore, it is required to extract the coordinates from the weekly IGS solutions, which also include estimates of the two mentioned ITRF sites, and to compare them with the extrapolated values. If no weekly IGS solution is available for the current session or station, then the stations of the last known fiducial site file will be stored in the new file. The defined threshold prevents that inappropriate stations lead to distortions in the datum definition. Reasons for such defective stations can be a noteless change in the receiver equipment or unpredictable geophysical events, such as earthquakes or land slides, which cause station movements that are inconsistent with their expected a priori coordinates. The selection of threshold values is founded on the analysis of weekly IGS residuals covering a time span of three years and is given in Table 5.6.

Table 5.6: Defined threshold for the selection of fiducial sites

Direction	Value, in [mm]
North	10
East	10
Up	15

Figure 5.4 illustrates the residuals between predicted coordinates and weekly IGS solutions for all 17 potential fiducial sites in this period.

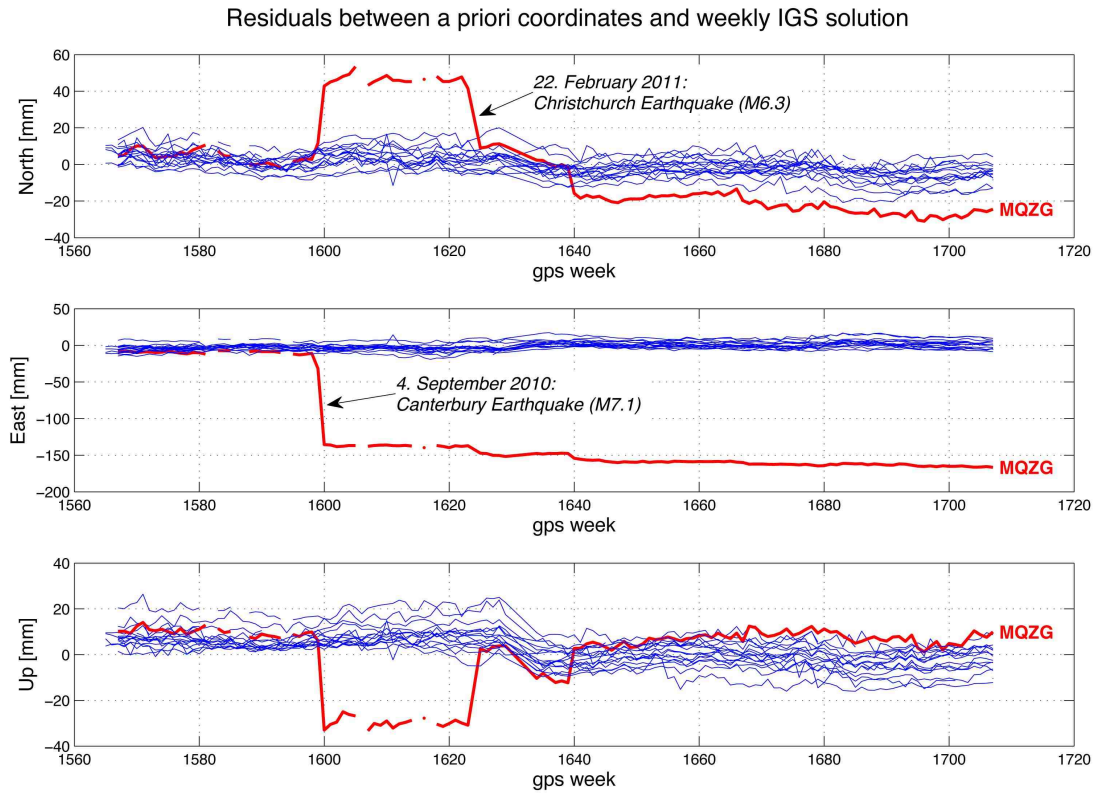

Figure 5.4: Residuals of the potential fiducial sites for the last three years

It is obvious that IGS station MQZG, located in Christchurch, New Zealand, is not an adequate fiducial site any more, after two major earthquakes hit the region in the past. A closer look at the remaining stations in Figure 5.5 reveals that most of the plotted residuals lie within the set threshold visualized by light green rectangles. A short statistic of the accepted residuals during this three year time span is given in Table 5.7.

Table 5.7: Statistic of accepted residuals within the set threshold

Direction	No. of stations	Total no. of observations	Accepted residuals
North			86.0 %
East	17	2185	88.4 %
Up			94.3 %

Inappropriate stations are excluded from the fiducial site file, but the percentage of accepted residuals shows a high probability that the chosen threshold does not exclude too many stations, which would lead to a lack of fiducial sites.

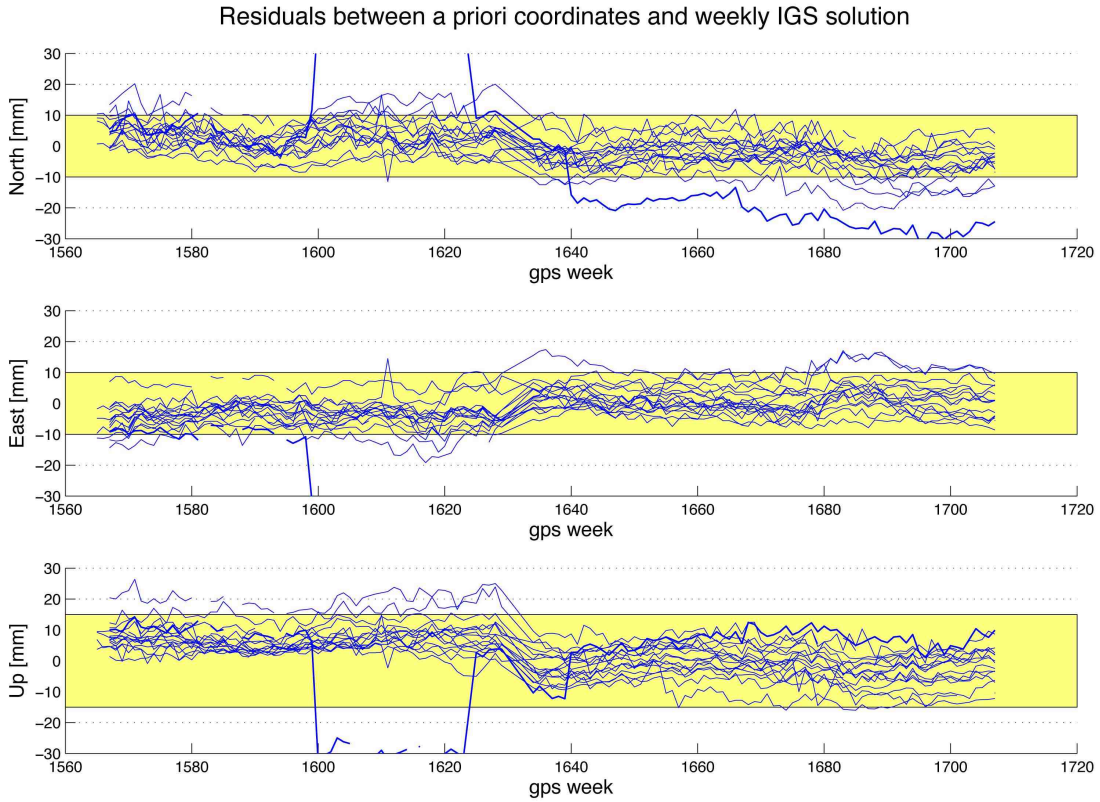

Figure 5.5: Residuals of the potential fiducial sites, accepted band in green

Additional output files of script REF_STA are given by a daily protocol, which lists all rejected fiducial site names and their accordant residuals (Figure 5.6), and a fiducial residual file, which indicates the weekly residuals of every IGS respectively ITRF station in North, East and Up component, including the rejected fiducial sites (Figure 5.7).

```
LIST OF REJECTED FIDUCIAL STATIONS,                    YEAR: 2012, DOY: 270
-------------------------------------------------------------------------------

Station name            Residuals (mm)
                      N           E           U
*********************************************
MQZG 50214M001      -25        -167          10
TOW2 50140M001      -12           9         -12
TIDB 50103M108      -12           5          -6
```

Figure 5.6: List of rejected fiducial sites for GPS week 1707, day 3

5.2.1.4 Prepare pole, orbit and clock information

The preparation of the precise orbit and clock information is essential for the data processing. The three Bernese scripts POLUPD, PRETAB and ORBGEN are responsible for these tasks,

```
FIDUCIAL RESIDUAL FILE                                        GPS WEEK: 1707
------------------------------------------------------------------------------

Station name              North       East         Up
****************       **.****    **.****    **.****
AUCK 50209M001           0.0022     0.0030     0.0042
MAC1 50135M001           0.0032     0.0086     0.0086
WGTN 50208M003           0.0084     0.0056     0.0104
MQZG 50214M001           0.0245     0.1665     0.0099
...
```

Figure 5.7: Residuals of all potential fiducial sites for GPS week 1707, in [m]

which can mainly be described as

- the conversion of the given precise orbit and pole files into the Bernese format,
- the transformation of the precise satellite's position into a celestial system and
- the generation of a standard orbit file.

The geocentric cartesian coordinates and clock information of each satellite are given in the precise orbit file, where the pole file contains the Earth rotation parameters, which are necessary for the transformation from the Earth-fixed into the celestial system and vice versa.

At first, the input (IGS-formatted) pole file has to be converted into a Bernese format. POLUPD is able to execute this step and supports several foreign formats of the input pole file, which extension has to be set to IEP. The conversion requires additional information about occurrent leap seconds, which are represented by the general Bernese file GPSUTC., and the chosen nutation and sub-daily pole models. The nutation model IAU2000 and the sub-daily pole model IERS2000 are selected in order to be consistent with the IERS Conventions 2010 (Petit & Luzum, 2010) and to describe the nutation and sub-daily tidal variations of the pole and the rotation of the Earth. These two models will be written to the header of the Bernese-formatted output pole file (extension ERP) and therefore have to be equally defined in the following scripts PRETAB and ORBGEN (Dach *et al.*, 2007).

PRETAB uses the input precise orbit file and the generated Bernese pole file in order to execute the transformation of the satellite's positions into the celestial system J2000.0, writes them into an intermediate tabular orbit file and extracts clock information from the precise orbit file. Again, the former discussed nutation and sub-daily pole models have to be taken into account.

ORBGEN creates a so-called standard orbit (STD) and a radiation pressure coefficient file. The standard orbit will be generated starting from the tabular orbit file. It is the result of a numerical integration of the equations of motions, it is a binary file, represents the satellite's positions in a geocentric celestial system and is mandatory for all following programs that access satellite orbit information, such as the major scripts for parameter estimation GPSEST and ADDNEQ2. Wherever a standard orbit is used, it has to be used together with the Bernese

pole file. The radiation pressure coefficient file is only required for the estimation of satellite orbits and therefore will not be mentioned anymore. Table 5.8 illustrates the additional models which are used for the computation of a standard orbit in the GPS time frame.

Table 5.8: Defined models for the standard orbit generation

Description	Model
Planetary ephemeris file	DE200
Coefficients of Earth potential	JGM3.
Ocean tides file	OT_CSRC

ORBGEN additionally produces a summary file, which shows that the fit of the tabular orbit positions is of the order of 1cm or better if the described input files were used (Dach *et al.*, 2007).

5.2.2 Preprocessing

Prior to the parameter adjustment and estimation of station coordinates, the gathered raw data run through a set of preprocessing steps. Fragmentary observations have to be excluded, receiver clocks have to be synchronized and appropriate baselines have to be formed, which marks the beginning of the relative positioning process using double differences of carrier phase measurements. The nature of carrier phases then leads to the effort of the cycle slip detection and ambiguity resolution and ends in a residual screening in order to detect remaining outliers so that the cleaned observations can be used for a final parameter estimation. Figure 5.8 illustrates the required scripts, which fulfill these steps, and represents the applied preprocessing strategy. Again, green names represent Bernese-internal programs, whereas red names stand for scripts which are developed from the author.

5.2.2.1 Import and conversion of observation data

The import of the gathered RINEX files results in the generation of four binary observation files for each station (code header and measurement, carrier header and measurement). The responsible script RXOBV3 does not only convert the input observation files, but performs checks on the contained observation period and the RINEX header. Station observations which do not coincide with the receiver and antenna characteristics in the station information file AUS.STA or show a number of observed epochs smaller than 1440, which equates to half a day of successful measurements considering a 30 s sampling interval, and therefore may degrade the network solution will not be used for the later processing.

```
…
# Convert and synchronize observation data
# ---------------------------------------
211 RXOBV3AP UNSW_GEN          ANY      1 112
212 RXOBV3_P UNSW_GEN          ANY      1 211
221 CODSPPAP UNSW_GEN          ANY      1 212
222 CODSPP_P UNSW_GEN          ANY      1 221
223 CODXTR   UNSW_GEN          ANY      1 222
#
# Form baselines, preprocess and screen phase data, save cluster NEQ files
# -------------------------------------------------------------------------
301 SNGDIF   UNSW_GEN          ANY      1 223
311 MAUPRPAP UNSW_GEN          ANY      1 301
312 MAUPRP_P UNSW_GEN          ANY      1 311
313 MPRXTR   UNSW_GEN          ANY      1 312
314 BAD_OBS  UNSW_GEN          ANY      1 313
321 GPSEDTAP UNSW_GEN          ANY      1 314
322 GPSEDT_P UNSW_EDT          ANY      1 321
331 GPSCHK   UNSW_GEN          ANY      1 322
#
# Compute ambiguity-float network solution, resolve phase ambiguities
# --------------------------------------------------------------------
401 ADDNEQ2  UNSW_GEN          ANY      1 331
402 GPSXTR   UNSW_GEN          ANY      1 401
411 GPSQIFAP UNSW_QIF          ANY      1 402
412 GPSQIF_P UNSW_QIF          ANY      1 411
413 GPSXTR   UNSW_QIF          ANY      1 412
```

Figure 5.8: Preprocessing scripts of NSW.PCF

5.2.2.2 Synchronization of receiver clocks

The script CODSPP uses the least-squares adjustment method to compute the corrections for synchronizing the receiver clocks with respect to GPS time. For this synchronization the linear combination L_3 of the zero-difference code measurements is used for a single point positioning in order to estimate a priori corrections with sufficient accuracy of less than 1 µs. L_3 is used to eliminate the ionospheric refraction, where the troposphere model is set to Saastamoinen. Considering the possible radial velocity of a GNSS satellite with respect to a station on Earth, the error in the geometric distance between satellite and station would be smaller than 1 mm if the receiver clock error is less than 1 µs. By comparison to the a priori coordinates, outliers and bad observations are additionally marked in the observation files.

5.2.2.3 Formation of baselines

This section marks the step of using single-differences of carrier phase measurements for the phase residual screening in order to detect cycle slips and for the double difference processing. Single differences describe baselines between the stations and therefore build up the inner geometry of the network. The selection of baselines is carried out using a strategy called 'OBS-MAX', which screens all possible and linear independent baselines of the network and their corresponding number of observations. Only the baselines with the highest number of observations will then be used for the creation of single differences. An additional criteria limits the baselines to a maximum length of 2000 km, which avoids very long baselines and

thereby a decreasing correlation of the station-dependent errors. Further settings can be seen in Table 5.9.

Table 5.9: Options in the creation of new baselines, script SNGDIF

Description	Selection
General options:	
Measurement type	Phase
Processing strategy	OBS-MAX
Simultaneous observations:	
Tolerance	1 s
Setting up new ambiguities:	
After an observations gap larger than	20 min
Baseline selection:	
Maximum baseline length considered	2000 km

5.2.2.4 Cycle slip detection

As described in Section 2.3.2, carrier phase observations are defined as the difference between the transmitted carrier phase from the satellite and the replica signal from the receiver. By the nature of signal processing, this measurement leads to a value between 0 and 1 cycles, respectively 0 and $2\,\pi$. At the beginning of the observation, the receiver initializes an integer counter which will be incremented by 1 at each time the fractional phase jumps from $2\,\pi$ to 0. Hence, the accumulated phase is given by the sum of the currently measured fractional phase and the integer counter. This initial integer number of cycles between satellite and receiver will be introduced as an unknown parameter called (integer) ambiguity and stays the same as long as there is no gap in the transmitted signal during the observation. Figure 5.9 illustrates the occurrence of such a loss of lock, in which the observed fractional phase executes a jump and leads to a discontinuity in the accumulated phase by an integer number of cycles.

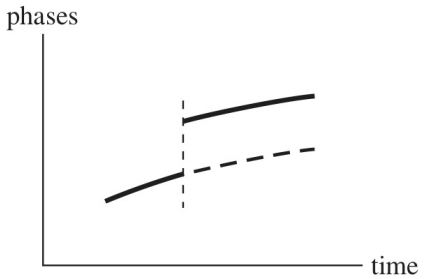

Figure 5.9: Event of a carrier phase cycle slip (Seeber, 2003)

This event of a cycle slip can be caused by several reasons (Dach *et al.*, 2007):

- shadowing effects of the transmitted signal due to vegetation, buildings, topography, etc.

- low signal-to-noise ratio

- dropout in the receiver software

- problems in the satellite's signal generator

The script MAUPRP fulfills a residual screening of the L_3 combination of the created single differences in order to detect these cycle slips and, if possible, to repair them. Table 5.10 specifies the settings of capital importance.

Table 5.10: General options of script MAUPRP for the cycle slip detection

Description	Selection
General setting:	
Screening mode, frequency to check	Combined (L_3)
Troposphere modeling:	
Zenith path delay and mapping function	NIELL
Mark observations:	
Below an elevation of	10 °
Minimum continuously observed time interval	301 s
Maximum gap within continuous observations	61 s
Epoch-different solution	
Frequency	L_3
Maximum value (observed-computed)	0.5 m
A priori baseline vector sigmas (X, Y and Z)	0.1 m
Cycle slip detection/correction:	
Minimum size of accepted cycle slip correction	10 cylces
Sigmas for L1 and L2 observations	0.002 m
Outlier rejection:	
Mark outliers up to a time interval of	181 s
Set up multiple ambiguities:	
If no cycle slip correction was possible	Yes
After an observation gap larger than	181 s

For the successful execution of this step, a priori station coordinates with an accuracy in dm-level and precise satellite orbits are essential. In detail, MAUPRP fulfills following tasks (Dach *et al.*, 2007):

- mark bad observations and exclude them from the processing if they show epochs of unpaired L1 and L2 measurements, small fragments of observations or satellite elevations lower than 10 °

- trace big outliers by executing a non-parametric screening

- calculate an epoch-different solution which serves as a reference for the cycle slip detection
- find the time intervals $[t_1, t_2]$ in all observations which were interrupted by cycle slips
- try to estimate the size of each cycle slip and correct all observations which are attached to the cycle slip event accordingly
- if a cycle slip can not be repaired, the subsequent observations will be marked as outliers respectively a new ambiguity parameter will be introduced

The following script MPRXTR creates a summary file and lists bad observation files, which contain hardly any carrier phase measurements. Script BAD_OBS deletes the corresponding zero and single difference files and repeats the last scripts beginning with the creation of baselines (SNGDIF), but without the bad observations.

5.2.2.5 Double difference phase residual screening

This task represents the first parameter estimation process and is used to clean the data from outliers and irrational observations respectively stations. It is split into four scripts which are responsible for the detection of outliers and one additional script which checks the screening results for defective stations.

1. GPSEST is one of the two main scripts for the parameter estimation and based on a least-squares adjustment. Residual files and cluster-wise normal equations will be created based on a double difference level, where all stations are loosely constrained on their a priori coordinates. Table 5.11 summarizes the general options which were set for this process[1]. It can be seen that the linear combination L_3 is used in order to eliminate the ionospheric propagation delays of the transmitted signals and that the NIELL mapping function models the dry component of the slant tropospheric path delay out of a Saastamoinen zenith path delay by the use of an elevation-dependent weighting of $1/cos^2(z)$. The remaining wet part will be estimated by the script with a sampling interval of 1 h.

2. RESRMS screens the previously produced post-fit residuals from script GPSEST and provides statistical information about the residuals in order to identify outliers. The resulting edit information file contains a list of observations which are considered as outliers. Criteria for the selection are given in Table 5.12.

3. SATMRK reads the measurements identified as outliers according to the edit information file and marks them in the Bernese observation files. The actual observations remain in the files, but the corresponding records are flagged as bad.

[1] More information to the specific options and models are given in Dach *et al.* (2007), page 141

Table 5.11: General options of script GPSEST in the first phase residual screening

Description	Selection
Observation selection:	
Satellite system	All (GPS and GLONASS)
Frequency	Linear combination L_3
Elevation cutoff angle	10 °
Tolerance for simultaneity	100 ms
Observation modeling:	
A priori sigma	1 mm
Elevation-dependent weighting	$cos^2(z)$
Type of computed residuals	Normalized
Correlation strategy	Baseline
A priori troposphere modeling:	
Zenith path delay and mapping function	DRY_NIELL
Handling of ambiguities	
Resolution strategy	None
Datum definition for stations coordinates	
Coordinate constrained	All
A priori sigma (N, E, U)	0.1 m
Estimation of tropospheric parameters	
Mapping function	WET_NIELL
Parameter spacing	1 h

Table 5.12: Criteria of outlier detection in script RESRMS

Description	Selection
General options:	
Frequency to check	L_3
Detect large residuals:	
Limit of phase measurement	0.0025 m
Detect bad data:	
Minimum continuously observed time interval	61 s
Detect ambiguities with few observations	YES
Minimum number of observations per ambiguity	3

4. GPSEST represents the same parameter estimation process as before with exactly the same options as in Table 5.11. In contrast to the first run, the marked observations are now excluded from the least-squares adjustment. Therefore, the resulting residual files and normal equations are cleaned from the detected outliers.

5. GPSCHK checks the cleaned residual files in order to detect bad stations based on their overall performance. Doubtful satellites or stations show large residuals respectively a high number of rejected data and will be listed in a deletion file. In that case, the corresponding observation files will be deleted and the previous scripts beginning with the creation of baselines (SNGDIF) will be repeated.

5.2.2.6 Ambiguity resolution

Generally, initial phase ambiguities are defined as integer numbers of full cycles, but in practice these ambiguities contain linear terms such as clock corrections and hardware delays which cannot be separated definitely and cause a real value character of the parameters. Therefore, the ambiguity resolution demands for processed double differences, where this linear effects are eliminated respectively reduced in such a way that the integer nature of the ambiguities can be reassumed. Two steps can be set up in order to resolve ambiguities:

1. Estimation of the initial phase ambiguity parameters as real values
2. Resolution of the ambiguities by adapting integers to the estimated real values

Bernese offers four different algorithms to solve these phase ambiguities: ROUND, SIGMA, SEARCH and QIF[1]. Basically the selection of the resolution strategy depends on three features, which can be seen in Table 5.13 together with the corresponding characteristic of the network NSW. Due to the long baselines in use, the Quasi Ionosphere-Free (QIF) strategy is appropriate for the processed network.

Table 5.13: Relevant features for the selection of the ambiguity resolution strategy and corresponding values of the processed network NSW

Description	Value
Number of observed carriers	2 (L1 & L2)
Maximum length of the baselines	2000 km
Session length	24 h

Based on the cluster-wise normal equations established by GPSEST, a network solution with real ambiguity values and tropospheric estimates will be calculated using ADDNEQ2,

[1]Details to these algorithms and their underlying approaches are given in Dach *et al.* (2007), page 172

which is the second major Bernese script for the parameter adjustment (next to GPSEST). This solution, which is called ambiguity-float solution, uses both signals L1 and L2 to create real valued estimates b_1 and b_2. Script GPSQIF will then perform the QIF algorithm and solve the single difference ambiguities for each baseline separately. Newly introduced input data sets are the tropospheric estimates from the previous float solution, ocean loading corrections and an ionospheric model, whereat the latter two were acquired from the Chalmers respectively AIUB data centres (Table 5.5).

The QIF strategy uses the linear combination L_3 to compute the corresponding ionosphere-free bias $\tilde{B}_3$ by taking the real values b_1 and b_2 into account, which can be written as

$$\tilde{B}_3 = \frac{c}{f_1^2 - f_2^2} \cdot (f_1 \cdot b_1 - f_2 \cdot b_2). \tag{5.1}$$

Dividing $\tilde{B}_3$ by the combined wavelength λ_3, the real valued L_3-bias $\tilde{b}_3$ can be expressed in narrow cycles

$$\tilde{b}_3 = \frac{\tilde{B}_3}{\lambda_3} = \tilde{B}_3 \cdot \frac{f_1 + f_2}{c} = \frac{f_1}{f_1 - f_2} \cdot b_1 - \frac{f_2}{f_1 - f_2} \cdot b_2. \tag{5.2}$$

By naming the correct integer ambiguities n_{1i} and n_{2j}, the corresponding L_3-bias can be written as

$$b_{3ij} = \frac{f_1}{f_1 - f_2} \cdot n_{1i} - \frac{f_2}{f_1 - f_2} \cdot n_{2j} \tag{5.3}$$

so that the difference between real valued and integer L_3-bias

$$d_{3ij} = |\tilde{b}_3 - b_{3ij}| \tag{5.4}$$

can be used as a criteria in order to find the pair of integer values n_{1i} and n_{2j} which results in the smallest deviation compared to the computed real valued L_3-bias (Dach *et al.*, 2007).

Due to the fact that the real valued ambiguity parameters are estimated separately for L1 and L2, the influence of the ionospheric refraction has to be considered in order to achieve sufficient estimates of b_1 and b_2. This is the reason why the deterministic model of the ionosphere provided by the AIUB has to be introduced. As a result of the separate processing of each baseline, the datum definition can simply be realized by fixing the coordinates of the first station of each baseline. Significant settings of the responsible script GPSQIF are given in Table 5.14. By applying this strategy, on average 90 % of the ambiguities are resolved to their integer values.

Table 5.14: Options of script GPSQIF for the ambiguity resolution

Description	Selection
Observation selection:	
Satellite system	GPS
Frequency	L1 & L2
Elevation cutoff angle	10 °
Tolerance for simultaneity	100 ms
Observation modeling:	
(same as in Table 5.11)	
A priori troposphere modeling:	
Zenith path delay and mapping function	DRY_NIELL
Handling of ambiguities	
Resolution strategy	QIF
Max. no. of ambiguities fixed per iteration step	5
Search Width for pairs of L1 and L2 ambiguities	0.5 WL cycles
Max. sigma of resolved NL ambiguities	0.03 cycles
Max. fractional part of resolved NL ambiguities	0.1 cycles
Datum definition for stations coordinates	
Coordinates fixed	first station

5.2.3 Final processing

The observations are cleaned and most of the ambiguities are resolved. This leads to the stage, where an ambiguity-fixed solution can be computed, which reduces the number of remaining, unknown parameters considerably. A final parameter estimation will compute daily tropospheric estimates and station coordinates, which will be verified by the means of a Helmert transformation and at the end will be combined into a weekly solution. The responsible scripts are shown in Figure 5.10 (same color denotation as in Figure 5.8).

The last four scripts do not belong to the actual process of parameter estimation, but are responsible for the generation of a protocol file containing the most important results (NSW_SUM), the storage of final output files to a specified directory (NSW_SAV) and the cleaning of data and output files from older sessions (NSW_DEL and BPE_CLN).

5.2.3.1 Ambiguity-fixed network solution

The integer ambiguities have been estimated and now have to be introduced as known parameters in a further parameter estimation GPSEST, which results in an ambiguity-fixed normal equation. Significant characteristics of this adjustment are the introduction of the estimated L1 and L2 integer ambiguities and the chosen correlation strategy called CORRECT. Due to the fact that this is a final analysis of the observation data, all correlations between the processed baselines should be taken into account. Therefore, this is the only script which does not model correlations within each baseline separately, but for each cluster, which is set to a

```
…
# Compute ambiguity-fixed network solution, create final NEQ/SNX/TRO files
# -------------------------------------------------------------------------
501 GPSESTAP UNSW_FIN          ANY      1 413
502 GPSEST_P UNSW_FIN          ANY      1 501
511 ADDNEQ2  UNSW_FIN          ANY      1 502
512 GPSXTR   UNSW_FIN          ANY      1 511
513 ADDNEQ2  UNSW_DAY          ANY      1 512
514 HELMR1   UNSW_FIN          ANY      1 513
521 ADDNEQ2  UNSW_RED          ANY      1 514
522 GPSXTR   UNSW_RED          ANY      1 521
#
# Create summary file, save results, and delete files
# ---------------------------------------------------
901 NSW_SUM  UNSW_GEN          ANY      1 522
902 NSW_SAV  UNSW_GEN          ANY      1 901
903 NSW_DEL  UNSW_GEN          ANY      1 902
904 BPE_CLN  UNSW_GEN          ANY      1 903
#
# End of BPE
# ----------
```

Figure 5.10: Final processing scripts of NSW.PCF

maximum number of 12 stations.

5.2.3.2 Computation of daily solutions

The ambiguity-fixed normal equations are then used for the determination of daily solutions by applying an appropriate datum definition approach to the processed network. Different approaches are executed (see Section 5.3), where the primary one is realized by a minimum constraint solution using three no-net-translation and no-net-rotation conditions imposed on the stations which are represented in the fiducial site file, as described in Section 5.2.1.3. Final products of this process are

- daily normal equations
- daily station coordinates
- daily zenith path delays with a sampling interval of 1 h

5.2.3.3 Verification through a Helmert transformation

Although the fiducial sites have been selected based on the residuals to their weekly IGS solution, script HELMR1 performs an additional verification of the fiducial sites. The estimated daily coordinates will be compared to the a priori station coordinates based on the means of a three parameter Helmert transformation. If discrepancies are larger than the set threshold in Table 5.15, the corresponding stations will be rejected from the fiducial site list and the daily solution will be recomputed.

Table 5.15: Verification of the daily estimation of fiducial site coordinates

Outlier criteria	Value
North	20 mm
East	20 mm
Up	40 mm

5.2.3.4 Computation of weekly solutions

Once the daily solutions are computed and verified, a final parameter estimation can be performed, which includes all normal equations of the current GPS week and consequently results in a weekly network solution. The strategy of the datum definition concurs with the final computation of daily solutions. Atmospheric parameters will be pre-eliminated so that only coordinate parameters remain. Final products of this process are

- weekly SINEX files
- weekly station coordinates
- weekly summary files, which contain single and total repeatability RMS values of the network

5.3 The definition of the geodetic datum

GNSS positioning mainly represents a differential method, as clock corrections and ambiguities have to be estimated efficiently by forming differences and linear combinations, before the measurements can be used for the computation of absolute positions. Although a priori coordinates of all stations are available, only a loose definition of the geodetic datum was applied in order to perform the estimation of unknown parameters (as can be seen in Table 5.11). After the removal of outliers and the estimation of clock corrections, cycle slips and integer ambiguities, the internal geometry of the processed network is very well determined so that it can be aligned to a defined reference frame using a specific datum definition approach (Dach *et al.*, 2007).

In a very small network of only a few stations this step can simply be made by fixing the network to the coordinates of (at minimum) one fiducial site. Regional and global networks demand certain constraints respectively conditions which define the geodetic datum. Bernese offers four strategies to define the datum[1]:

- Free network solution

[1]Details to these datum definition types are given in Dach *et al.* (2007), page 215

- Minimum constraint solution

- Constraining fiducial coordinates

- Fixing fiducial coordinates

Due to the fact that the results from a free network solution do not refer to a defined reference frame and the fixing of fiducial station coordinates leads to a distortion of the network solution if only one fiducial site shows inaccurate a priori coordinates, the following sections will focus on both the strategy of constraining fiducial coordinates and the minimum constraint solution, but especially on the latter strategy.

5.3.1 Minimum constraint solution

The aim of the minimum constraint solution is to use network conditions, so-called minimum constraint conditions, in order to define the geodetic datum without constraining or fixing individual station coordinates, but by constraining the terms of a seven parameter transformation. Therefore, two reference frames have to be introduced:

- one reference frame containing the a priori coordinates $\tilde{\mathbf{X}}_\mathbf{i}$ of the selected fiducial sites

- one reference frame containing the resulting coordinates $\mathbf{X_i}$ of the network solution

The corresponding transformation can then be written as

$$\begin{pmatrix} \tilde{X}_i \\ \tilde{Y}_i \\ \tilde{Z}_i \end{pmatrix} = \begin{pmatrix} \Delta X \\ \Delta Y \\ \Delta Z \end{pmatrix} + (1+\mu) \begin{pmatrix} 1 & \gamma & -\beta \\ -\gamma & 1 & \alpha \\ \beta & -\alpha & 1 \end{pmatrix} \begin{pmatrix} X_i \\ Y_i \\ Z_i \end{pmatrix} \tag{5.5}$$

or in the linearized form, assuming that there are only small rotations involved,

$$\begin{pmatrix} \tilde{X}_i \\ \tilde{Y}_i \\ \tilde{Z}_i \end{pmatrix} = \begin{pmatrix} X_i \\ Y_i \\ Z_i \end{pmatrix} + \begin{pmatrix} 1 & 0 & 0 & 0 & -Z_i & Y_i & X_i \\ 0 & 1 & 0 & Z_i & 0 & -X_i & Y_i \\ 0 & 0 & 1 & -Y_i & X_i & 0 & Z_i \end{pmatrix} \begin{pmatrix} \Delta X \\ \Delta Y \\ \Delta Z \\ \alpha \\ \beta \\ \gamma \\ \mu \end{pmatrix}. \tag{5.6}$$

The minimum constraint conditions can set certain transformation parameters to zero and thereby allow the avoidance of translations, rotations or scales of the network in order to perform a best-fit transformation using a minimum number of constraints. The corresponding conditions are split in three terms:

- no-net-translation (NNT): parameters ΔX, ΔY and ΔZ are set to zero

- no-net-rotation (NNR): parameters α, β and γ are set to zero

- no-net-scale (NNS): parameter μ is set to zero

In fact, the realization of the constraints is carried out by a very small internally defined a priori sigma of the specific parameters and therefore leads to a strong weight, as can be seen in Table 5.16.

Table 5.16: A priori sigma of the specific minimum constraint conditions

Description	Sigma
Translation	0.000 01 m
Rotation	0.000 10 rad
Scale	0.001 00 ppm

Based on the solution type, different conditions should be set for the definition of the datum. If e.g. precise orbits are applied on a global network, the processed network solution should show a very accurate orientation and therefore do not need to be rotated, otherwise the transformation would eventually decrease the quality of the resulting coordinates. According to Dach *et al.* (2007), it can be proved that usually the barycentre of the computed network solution coincides with the barycentre of the a priori fiducial site coordinates, which supports the no-net-translation condition.

This leads to the conclusion that a minimum constraint solution using a NNT and NNR condition would serve as a good strategy for the geodetic datum definition and therefore yields to the possibly most accurate station coordinates (Table 5.17).

Table 5.17: Primary approach for the definition of the geodetic datum

Description	Setting
NNT & NNR approach:	
Datum definition type	Minimum constraint solution
Minimum constraint conditions	NNT and NNR
Source of involved reference stations	Fiducial site file

The resulting weekly coordinates of this approach will be used for the velocity estimation and finally will be compared to existing IGS08/ITRF2008 and NNR-NUVEL-1A solutions according to repeatability and accuracy. For an additional verification and comparison, three other approaches are applied, as defined in Table 5.18.

Table 5.18: Secondary approaches for the definition of the geodetic datum

Description	Setting
NNT approach:	
Datum definition type	Minimum constraint solution
Minimum constraint conditions	only NNT
Source of involved reference stations	Fiducial site file
NNR approach:	
Datum definition type	Minimum constraint solution
Minimum constraint conditions	only NNR
Source of involved reference stations	Fiducial site file
No conditions approach:	
Datum definition type	Minimum constraint solution
Minimum constraint conditions	-
Source of involved reference stations	Fiducial site file

5.3.2 Constraining of fiducial coordinates

Another approach is to constrain specific fiducial sites by introducing coordinate sigmas. The selection of fiducial files can e.g. be done by flags, manually or with a file, which contains the fiducial sites and their corresponding sigmas in the North, East and Up components. Due to the fact that during the preparation work in Section 5.2.1.3 residuals between the a priori coordinates and the weekly IGS solution were computed and stored in the form of a weekly residual file (Figure 5.7), this data set can be used in order to define sigmas of constraining for the individual fiducial sites. This strategy is named the tertiary approach (Table 5.19).

Table 5.19: Tertiary approach for the definition of the geodetic datum

Description	Setting
Coordinate constraints approach:	
Datum definition type	Coordinates constrained
Source of reference stations and sigmas	Fiducial residual file

The results in terms of coordinate solutions of all approaches are described in Section 6.1.

5.4 Velocity estimation

The computation of station velocities in X, Y and Z is carried out by the use of a regression line which will be constructed based on the determined weekly coordinates of the given time span[1]. The slope of the regression line of each station can then be used for the computation

[1]The calculation was performed by means of The MathWorks™ MATLAB® 2009

of the velocity in units of mm/year. If the station movement does not show a regular trend, but performs conspicuous jumps due to outstanding events such as earthquakes or equipment changes, then the superposed regression line does not represent the actual station movement any more. An example is given in Figure 5.11, where the Z component of station MQZG illustrates the event of several earthquakes and the resulting improper regression line.

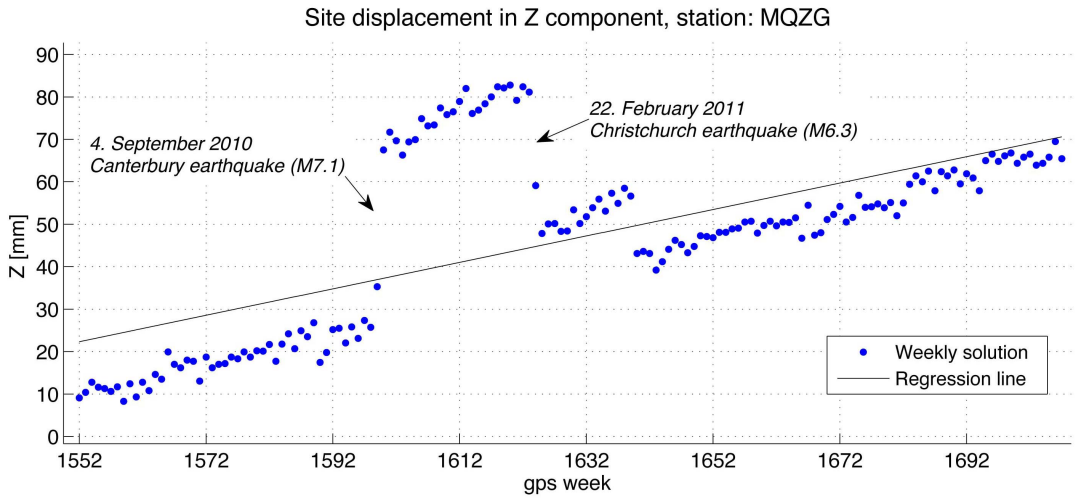

Figure 5.11: Wrongly computed regression line of station MQZG (Christchurch, New Zealand)

Therefore, the weekly solutions will be screened for three-dimensional coordinate jumps bigger than a defined limit of 15 mm. The corresponding time information will then be used in order to split the regression line into separate parts. In fact, MQZG is the only station in network NSW which causes such significant jumps. The resulting individual regression lines are shown in Figure 5.12.

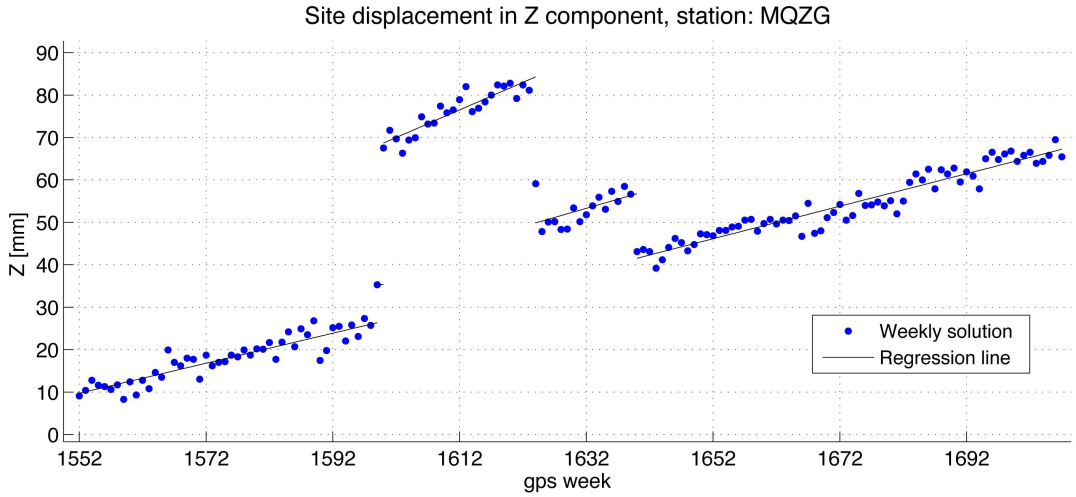

Figure 5.12: Regression line of station MQZG is split into separate parts

Assuming that the station does not change its direction of movement after such jumps considerably, which can be proved in the nearly parallel regression lines in Figure 5.12, the individual regression lines can be used in order to eliminate the jumps and to raise the separate coordinate trends to the same level so that a final regression line can be calculated on the basis of the corrected relative coordinates (Figure 5.13).

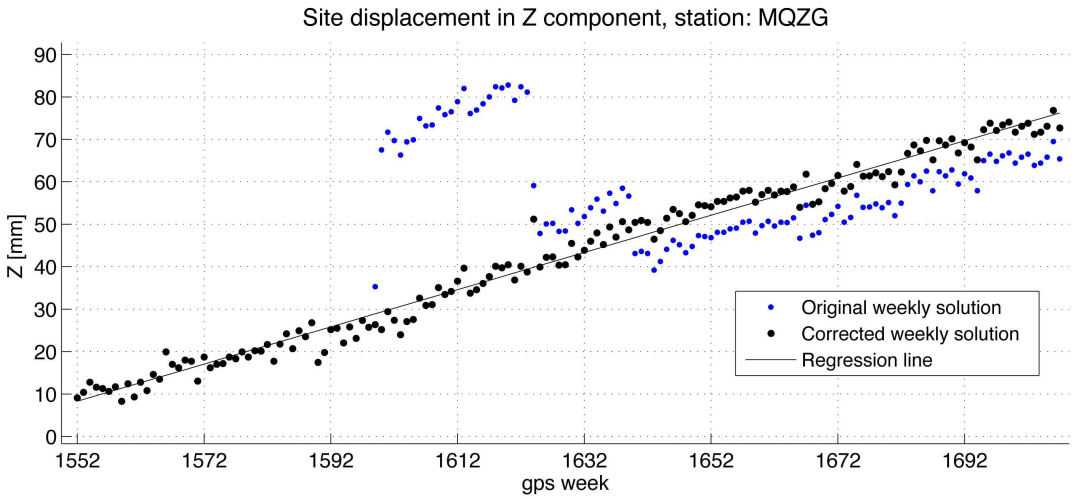

Figure 5.13: New regression line based on the leveling of the coordinate trends

If a station does not perform any jumps, then the regression line will be applied on the coordinates from the original weekly solution. The resulting station velocities in *X*, *Y* and *Z* will be stored in a text file, as shown for station AUCK (Auckland, New Zealand), CEDU (Ceduna, Australia) and MQZG (Christchurch, New Zealand) in Figure 5.14.

```
FINAL STATION VELOCITIES                                          13-NOV-12
-------------------------------------------------------------------------
LOCAL GEODETIC DATUM: IGS08              EPOCHS: 10/2009 - 09/2012

NUM  STATION NAME          X (MM/YR)     Y (MM/YR)     Z (MM/YR)     FLAG

  1  AUCK 50209M001          -21.2          -1.7          32.8        IGS08
  2  CEDU 50138M001          -42.0           2.1          49.9        IGS08
  3  MQZG 50214M001           -7.1          42.9          22.7        IGS08


Meaning of flags:
-----------------
IGS08 : IGS Station
```

Figure 5.14: Example of a resulting velocity file of three stations

A detailed description of the resulting velocities of the whole network is given in Section 6.2. The velocity solution of the first approach is shown in Appendix A and represents all stations of the processed network, whereas Appendix B and C represent a comparison of the secondary and tertiary approaches with respect to the IGS08/ITRF2008 velocities respectively

the NUVEL plate motion model.

The standard deviation of the estimated velocity can be computed by the use of σ_x of the linear regression, which is given by

$$\sigma_{\mathbf{x}} = \sqrt{\frac{1}{n}\sum(\mathbf{X}_{\mathbf{observed}} - \mathbf{X}_{\mathbf{regression}})^2}, \tag{5.7}$$

where $\mathbf{X}_{\mathbf{observed}}$ represents the processed weekly coordinates, $\mathbf{X}_{\mathbf{regression}}$ contains the corresponding coordinates of the regression line and n is the number of weekly solutions. Following the law or error propagation, the resulting standard deviation of the velocity is then described as

$$\sigma_{\mathbf{v}} = \frac{1}{t}\sigma_{\mathbf{x}}, \tag{5.8}$$

where t is the observed time span in terms of years. The output file, which represents the achieved standard deviation of the station velocities in $\mathrm{mm\,yr^{-1}}$, is illustrated in Figure 5.15.

```
STANDARD DEVIATION OF FINAL STATION VELOCITIES                  13-NOV-12
-------------------------------------------------------------------------
LOCAL GEODETIC DATUM: IGS08             EPOCHS: 10/2009 - 09/2012

NUM  STATION NAME          X (MM/YR)     Y (MM/YR)     Z (MM/YR)     FLAG

  1  AUCK 50209M001          0.84          0.65          0.70        IGS08
  2  CEDU 50138M001          0.63          0.74          0.74        IGS08
  3  MQZG 50214M001          1.09          0.61          0.88        IGS08


Meaning of flags:
-----------------
IGS08 : IGS Station
```

Figure 5.15: Corresponding standard deviations of the estimated velocities

In order to visualize the station velocity in a map projection, the cartesian coordinate components of the computed regression have to be transformed to longitude and latitude values λ and ϕ prior to the velocity estimation by using equation

$$\lambda = \arctan\frac{Y}{X} \cdot \frac{180^\circ}{\pi} \tag{5.9}$$

and

$$\phi = \arctan\frac{Z}{\sqrt{X^2+Y^2}\cdot(1-e^2)} \cdot \frac{180^\circ}{\pi}, \tag{5.10}$$

together with an eccentricity parameter $e = 0.081\,819\,190\,842\,621$, taken from the WGS 84 ellipsoid.

Chapter 6

Results

Based on the processed weekly solutions of the different approaches, a closer look at the analysis and evaluation of the obtained results can now be taken. The main focus lies on the separate assessment of coordinate and velocity solutions, the achieved tropospheric parameters and a final conclusion of both gained findings and occurrent problems.

As the NNT & NNR approach is the primary approach, it contains the largest number of processed sessions and represents a computed period of about three years. Due to the long processing effort and calculation time, the secondary and tertiary approach are limited to a observation period of about nine months, which is assumed to be sufficient in order to get an insight into the resulting coordinate solutions and to compare it to the primary approach. The processed time span of all approaches is given in Table 6.1.

Table 6.1: Observed time span of each processing approach

Description	Period in [months]	Start date	End date
Primary approach:			
NNT & NNR	36	October 4th, 2009	September 29th, 2012
Secondary approaches:			
NNT			
NNR			
No conditions	9	January 1st, 2012	September 29th, 2012
Tertiary approaches:			
Coordinate constraints	9	January 1st, 2012	September 29th, 2012

6.1 Coordinate solutions

This section distinguishes between the achieved weekly repeatability of the whole network and the impact of the different datum definition approaches with respect to the final position

of the used fiducial sites.

The weekly repeatability is defined as the precision of the resulting weekly solution if this multi-session result is computed by the combination of several daily solutions. It acts on the assumption that each daily solution was obtained through the same measurement and processing method and the same underlying conditions. The achieved repeatability is therefore a result of the combination of at maximum seven daily solutions from the same GPS week and can be described as single repeatability for each station and total repeatability, which summarizes the single repeatabilities of the whole network for one week.

While the repeatability describes the precision of the weekly solution, the actual resulting station coordinates and their biases to their "true" position have to be considered with respect to translations and rotations, assuming that the global weekly IGS solution represents the most accurate estimation of station coordinates and therefore acts as reference.

6.1.1 Repeatability

In order to establish a legitimate comparison of the separate datum definition approaches, Table 6.2 represents the mean total repeatabilities of the shared time span of available solutions, which is given by a period of nine months from January 1st, 2012 to the September 29th, 2012.

Table 6.2: Mean value and standard deviation of the total repeatability over nine 9 months

Description	Mean repeatability ± std. dev., in [mm]		
	N	*E*	*U*
Primary approach:			
NNT & NNR	1.3 ± 0.19	1.2 ± 0.23	4.1 ± 0.78
Secondary approaches:			
NNT	1.2 ± 0.18	1.2 ± 0.21	4.2 ± 1.08
NNR	1.3 ± 0.19	1.2 ± 0.26	4.1 ± 0.80
No conditions	1.2 ± 0.17	1.2 ± 0.25	4.2 ± 0.93
Tertiary approaches:			
Coordinate constraints	1.2 ± 0.17	1.2 ± 0.21	3.9 ± 0.75

All approaches result in approximately the same range of total repeatabilities, where the solutions in North and East of nearly 1 mm stick out appreciably, compared to the Up component of around 4 mm. This is mainly caused by the general aspect that several parameters, such as the strategy of ambiguity resolution, the limiting elevation angles, the satellite constellation, the correlation with tropospheric parameters and the geometry of the station network directly affect the height solution.

By taking a closer look on the three year time series of the primary approach in Figure 6.1, certain peaks in the total repeatability do not describe the overall quality of the network, but can be linked to the performance of only one single station, such as station MQZG

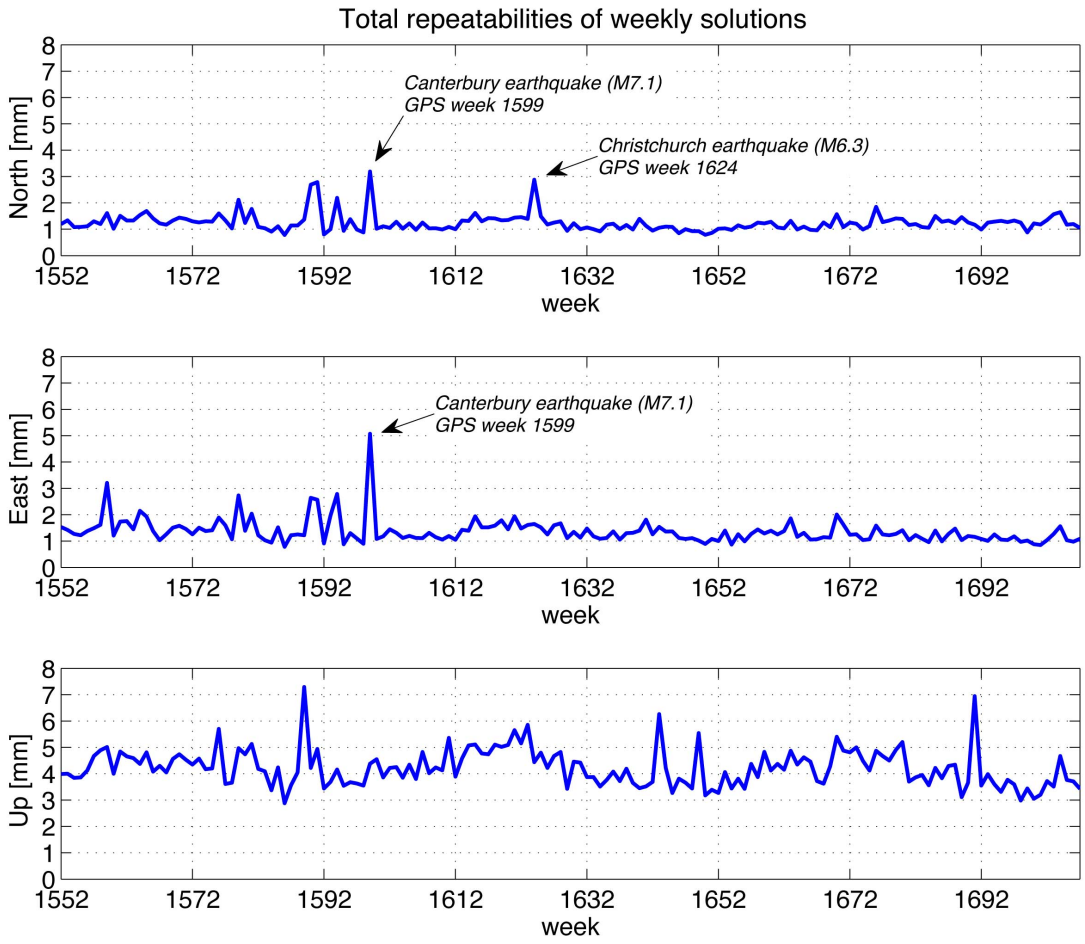

Figure 6.1: Total repeatability of the primary approach, based on three years of data sets

(Christchurch, New Zealand). As mentioned earlier, two earthquakes caused coordinate jumps of that station and therefore big single repeatabilities in the corresponding weeks, which also affected the resulting total repeatability.

Table 6.3 illustrates the single repeatabilities of a few stations in the two respective weeks, where it can be seen that only station MQZG is out of scale and hence caused the rise in the total repeatability, whereat the other stations remained as good as in the trend shown in Table 6.2.

6.1.2 Impacts of constraining

While the repeatability does not indicate disadvantages of the secondary and tertiary approaches, the final coordinate solutions reveal a big impact on the translation and rotation of station coordinates based on the selected definition of the geodetic datum. Considering the weekly IGS solution as a highly accurate adjustment of all globally distributed IGS reference sites (see Section 3.2.2), this weekly data set, which was already used for the selection of fidu-

Table 6.3: Single repeatability of station MQZG in the event of two earthquakes, compared to two other untroubled stations, primary approach

GPS week	Station name		Nearby event	Single repeatability, in [mm]		
				N	*E*	*U*
1599	AUCK	50209M001	-	0.6	1.1	4.2
	CEDU	50138M001	-	0.8	0.2	3.2
	MQZG	50214M001	Earthquake	25.4	42.1	12.2
1624	AUCK	50209M001	-	1.5	0.8	3.4
	CEDU	50138M001	-	0.8	0.7	2.6
	MQZG	50214M001	Earthquake	22.2	7.6	3.8

cial sites (see Section 5.2.1.3), will act as a reference in order to demonstrate the coordinate differences to the network solution.

6.1.2.1 Primary approach

The primary approach uses the NNT and NNR conditions to only allow a scale of the processed station network in order to fit into the a priori fiducial site coordinates. Therefore, the comparison of this approach to the weekly IGS solution shows the smallest coordinate difference in all axis for the overall network. Station AUCK (Auckland, New Zealand) is a good representative station of the network and is used for the illustration of the relative site displacement of both the given IGS solution and the computed weekly coordinates (Figure 6.2), where the reference coordinates are described by the IGS solution of the first epoch (GPS week 1552).

The processed network contains a number of 15 IGS and two ITRF stations (blue triangles in Figure 4.3) which are also included in the weekly IGS solutions and therefore can be compared to each other. By calculating the residuals of every one of these sites in X, Y and Z and combining them to mean residuals along the observed time span, it can be shown that these stations vary in a range of up to 10 mm from the given IGS coordinates (Figure 6.3).

The abrupt decrease of the mean residual in Z direction at GPS week 1632 (corresponding to April 17th, 2011) in Figure 6.3 can most probably be explained by the fact that in the IGS solution, 12 out of 17 analyzed stations perform a coordinate jump of more than 10 mm at this time. This shift of the IGS solution is also visible in the Z component of station AUCK in Figure 6.2. The cause for this discontinuity can be found in the switch from the reference frame IGS05 to the latest realization IGS08 and the use of an updated set of satellite and ground antenna calibrations (igs08.atx) which became effective on April 17th, 2011. Prior to that time, the IGS used IGS05 and igs05.atx in order to process their global network, whereas the entire computation of network NSW is based on the current reference frame IGS08 and

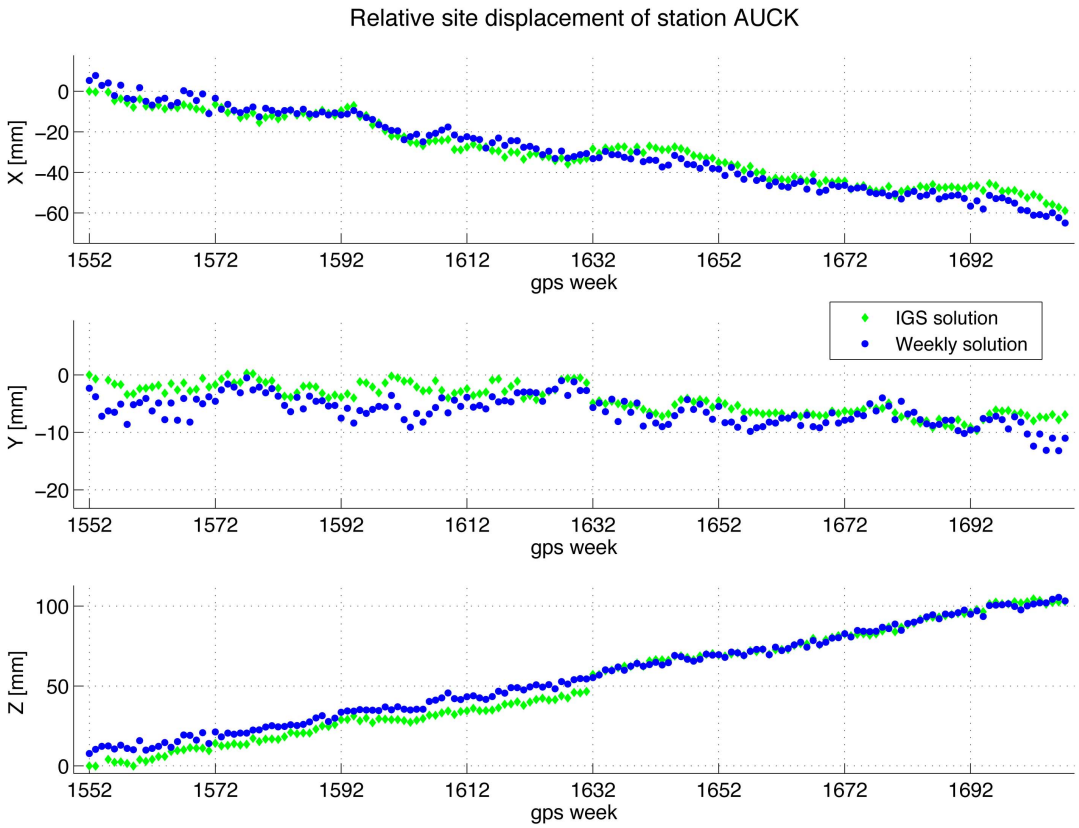

Figure 6.2: Relative components of the final weekly coordinates of the primary approach (blue) and IGS solution (green) with respect to the first weekly IGS solution of GPS week 1552, based on data sets of three years

antenna calibration file igs08.atx. Due to this alignment of the underlying framework of both solutions beginning with GPS week 1632, it is coherent that the later residuals show smaller values, especially in the Z component.

6.1.2.2 Secondary and tertiary approaches

Regarding the secondary and tertiary approaches of the datum definition, the same analysis of the mean IGS residuals can be performed as already described above. Figure 6.4 faces the two secondary approaches of a separate NNT and NNR condition and the tertiary approach of constraining fiducial site coordinates by using certain station sigmas. The same notation is used as in Figure 6.3, where the dark lines represent the mean value of the residuals and the lighter bands stand for the corresponding standard deviation.

The "NNT" approach shows very low residuals close to zero, similar to the primary approach which applied a combination of a NNT and NNR condition. In fact, there is a high correlation between these two strategies of defining the datum as given in Table 6.4, considering the shared time span of processing. Hence, it can be assumed that though the "NNT"

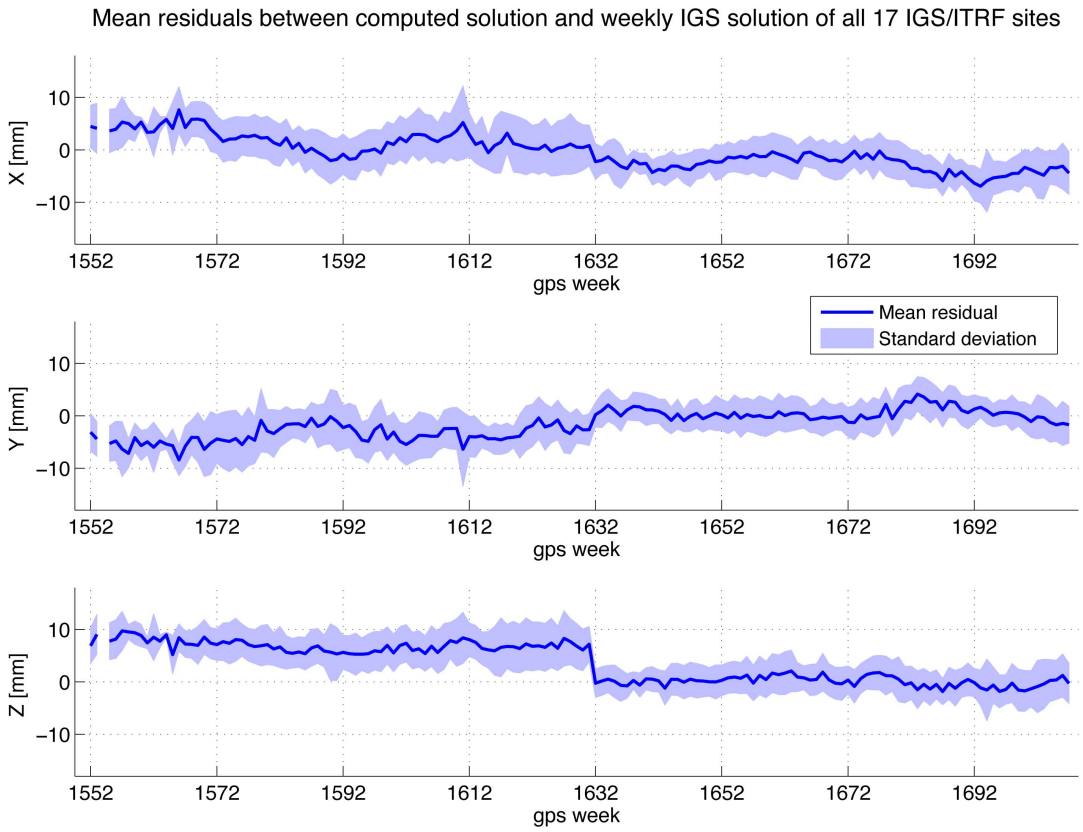

Figure 6.3: Mean residuals and standard deviations between computed coordinates of the primary approach and given IGS solution ($\mathbf{x}_{Calc} - \mathbf{x}_{IGS}$), based on data sets of three years. Note the impact of the switch to IGS08 and igs08.atx in the IGS solution at GPS week 1632

approach is allowed to perform a rotation of the network, the resulting estimates of the rotation parameters are very close to zero and therefore do not disturb the network solution significantly.

Table 6.4: Correlation coefficient between primary approach "NNT & NNR" and secondary approach "NNT", based on data sets of nine months

Approaches	Correlation coefficients		
	X	Y	Z
Primary vs. secondary ("NNT")	0.98	0.93	0.90

Another interesting aspect is the result of the two remaining secondary approaches which use a no-net-rotation condition respectively no minimum constraint conditions at all. Both strategies show the highest IGS residuals in a range of up to 40 - 60 mm. The "No conditions" approach is not plotted in Figure 6.4, because it overlaps with the "NNR" approach almost completely. The resulting correlation coefficients, given in Table 6.5, coincide with the assumption

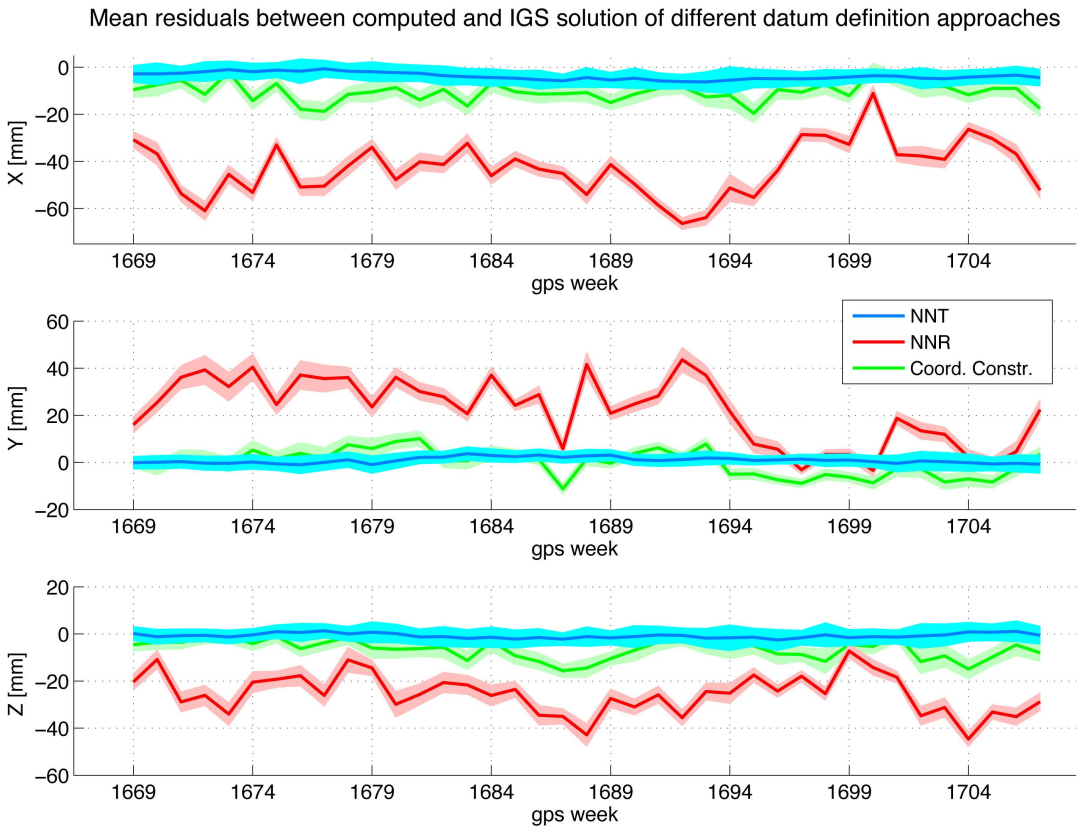

Figure 6.4: Comparison of "NNT" , "NNR" and "Coordinate constraints" approach with respect to the mean residuals between computed coordinates and IGS solution ($\mathbf{x}_{Calc} - \mathbf{x}_{IGS}$), based on data sets of nine months

that the exclusion of the no-net-rotation condition does not lead to essential distortions of the station network and therefore results in similar IGS residuals as if a no-net-rotation condition was used.

Table 6.5: Correlation coefficient between secondary approaches "NNR" and "No conditions", based on data sets of nine months

Approaches	Correlation coefficients		
	X	Y	Z
"NNR" vs. "No conditions"	0.99	0.99	0.98

The "Coordinate constraints" approach shows better results than the "NNR" and "No conditions" solutions, but still underlies undesirable coordinate shifts within a range of approximately 10 - 20 mm. A summarized conclusion representing one mean value and standard deviation of each approach for the shared time span is provided in Table 6.6.

Table 6.6: Mean value and standard deviation of the IGS residuals ($\mathbf{x}_{Calc} - \mathbf{x}_{IGS}$) for the whole time series of nine months

Description	Mean residual ± std. dev., in [mm]		
	X	Y	Z
Primary approach:			
NNT & NNR	-4.0 ± 1.62	0.8 ± 1.52	-0.5 ± 0.95
Secondary approaches:			
NNT	-3.8 ± 1.51	0.9 ± 1.27	-0.8 ± 1.01
NNR	-42.9 ± 11.45	22.1 ± 13.96	-25.4 ± 8.49
No conditions	-42.8 ± 11.27	21.2 ± 14.34	-27.5 ± 9.35
Tertiary approaches:			
Coord. constraints	-10.6 ± 4.07	-0.2 ± 5.52	-6.6 ± 4.02

6.2 Velocity solutions

This section leads to the main purpose of this thesis, namely the evaluation of station velocities from a regional network. The findings of the previous Section 6.1 suggest that only two approaches result in highly accurate coordinate solutions regarding repeatabilities and residuals to existing IGS solutions. Although the repeatability of all approaches is satisfying, the mean IGS residuals and standard deviations of the "NNR", "No conditions" and "Coordinate constraints" approaches show a high uncertainty of the final station coordinates, which can be seen in Table 6.6 and Figure 6.4, and are therefore insufficient for the estimation of velocities, which will be verified in the following section.

The two remaining, successful approaches were both realized through a minimum constraint solution using

- a no-net-translation and no-net-rotation condition (primary approach "NNT & NNR")
- a no-net-translation condition only (secondary approach "NNT"),

where the primary approach represents the most promising strategy for the velocity estimation and analysis.

6.2.1 Velocity field of the primary approach

Due to the fact that both mentioned successful solutions show approximately the same quality, the focus now lies on the primary datum definition approach, which contains a much longer observation period of three years. By considering the three year time series of weekly coordinates, the station velocities of the whole network can be calculated based on the strategy described in Section 5.4. The obtained polar components of each velocity vector can be used to project the network velocities onto a regional map by scaling the velocities appropriately (Figure 6.5).

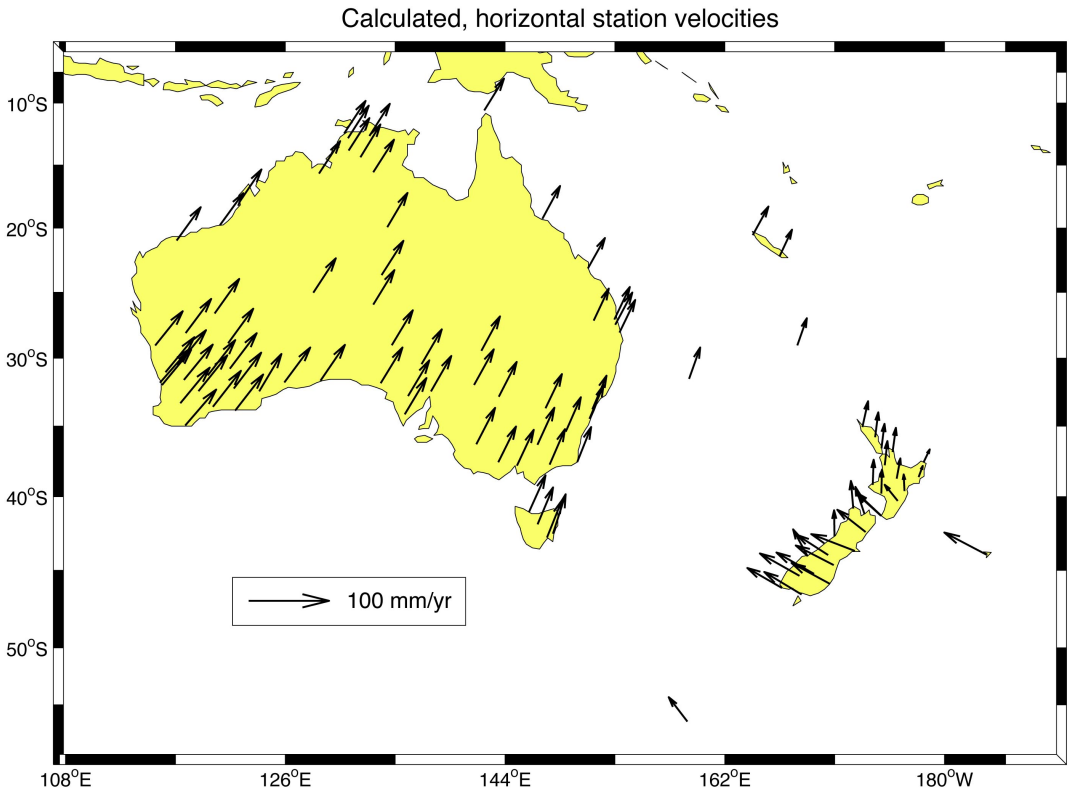

Figure 6.5: Horizontal components of the final velocity solution of network NSW containing 97 stations, primary approach based on data sets of three years

The plot shows a quite concurring velocity of all stations on the Australian continent, where the general movement of the corresponding Australian plate can be described in form of mean velocities in X, Y and Z components of the IGS08 reference frame (Table 6.7) or in form of an absolute value and azimuth of the mean velocity vector as given in Table 6.8.

Table 6.7: Movement of the Australian plate in X, Y and Z component, calculated by the use of 21 station velocities, primary approach based on data sets of three years

Description	Mean velocity ± std. dev., in $[\mathrm{mm\,yr^{-1}}]$		
	X	Y	Z
Australian continent	-42.2 ± 6.08	1.7 ± 8.67	50.7 ± 3.16

The calculation is based on the velocity vectors of 21 stations which are located on the mainland of Australia and show the longest available observation period of three years. The standard deviations of the resulting velocity and azimuth values indicate that there may also be a slight rotation involved.

Table 6.8: Movement of the Australian plate, calculated by the use of 21 station velocities, primary approach based on data sets of three years

Description	Mean value ± std. dev.
Absolute velocity	66.8 ± 3.42 mm yr^{-1}
Azimuth	33.0 ± 5.03 °
Approx. compass direction	NNE - NE

The station movement in the region of New Zealand shows a more complicated characteristic due to the near course of the plate boundary between the Pacific and Australian plate. A closer look at these velocities will be given in Section 6.2.4.

By combining the standard deviations of the velocity estimates of the 97 stations, the resulting mean standard deviation suggests an accuracy of the whole network at the 1 mm yr^{-1} level. The achieved standard deviations in the X, Y and Z components are provided in Table 6.9.

Table 6.9: Mean standard deviation of the final velocity solution of network NSW, primary approach based on data sets of three years

Description	Mean standard deviation, in [mm yr^{-1}]		
	X	Y	Z
Primary approach:			
NNT & NNR	1.06	1.04	0.97

A detailed description of the resulting velocity and standard deviation of each station is provided in the tables of Appendix A.

6.2.2 Comparison to the IGS08/ITRF2008 velocities

Similar to Section 6.1.2, where the station coordinates were compared to the weekly IGS solution, a comparison of the computed velocities of the 17 IGS/ITRF stations in contrast to the given IGS08 respectively ITRF2008 velocities can now be examined. It should be mentioned that stations WGTN and WGTT represent nearby ITRF stations and therefore will be compared with their corresponding ITRF2008 velocity. Regarding to the primary approach, Figure 6.6 visualizes the magnitude of the velocity difference for each single IGS/ITRF station using bars in the X, Y and Z components.

It becomes conspicuous that the velocity differences of station MQZG show high values compared to the other stations, which may be caused by the special alignment of the station's regression line, as described in Section 5.4. The mean velocity difference of all IGS/ITRF stations ranges at about 1 - 2 mm yr^{-1} per component for the primary approach (Table 6.10).

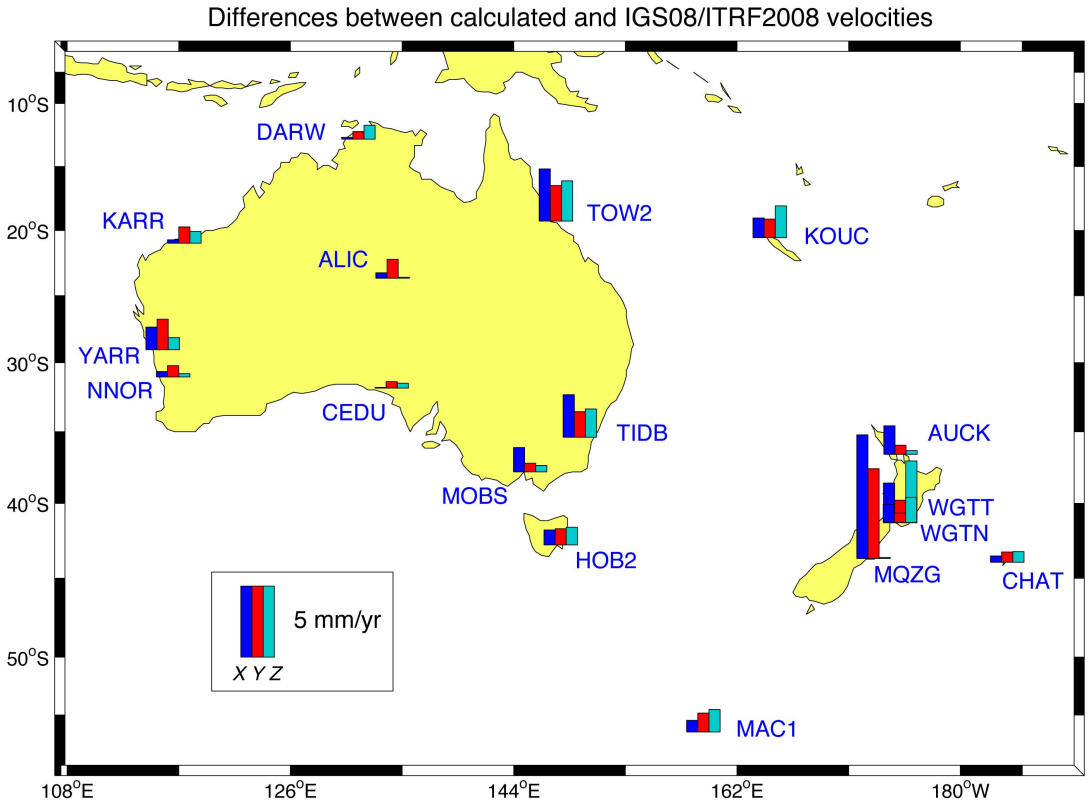

Figure 6.6: Absolute velocity differences of the IGS/ITRF stations with respect to the IGS08/ITRF2008 velocities, primary approach based on data sets of three years

Table 6.10: Mean velocity difference and standard deviation with respect to the IGS08/ITRF2008 velocities ($\mathbf{v}_{Calc} - \mathbf{v}_{IGS08/ITRF2008}$) representing an overview of all IGS/ITRF stations, primary approach based on data sets of three years

Description	Mean velocity difference ± std. dev., in [mm yr^{-1}]		
	X	Y	Z
Primary approach:			
NNT & NNR	1.7 ± 2.51	-0.1 ± 2.27	0.7 ± 1.77

By taking the other datum definition approaches into account, it can be seen that these strategies, with exception of the secondary approach "NNT", show much higher discrepancies compared to the IGS08/ITRF2008 velocity sets. Table 6.11 reflects the results of the secondary and tertiary approaches, which lead to velocity differences at the cm level for the remaining "NNR", "No conditions" and "Coordinate constraints" approaches using an observation period of nine months.

Figures of the station-specific velocity differences of the secondary and tertiary approaches

Table 6.11: Mean velocity difference and standard deviation with respect to the IGS08/ITRF2008 velocities ($\mathbf{v}_{Calc} - \mathbf{v}_{IGS08/ITRF2008}$) representing an overview of all IGS/ITRF station, secondary and tertiary approaches based on data sets of nine months

Description	Mean velocity difference ± std. dev., in [mm yr^{-1}]		
	X	Y	Z
Secondary approaches:			
NNT	2.1 ± 4.92	0.4 ± 9.48	0.3 ± 6.30
NNR	16.2 ± 12.10	-32.9 ± 35.56	-9.7 ± 5.85
No conditions	18.1 ± 14.65	-35.3 ± 24.45	-6.8 ± 7.96
Tertiary approaches:			
Coord. constraints	3.8 ± 13.91	-9.8 ± 19.17	-5.9 ± 5.64

can be seen in Appendix B.

6.2.3 Comparison to the NNR-NUVEL-1A plate motion model

In contrast to the prior comparison, ground velocities which are based on the NNR-NUVEL-1A plate motion model can be computed for any location on Earth and therefore for the whole network of 97 stations. The individual velocities can be acquired through several plate motion calculators, e.g. by an online program operated by the University Navstar Consortium[1] (UNAVCO, 2012). Again, the main focus is on the primary approach and leads to an illustration of the corresponding velocity differences of all IGS/ITRF sites in Figure 6.7. In order to keep track of the plot, the velocities of the remaining APREF sites are not visualized in the figure, whereat the following calculations include all 97 stations of the network.

It can be seen that the velocity differences on the Australian continent show similar dimensions as in the confrontation with IGS08/ITRF2008 velocities, including Tasmania and New Caledonia. In the region of New Zealand, especially along the plate boundary, the discrepancies are many times higher. A closer look at the disparities in New Zealand will be given in the next Section 6.2.4. The statistic of the mean differences is therefore split up into two groups representing Australia (including New Caledonia) and New Zealand. Table 6.12 describes the mean velocity values of both groups for the primary approach.

Whereas the secondary approach "NNT" shows a kindred increase of the velocity difference in the New Zealand region and represents the second-best results, the remaining approaches do not exhibit a geographical distribution of velocity discrepancies and therefore will not be split into regional groups as seen in Table 6.13.

An illustration of the station-specific velocity differences of the secondary and tertiary approaches is given in Appendix C.

[1] http://www.unavco.org/

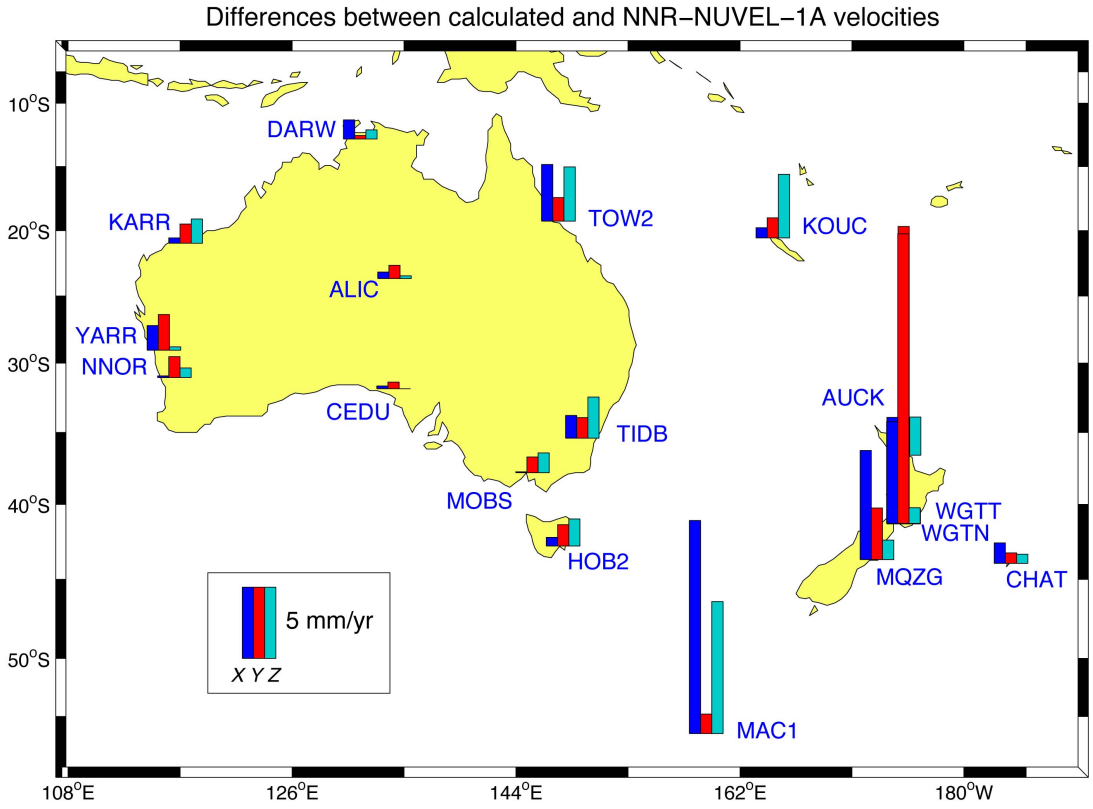

Figure 6.7: Absolute velocity differences of the IGS/ITRF stations with respect to the NNR-NUVEL-1A plate motion model, primary approach based on data sets of three years

Table 6.12: Mean velocity difference and standard deviation with respect to the NNR-NUVEL-1A plate motion model ($\mathbf{v}_{Calc} - \mathbf{v}_{NUVEL}$) representing an overview of the Australian (including New Caledonian) and New Zealand stations, primary approach based on data sets of three years

Primary approach: NNT & NNR	No. of sites	Mean velocity difference ± std. dev., in $[\mathrm{mm\,yr^{-1}}]$		
		X	Y	Z
Australia	68	1.1 ± 1.95	-1.4 ± 1.59	1.1 ± 2.33
New Zealand	29	2.7 ± 5.14	2.3 ± 7.56	0.0 ± 4.75

Table 6.13: Mean velocity difference and standard deviation with respect to the NNR-NUVEL-1A plate motion model ($\mathbf{v}_{Calc} - \mathbf{v}_{NUVEL}$), secondary and tertiary approach based on data sets of three months

Secondary and tertiary approaches	Mean velocity difference ± std. dev., in [mm yr^{-1}]		
	X	Y	Z
NNT			
Australia	0.4 ± 5.87	-1.4 ± 5.26	1.7 ± 5.20
New Zealand	3.2 ± 6.85	1.0 ± 9.95	1.4 ± 5.93
NNR			
Whole network	19.5 ± 9.66	-40.1 ± 16.48	-8.9 ± 6.35
No conditions			
Whole network	22.2 ± 10.59	-40.3 ± 12.30	-7.7 ± 6.42
Coord. constraints			
Whole network	4.9 ± 9.12	-13.1 ± 9.95	- 5.5 ± 6.39

6.2.4 Velocity field of New Zealand

New Zealand is in an awkward position because of its location on a junction between the Australian and the Pacific plate, which leads to the case that this region is exposed to a high tectonic activity. Fortunately, the country is a well developed nation and has the ability to do geophysical research and surveys so that the density of available GNSS reference stations is quite high. Though the focus of this thesis lies on the accurate determination of reference site velocities and not on the geophysical interpretation of plate tectonics, the obtained velocities in this region will shortly be discussed.

Considering the length and azimuth of every velocity vector, similar station movements of approximately 50 mm yr^{-1} can be arranged into one group represented by the blue vectors in Figure 6.8 and may be assigned to the movement of the Pacific plate. This assumption shows a good accordance with the NUVEL plate boundary given by the red line and the given velocities in the right plot. An exception is represented by the nearby stations WGTN and WGTT (see black circles). Whereas the remaining black velocity vectors reveal smaller velocities for both the processed solution and the NUVEL model, the azimuths of both velocity fields differ considerably, especially near the given junction. At which the NUVEL motion of the Australian plate shows a homogeneous movement to the North, the calculated diverse azimuths suggest that the velocity characteristic close to the plate boundary is more complicated and that the reliable assignment of plate affiliations can therefore pose a challenge in such zones.

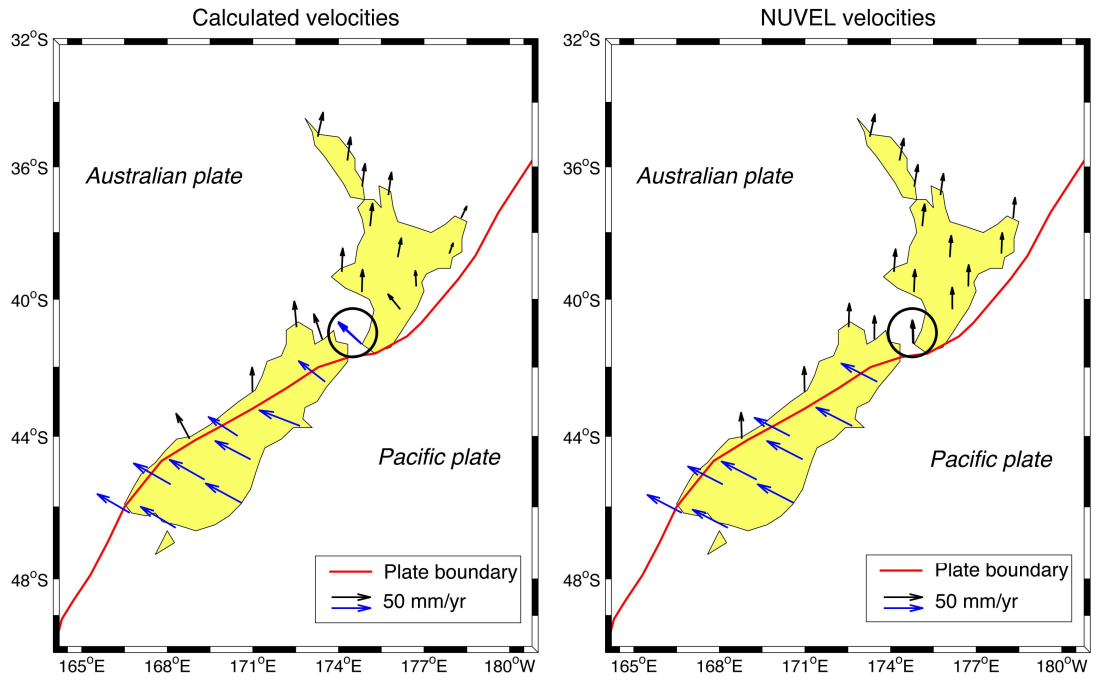

Figure 6.8: Estimated velocities in the region of New Zealand (left plot) in comparison with the NNR-NUVEL-1A velocities (right plot), plate boundary in red, primary approach based on data sets of three years. Note stations WGTN and WGTT at the south side of the northern island (black circles)

6.3 Tropospheric estimates

Next to the station coordinates, the final parameter estimation produces tropospheric estimates in form of zenith path delays on an hourly basis. Whereas the wet part of the zenith delay is estimated by this process, the dry component was introduced as an a priori value from the NIELL model[1], which is represented by the Saastamoinen zenith path delay and the NIELL mapping function. It is an empiric model, which means that no weather data is involved. Hence, it is interesting to compare the results with other tropospheric solutions which use a numeric weather model.

Amongst others, the *GGOS Atmosphere* project[2], established at the Institute of Geodesy and Geophysics at the Vienna University of Technology, provides consistent models for the estimation of hydrostatic and wet zenith delays. These models use data from numeric weather models (e.g. from the European Centre for Medium-Range Weather Forecast, ECMWF) and the Vienna Mapping Functions (VMF1) in order to provide these atmospheric parameters on a global grid and also for a set of IGS and VLBI stations.

[1] Details to the available models are given in Dach *et al.* (2007), page 244
[2] Details to GGOS Atmosphere are given in Böhm *et al.* (2006) and http://ggosatm.hg.tuwien.ac.at/

Regarding to the investigative network, 16 out of 17 regional IGS/ITRF sites are within the GGOS Atmosphere data set showing a sampling interval of 6 h. These parameters can be compared to the tropospheric estimates of the processed solution by summarizing the dry and wet component to a total zenith delay and computing the bias for each IGS/ITRF station, whereat the GGOS data set acts as a reference. Furthermore the biases of the 16 stations can be merged into one mean bias representing the whole network. This mean bias and its corresponding standard deviation is given in Table 6.14.

Table 6.14: Mean bias and standard deviation of the total zenith delay with respect to the GGOS atmosphere data set ($d_{Calc} - d_{GGOS}$) representing 16 IGS/ITRF stations covering the whole observation period, primary approach based on data sets of three years

Description	Mean bias ± std. dev., in [mm]
Primary approach: NNT & NNR	4.6 ± 16.45

Figure 6.9 illustrates the deviation of the calculated mean bias of all stations over a time span of three years and reveals that the magnitude shows a range of approximately 10 mm.

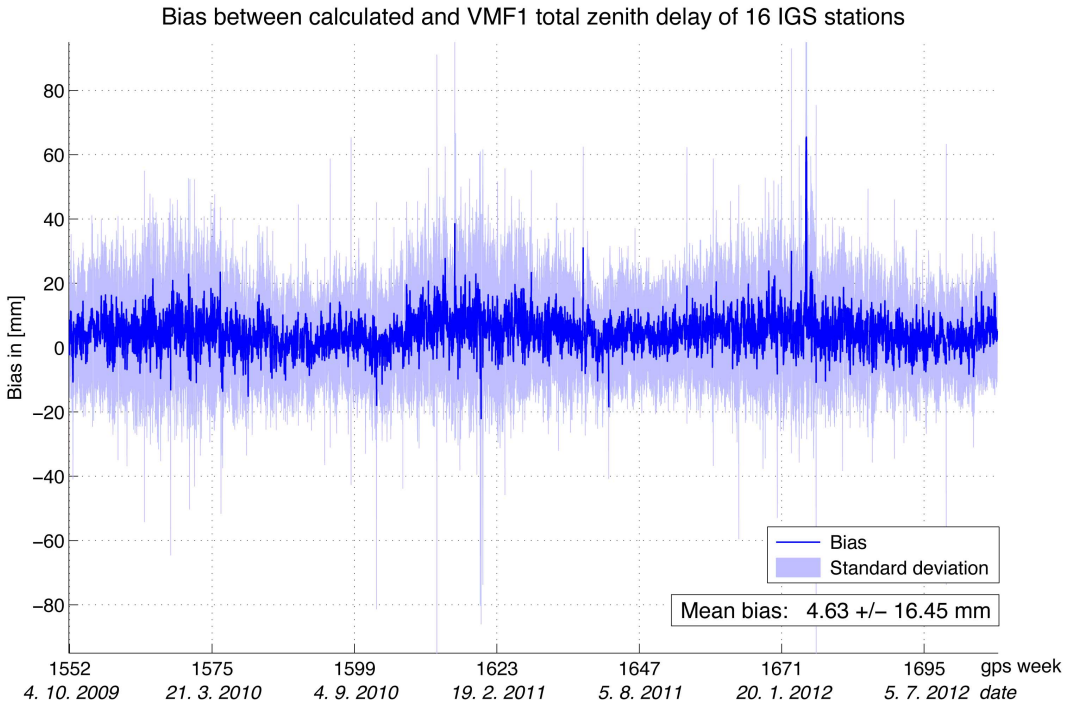

Figure 6.9: Mean bias and standard deviation of the total zenith delay with respect to the GGOS atmosphere data set ($d_{Calc} - d_{GGOS}$) representing 16 IGS/ITRF stations, primary approach based on data sets of three years

Chapter 7

Conclusion

The outcome of this thesis shows that the objective to determine utmost accurate GNSS reference site coordinates and furthermore velocities demand for both a multitude of adequate input data sets and a complex post-processing strategy. If the contributing elements are grouped with respect to the signal propagation from the satellite to the ground station, the chosen strategy includes the use of precise satellite orbits, an appropriate method to eliminate ionospheric and tropospheric effects, the synchronization of receiver clocks and the consideration of gravitational forces which cause temporal loading effects in each station due to the dynamics of the ocean and the celestial bodies. In addition, long observation periods of 24 h for each session allow a proper adjustment in order to clean the data from outliers, to detect cycle slips and to perform a successful resolution of ambiguities.

Regarding the different approaches of a suitable datum definition, it turns out that a minimum constraint solution using a no-net-translation and no-net-rotation condition provides the most accurate results in repeatability and residuals with respect to the given weekly IGS solutions. This solution is given by the primary approach. It can be assumed that the avoidance of a translation and rotation of the regional network of 97 stations is desirable and reasonable, because the precise orbits already define an accurate orientation of the whole network, where the a priori coordinates of the datum defining fiducial sites reveal the uselessness of a network shift. The removal of one of these conditions shows that the no-net-translation condition has a much bigger impact on the results than the no-net-rotation. It has been shown that the second approach, which uses a no-net-translation condition only, leads to very small rotation rates of the network so that the solution is very close to the primary approach. It is obvious that an important aspect of the minimum constraint solution is the accuracy of the a priori fiducial site coordinates. For that reason, extrapolated IGS08/ITRF2008 coordinate sets of 17 fiducial sites are in use, including an additional script (REF_STA) which rejects defective stations from the datum definition.

The achieved coordinate accuracies are summarized in Table 7.1 and cover an observation period of one and a half years, in which the processed and the given weekly IGS08 solutions underly the same terrestrial reference frame IGS08 and antenna calibration file igs08.atx, be-

ginning with GPS week 1632 (April 17th, 2011).

Table 7.1: Mean value and standard deviation of the total weekly repeatabilities and residuals with respect to the weekly IGS solutions ($\mathbf{x}_{Calc} - \mathbf{x}_{IGS}$) for a time series of one and a half years (period of equal use of reference frame IGS08 and antenna calibrations file igs08.atx), primary and most accurate approach

Description	Mean value ± std. dev., in [mm]		
	X	Y	Z
NNT & NNR:			
Total repeatabilities	1.2 ± 0.19	1.2 ± 0.23	4.0 ± 0.71
Weekly IGS residuals	-2.9 ± 3.23	0.5 ± 3.05	-0.1 ± 3.24

These final coordinate solutions of the primary approach are suitable for a further velocity estimation, although the mean residuals with respect to the weekly IGS solutions still show a range of several mm. The reason for these remaining uncertainties may lie in the geometric dimension of the network. While the stations of network NSW represent a limited regional network in Oceania and include only 17 datum defining IGS/ITRF sites, the compared IGS solutions were processed from a global, well distributed network of more than 250 IGS stations and therefore show a higher stability according to the orientation in space and the alignment in the corresponding terrestrial reference frame.

Whereas the mentioned datum definition approaches show IGS residuals in mm level, the remaining strategies of using either a no-net-rotation condition only, no conditions at all or a coordinate constraint of separate fiducial sites perform translations of the network and lead to higher residuals of up to several cm. Therefore, this error will be propagated in the following velocity estimation and will result in uncertainties of some cm yr^{-1}, which represents the actual dimension of plate velocities and hence is futile.

In contrast, the calculated velocity field of the primary approach shows much more satisfying results as can be seen in the mean standard deviation of approximately 1 mm yr^{-1} in X, Y and Z of all station velocities (Table 6.9) and the comparison with the given IGS08/ITRF2008 velocities of 17 IGS/ITRF stations as shown in Table 7.2.

These results illustrate that the velocity determination of a regional GNSS network can reach accuracies of a few mm yr^{-1} even after rather short observation periods of three years. An improvement of this solution may be achieved by two basic concepts. On the one hand, the global extension of the network and the integration of a higher number of fiducial IGS sites may improve the coordinate solution and further the final velocities. On the other hand, the computation of velocities of course depends on the observed period of time. Therefore, a longer time span of processed coordinates up to 10 years or more would increase the accuracy and the reliability of the station velocities.

A final additional remark completes this thesis and covers a comparison with the geophys-

Table 7.2: Mean velocity difference and standard deviation with respect to the IGS08/ITRF2008 velocities ($\mathbf{v}_{Calc} - \mathbf{v}_{IGS08/ITRF2008}$) representing an overview of all IGS/ITRF stations, primary approach based on data sets of three years

Description	Mean velocity difference ± std. dev., in [mm yr^{-1}]		
	X	Y	Z
Primary approach:			
NNT & NNR	1.7 ± 2.51	-0.1 ± 2.27	0.7 ± 1.77

ical NNR-NUVEL-1A velocity model and the estimated tropospheric zenith delay. It appears that the processed station velocities near the plate boundary in New Zealand show varying azimuths and therefore differ from the homogenous NUVEL velocities (Figure 6.8). Hence, the geodetic examination in this region visualizes that the course of ground motion near the plate boundary shows a higher complexity and makes a clear separation of stations to specific tectonic plates much more difficult. A comparison of the estimated total zenith delays using a NIELL model with results from a numeric weather model indicate mean absolute biases of less than 10 mm (Figure 6.9). A future implementation of modern tropospheric models which include numeric weather models in the processing software would therefore eliminate the weakness in the estimation of tropospheric delays and furthermore might show a positive impact on the final network solution.

Appendix A

Velocity solution of the primary approach

A.1 Final site velocities of network NSW

Table A.1: Final station velocities of network NSW and corresponding number of observed weeks, part 1 of primary approach, based on data sets of three years from October 4th, 2009 until September 29th, 2012, reference frame: IGS08 (Meaning of flag: IGS08 ... IGS site, ITR08 ... ITRF site, A ... APREF site)

No.	Station name		Velocity in [mm yr^{-1}]			No. of obs.	Flag
			X	Y	Z	in [weeks]	
1	ALBY	50191M001	-48.6	11.0	47.6	156	A
2	ALIC	50137M001	-40.1	-6.6	54.0	155	IGS08
3	ANDA	59971M001	-39.8	-0.7	50.0	118	A
4	ARUB	59946M001	-43.9	2.1	50.4	39	A
5	AUCK	50209M001	-21.2	-1.7	32.8	156	IGS08
6	BALA	59947M001	-35.2	0.6	59.3	39	A
7	BBOO	59997M001	-41.3	1.7	49.3	156	A
8	BDLE	50196M001	-35.7	1.8	46.4	119	A
9	BEEC	59986M001	-37.7	0.8	49.6	112	A
10	BKNL	59951M001	-35.2	-5.0	53.7	55	A
11	BLUF	50234M001	-17.2	36.5	21.6	156	A
12	BRO1	50176M003	-39.2	-7.2	56.6	117	A
13	BURA	50193M001	-47.7	8.5	50.0	154	A
14	CBLT	59979M001	-26.9	-11.4	52.1	34	A
15	CEDU	50138M001	-42.0	2.1	49.9	155	IGS08
16	CHAT	50207M001	-25.6	38.3	23.3	124	IGS08
17	COOB	59970M001	-40.7	-0.7	51.1	128	A
18	CORM	50226M001	-21.9	-2.2	31.8	156	A
19	CUT0	59945M001	-45.8	6.4	52.1	55	A

Table A.2: Final station velocities of network NSW and corresponding number of observed weeks, part 2 of primary approach, based on data sets of three years from October 4th, 2009 until September 29th, 2012, reference frame: IGS08 (Meaning of flag: IGS08 ... IGS site, ITR08 ... ITRF site, A ... APREF site)

No.	Station name		Velocity in $[\mathrm{mm\,yr^{-1}}]$			No. of obs.	Flag
			X	Y	Z	in [weeks]	
20	DALB	AUM000095	-28.8	-9.1	50.0	53	A
21	DARW	50134M001	-35.0	-15.0	56.9	153	IGS08
22	DNVK	50224M001	-12.6	14.8	21.2	156	A
23	DODA	59985M001	-34.2	-15.2	56.6	144	A
24	DUND	50212M003	-14.4	36.7	22.5	156	A
25	ESPA	50177M002	-47.1	8.9	48.6	156	A
26	GABO	59983M001	-34.7	1.6	45.6	117	A
27	GISB	50223M001	-11.1	-4.1	13.5	156	A
28	GLDB	50230M001	-25.7	5.9	33.2	153	A
29	HAAS	50237M001	-22.5	18.4	31.2	156	A
30	HAMT	50222M001	-24.4	-0.9	29.4	156	A
31	HAST	50221M001	-14.7	1.8	21.4	156	A
32	HIKB	50225M001	-10.1	-6.5	17.0	156	A
33	HIL1	50141S001	-46.4	6.1	49.8	156	A
34	HNIS	59959M001	-27.2	-22.9	56.3	79	A
35	HOB2	50116M004	-38.6	7.4	42.0	156	IGS08
36	HOKI	50211M001	-25.8	4.5	28.9	156	A
37	HYDN	50195M001	-47.7	8.9	49.9	155	A
38	IHOE	59962M001	-36.9	-1.3	49.0	117	A
39	JAB2	50136M002	-32.5	-17.0	56.6	152	A
40	KAIK	50231M001	-16.2	30.2	27.4	156	A
41	KALG	50188M001	-46.0	5.8	50.8	156	A
42	KARR	50139M001	-44.5	2.4	53.4	156	IGS08
43	KAT1	59968M001	-33.4	-14.3	57.3	131	A
44	KELN	50197M001	-47.2	8.0	50.2	153	A
45	KOUC	92727S001	-20.7	-20.4	47.6	154	IGS08
46	KTIA	50241M001	-21.3	-4.6	36.1	68	A
47	KUNU	59995M001	-36.9	-11.2	55.5	150	A
48	LARR	59984M001	-33.6	-15.4	56.6	148	A
49	LDHI	AUM000006	-30.3	-4.1	43.9	82	A
50	LEXA	50236M001	-14.9	37.5	22.6	155	A
51	LIAW	50192M001	-39.0	6.9	42.5	155	A
52	LKYA	59952M001	-35.0	-16.6	57.2	60	A
53	LONA	59957M001	-44.1	4.9	50.9	74	A
54	MAC1	50135M001	-20.0	20.0	19.2	156	IGS08
55	MAVL	50235M001	-14.7	39.5	24.0	151	A
56	MOBS	50182M001	-38.2	3.3	45.4	155	IGS08
57	MQZG	50214M001	-7.1	42.9	22.7	156	IGS08
58	MTCV	59965M001	-39.6	-3.7	53.3	107	A

Table A.3: Final station velocities of network NSW and corresponding number of observed weeks, part 3 of primary approach, based on data sets of three years from October 4th, 2009 until September 29th, 2012, reference frame: IGS08 (Meaning of flag: IGS08 ... IGS site, ITR08 ... ITRF site, A ... APREF site)

No.	Station name		Velocity in [mm yr^{-1}]			No. of obs.	Flag
			X	Y	Z	in [weeks]	
59	MTEM	59954M001	-40.9	5.1	43.3	73	A
60	MTJO	50204M001	-16.5	32.7	20.8	156	A
61	MTMA	59958M001	-43.9	5.7	51.3	83	A
62	NHIL	59960M001	-40.2	3.4	47.0	114	A
63	NLSN	50232M001	-22.8	12.0	33.5	156	A
64	NNOR	50181M001	-47.5	8.8	50.1	156	IGS08
65	NORF	50189M001	-23.4	-8.7	40.1	155	A
66	NORS	50194M001	-46.6	7.5	49.9	156	A
67	NPLY	50227M001	-23.5	1.4	31.4	156	A
68	NRMD	92701M005	-19.5	-15.4	43.7	152	A
69	PTKL	50145M004	-33.3	-1.7	46.5	106	A
70	PYGR	50240M001	-17.8	35.4	15.6	72	A
71	RAVN	59967M001	-45.6	8.0	50.2	120	A
72	RHPT	50187M001	-39.2	5.7	43.3	152	A
73	ROBI	59976M001	-29.5	-10.2	50.3	34	A
74	RSBY	59953M001	-27.5	-14.6	49.8	60	A
75	SA45	59987M001	-39.4	-0.0	50.1	156	A
76	SPBY	50162M004	-40.5	10.7	44.0	154	A
77	SYDN	50124M003	-34.5	-1.6	45.8	156	A
78	TAUP	50217M001	-18.6	-2.9	25.7	156	A
79	TBOB	59963M001	-35.6	-5.0	51.7	103	A
80	TIDB	50103M108	-33.9	-0.8	47.2	140	IGS08
81	TOW2	50140M001	-26.4	-17.4	56.3	156	IGS08
82	UCLA	50153M002	-44.6	3.8	50.2	36	A
83	WAGN	59966M001	-46.8	9.3	49.6	131	A
84	WAIM	50239M001	-10.7	37.2	24.4	156	A
85	WANG	50228M001	-22.4	1.3	29.5	156	A
86	WARA	50198M001	-41.2	-2.1	53.8	127	A
87	WGTN	50208M003	-16.0	26.9	29.0	156	ITR08
88	WGTT	50208S004	-16.4	26.2	29.1	155	ITR08
89	WHNG	50218M001	-22.1	-1.7	33.1	156	A
90	WILU	59964M001	-43.6	3.9	52.7	92	A
91	WLAL	59950M001	-41.5	-3.8	53.0	45	A
92	WMGA	59961M001	-35.8	-10.0	57.2	102	A
93	WOOL	50143M003	-28.1	-13.0	51.1	34	A
94	WWLG	59988M001	-33.6	-3.0	48.8	134	A
95	YARR	50107M006	-45.4	6.2	51.5	135	IGS08
96	YEEL	59996M001	-42.2	3.2	48.7	156	A
97	YELO	50199M001	-46.4	7.0	50.5	156	A

A.2 Standard deviation of the final site velocities of network NSW

Table A.4: Standard deviation of the station velocities of network NSW and corresponding number of observed weeks, part 1 of primary approach, based on data sets of three years from October 4th, 2009 until September 29th, 2012, reference frame: IGS08 (Meaning of flag: IGS08 ... IGS site, ITR08 ... ITRF site, A ... APREF site)

No.	Station name		Std. dev. of velocity in $[\mathrm{mm\,yr^{-1}}]$			No. of obs.	Flag
			X	Y	Z	in [weeks]	
1	ALBY	50191M001	0.91	0.86	0.68	156	A
2	ALIC	50137M001	1.60	1.72	0.96	155	IGS08
3	ANDA	59971M001	0.99	1.02	1.12	118	A
4	ARUB	59946M001	1.19	1.66	1.65	39	A
5	AUCK	50209M001	0.84	0.65	0.70	156	IGS08
6	BALA	59947M001	1.54	2.02	2.83	39	A
7	BBOO	59997M001	0.65	0.73	0.78	156	A
8	BDLE	50196M001	0.79	0.69	0.84	119	A
9	BEEC	59986M001	1.22	0.77	1.53	112	A
10	BKNL	59951M001	1.62	1.49	1.69	55	A
11	BLUF	50234M001	1.00	0.72	0.96	156	A
12	BRO1	50176M003	0.93	1.36	0.62	117	A
13	BURA	50193M001	0.80	0.89	0.67	154	A
14	CBLT	59979M001	1.99	0.73	1.14	34	A
15	CEDU	50138M001	0.63	0.74	0.73	155	IGS08
16	CHAT	50207M001	1.26	0.79	1.21	124	IGS08
17	COOB	59970M001	1.08	1.15	1.13	128	A
18	CORM	50226M001	0.85	0.75	0.76	156	A
19	CUT0	59945M001	1.03	1.70	1.15	55	A
20	DALB	AUM000095	1.34	0.99	1.20	53	A
21	DARW	50134M001	1.09	1.34	1.05	153	IGS08
22	DNVK	50224M001	0.86	1.02	1.04	156	A
23	DODA	59985M001	1.33	1.50	0.72	144	A
24	DUND	50212M003	0.67	0.64	0.75	156	A
25	ESPA	50177M002	0.79	1.05	0.76	156	A
26	GABO	59983M001	0.83	0.86	1.06	117	A
27	GISB	50223M001	2.07	2.64	1.07	156	A
28	GLDB	50230M001	0.90	0.61	0.88	153	A

Table A.5: Standard deviation of the station velocities of network NSW and corresponding number of observed weeks, part 2 of primary approach, based on data sets of three years from October 4th, 2009 until September 29th, 2012, reference frame: IGS08 (Meaning of flag: IGS08 ... IGS site, ITR08 ... ITRF site, A ... APREF site)

No.	Station name		Std. dev. of velocity in $[\mathrm{mm\,yr^{-1}}]$			No. of obs.	Flag
			X	Y	Z	in [weeks]	
29	HAAS	50237M001	1.19	0.87	1.14	156	A
30	HAMT	50222M001	0.96	0.67	0.90	156	A
31	HAST	50221M001	1.01	1.06	0.77	156	A
32	HIKB	50225M001	0.92	0.74	0.74	156	A
33	HIL1	50141S001	0.80	1.08	0.81	156	A
34	HNIS	59959M001	1.91	1.26	0.64	79	A
35	HOB2	50116M004	0.72	0.62	0.73	156	IGS08
36	HOKI	50211M001	0.77	0.88	1.00	156	A
37	HYDN	50195M001	0.81	0.94	0.65	155	A
38	IHOE	59962M001	1.20	1.07	1.32	117	A
39	JAB2	50136M002	1.03	1.14	0.72	152	A
40	KAIK	50231M001	0.99	0.69	1.01	156	A
41	KALG	50188M001	0.69	0.87	0.70	156	A
42	KARR	50139M001	0.88	1.43	0.68	156	IGS08
43	KAT1	59968M001	1.55	1.47	0.72	131	A
44	KELN	50197M001	0.82	1.08	0.77	153	A
45	KOUC	92727S001	1.39	0.87	0.79	154	IGS08
46	KTIA	50241M001	1.22	0.89	1.02	68	A
47	KUNU	59995M001	0.90	1.25	0.61	150	A
48	LARR	59984M001	1.29	1.45	0.71	148	A
49	LDHI	AUM000006	1.31	1.08	1.34	82	A
50	LEXA	50236M001	0.89	0.77	0.86	155	A
51	LIAW	50192M001	0.61	0.56	0.72	155	A
52	LKYA	59952M001	2.57	2.97	1.50	60	A
53	LONA	59957M001	0.82	1.92	1.36	74	A
54	MAC1	50135M001	0.85	0.57	1.25	156	IGS08
55	MAVL	50235M001	1.71	1.55	1.40	151	A
56	MOBS	50182M001	0.72	0.62	0.86	155	IGS08
57	MQZG	50214M001	1.09	0.61	0.88	156	IGS08
58	MTCV	59965M001	1.17	1.18	1.00	107	A
59	MTEM	59954M001	1.35	1.50	1.85	73	A
60	MTJO	50204M001	0.92	0.67	0.84	156	A
61	MTMA	59958M001	1.02	1.68	1.05	83	A
62	NHIL	59960M001	0.75	0.76	1.07	114	A
63	NLSN	50232M001	0.87	0.69	0.83	156	A
64	NNOR	50181M001	0.74	0.91	0.63	156	IGS08
65	NORF	50189M001	1.13	0.68	0.70	155	A

Table A.6: Standard deviation of the station velocities of network NSW and corresponding number of observed weeks, part 3 of primary approach, based on data sets of three years from October 4th, 2009 until September 29th, 2012, reference frame: IGS08 (Meaning of flag: IGS08 ... IGS site, ITR08 ... ITRF site, A ... APREF site)

No.	Station name		Std. dev. of velocity in $[\mathrm{mm\,yr^{-1}}]$			No. of obs.	Flag
			X	Y	Z	in [weeks]	
66	NORS	50194M001	0.73	0.85	0.65	156	A
67	NPLY	50227M001	1.03	0.69	0.81	156	A
68	NRMD	92701M005	1.30	0.85	0.81	152	A
69	PTKL	50145M004	1.06	0.79	1.11	106	A
70	PYGR	50240M001	1.32	0.89	1.12	72	A
71	RAVN	59967M001	0.66	0.83	0.60	120	A
72	RHPT	50187M001	0.64	0.63	0.76	152	A
73	ROBI	59976M001	1.66	0.92	1.20	34	A
74	RSBY	59953M001	1.97	1.12	0.91	60	A
75	SA45	59987M001	0.74	0.78	0.88	156	A
76	SPBY	50162M004	0.73	0.76	0.99	154	A
77	SYDN	50124M003	0.68	0.56	0.75	156	A
78	TAUP	50217M001	1.06	0.63	1.38	156	A
79	TBOB	59963M001	1.10	0.84	1.08	103	A
80	TIDB	50103M108	0.75	0.62	0.85	140	IGS08
81	TOW2	50140M001	1.12	0.89	0.91	156	IGS08
82	UCLA	50153M002	1.41	1.79	1.95	36	A
83	WAGN	59966M001	0.83	1.04	0.72	131	A
84	WAIM	50239M001	1.16	0.71	0.86	156	A
85	WANG	50228M001	0.83	1.02	0.79	156	A
86	WARA	50198M001	0.81	1.00	0.72	127	A
87	WGTN	50208M003	0.69	0.72	0.68	156	ITR08
88	WGTT	50208S004	0.87	0.98	0.90	155	ITR08
89	WHNG	50218M001	1.02	0.68	0.94	156	A
90	WILU	59964M001	0.77	1.43	0.96	92	A
91	WLAL	59950M001	1.73	3.31	1.49	45	A
92	WMGA	59961M001	1.05	1.17	0.75	102	A
93	WOOL	50143M003	1.39	0.82	0.97	34	A
94	WWLG	59988M001	0.91	0.64	0.98	134	A
95	YARR	50107M006	0.83	1.04	0.70	135	IGS08
96	YEEL	59996M001	0.57	0.74	0.78	156	A
97	YELO	50199M001	0.73	0.83	0.65	156	A

A.3 Comparison to the IGS08/ITRF2008 site velocities

Table A.7: Velocity differences of 17 IGS/ITRF sites of network NSW with respect to the given IGS08/ITRF2008 velocities ($\mathbf{v}_{Calc} - \mathbf{v}_{IGS08/ITRF2008}$), primary approach based on data sets of three years from October 4th, 2009 until September 29th, 2012, reference frame: IGS08 (Meaning of flag: IGS08 ... IGS site, ITR08 ... ITRF site)

No.	Station name		Velocity difference in [mm yr^{-1}]			No. of obs.	Flag
			X	Y	Z	in [weeks]	
2	ALIC	50137M001	-0.5	-1.6	-0.1	155	IGS08
5	AUCK	50209M001	2.3	0.7	0.3	156	IGS08
15	CEDU	50138M001	-0.1	0.5	-0.4	155	IGS08
16	CHAT	50207M001	-0.5	-0.8	-0.8	124	IGS08
21	DARW	50134M001	-0.2	-0.7	-1.2	153	IGS08
35	HOB2	50116M004	1.1	-1.2	1.3	156	IGS08
42	KARR	50139M001	-0.3	1.4	-1.0	156	IGS08
45	KOUC	92727S001	1.7	-1.6	2.7	154	IGS08
54	MAC1	50135M001	-0.8	1.2	-1.5	156	IGS08
56	MOBS	50182M001	1.9	-0.7	-0.5	155	IGS08
57	MQZG	50214M001	9.4	6.8	-0.1	156	IGS08
64	NNOR	50181M001	0.4	-0.9	0.3	156	IGS08
80	TIDB	50103M108	3.4	-2.0	2.3	140	IGS08
81	TOW2	50140M001	4.5	-3.1	3.5	156	IGS08
87	WGTN	50208M003	3.0	1.7	4.7	156	ITR08
88	WGTT	50208S004	1.3	0.7	1.9	155	ITR08
95	YARR	50107M006	1.9	-2.5	1.0	135	IGS08

A.4 Comparison to the NNR-NUVEL-1A plate motion model

Table A.8: Velocity differences of 17 IGS/ITRF sites of network NSW with respect to the given NNR-NUVEL-1A plate motion model ($\mathbf{v}_{Calc} - \mathbf{v}_{NUVEL}$), primary approach based on data sets of three years from October 4th, 2009 until September 29th, 2012, reference frame: IGS08 (Meaning of flag: IGS08 ... IGS site, ITR08 ... ITRF site)

No.	Station name		Velocity difference in [mm yr^{-1}]			No. of obs.	Flag
			X	Y	Z	in [weeks]	
2	ALIC	50137M001	-0.5	-1.1	0.2	155	IGS08
5	AUCK	50209M001	1.0	0.7	3.0	156	IGS08
15	CEDU	50138M001	-0.2	-0.5	0.0	155	IGS08
16	CHAT	50207M001	-1.5	-0.8	0.7	124	IGS08
21	DARW	50134M001	1.7	-0.3	-0.8	153	IGS08
35	HOB2	50116M004	-0.6	-1.6	2.0	156	IGS08
42	KARR	50139M001	0.5	1.7	-2.1	156	IGS08
45	KOUC	92727S001	0.9	-1.7	5.5	154	IGS08
54	MAC1	50135M001	14.9	1.3	-9.0	156	IGS08
56	MOBS	50182M001	-0.1	-1.2	1.5	155	IGS08
57	MQZG	50214M001	8.3	3.8	1.4	156	IGS08
64	NNOR	50181M001	0.1	-1.7	-0.8	156	IGS08
80	TIDB	50103M108	1.8	-1.6	3.3	140	IGS08
81	TOW2	50140M001	4.9	-2.0	4.7	156	IGS08
87	WGTN	50208M003	8.2	24.1	1.2	156	ITR08
88	WGTT	50208S004	7.8	23.4	1.2	155	ITR08
95	YARR	50107M006	2.0	-3.0	-0.3	135	IGS08

Appendix B

Secondary and tertiary solutions with respect to the IGS08/ITRF2008 velocities

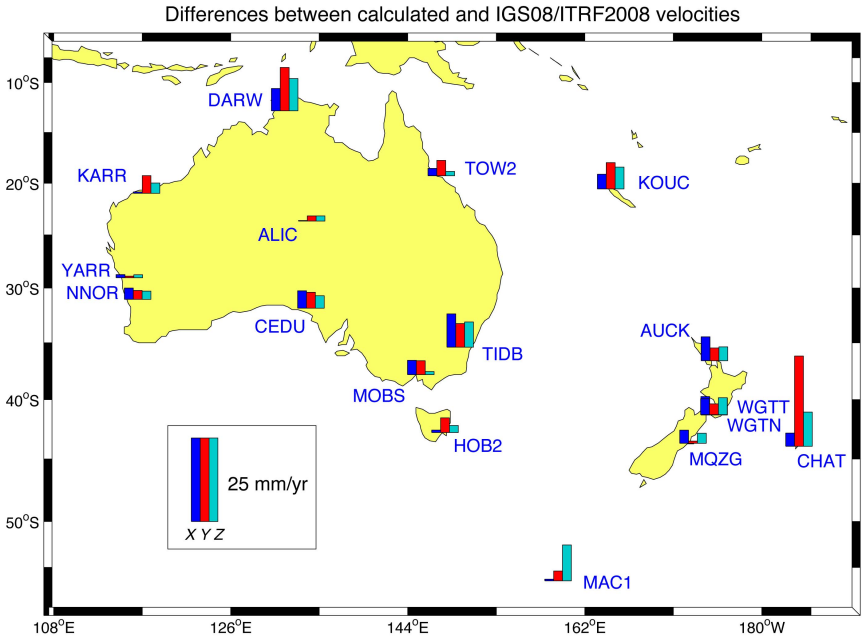

Figure B.1: Absolute velocity differences of 17 IGS/ITRF sites of network NSW with respect to the given IGS08/ITRF2008 velocities, secondary approach using a no-net-translation condition, based on data sets of nine months from January 1st, 2012 until September 29th, 2012, reference frame: IGS08

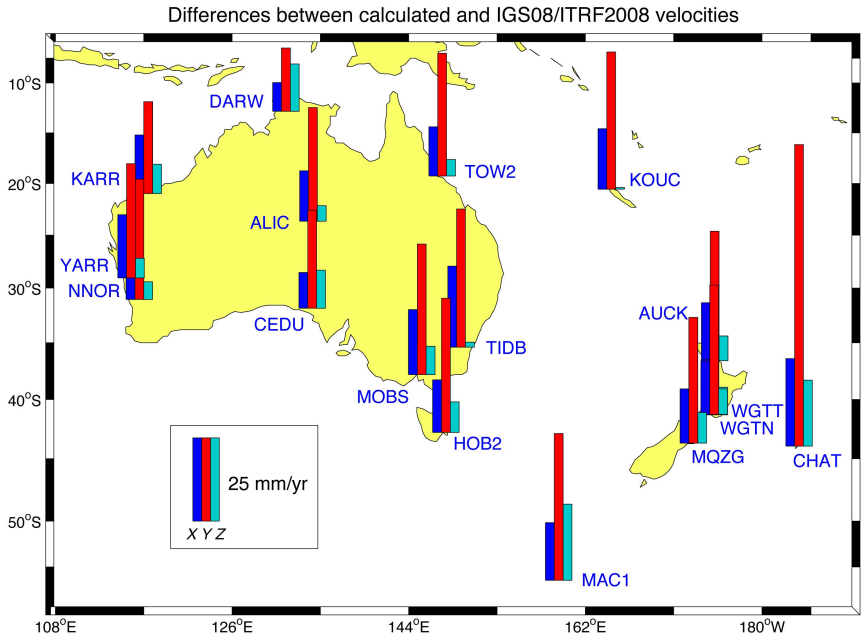

Figure B.2: Absolute velocity differences of 17 IGS/ITRF sites of network NSW with respect to the given IGS08/ITRF2008 velocities, secondary approach using a no-net-rotation condition, based on data sets of nine months from January 1st, 2012 until September 29th, 2012, reference frame: IGS08

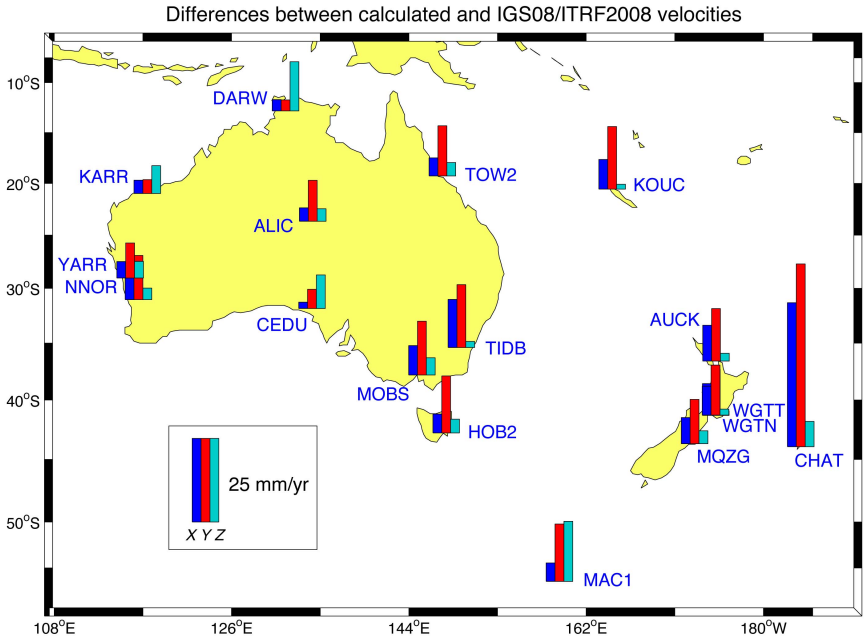

Figure B.3: Absolute velocity differences of 17 IGS/ITRF sites of network NSW with respect to the given IGS08/ITRF2008 velocities, tertiary approach using coordinate constraints, based on data sets of nine months from January 1st, 2012 until September 29th, 2012, reference frame: IGS08

Appendix C

Secondary and tertiary solutions with respect to the NNR-NUVEL-1A plate motion model

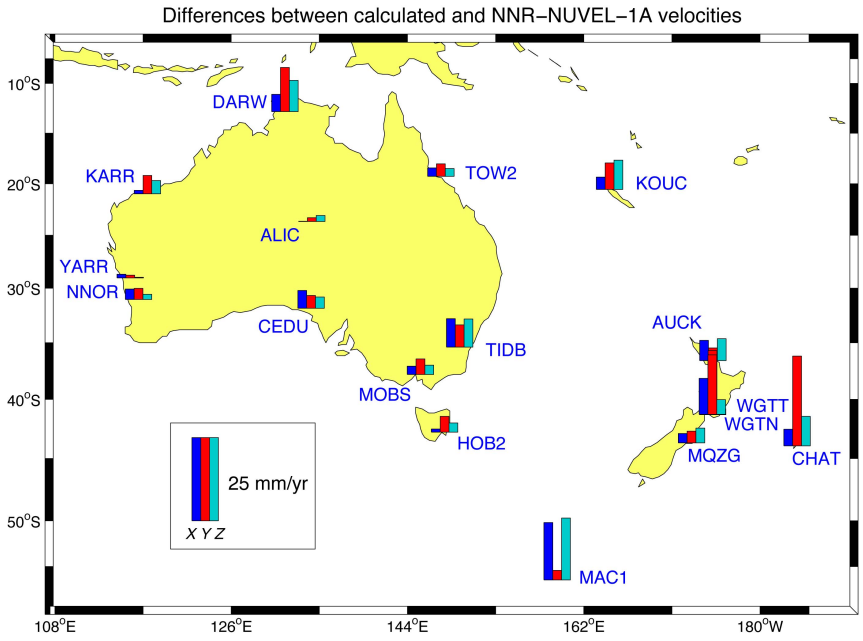

Figure C.1: Absolute velocity differences of 17 IGS/ITRF sites of network NSW with respect to the given NNR-NUVEL-1A plate motion model, secondary approach using a no-net-translation condition, based on data sets of nine months from January 1st, 2012 until September 29th, 2012

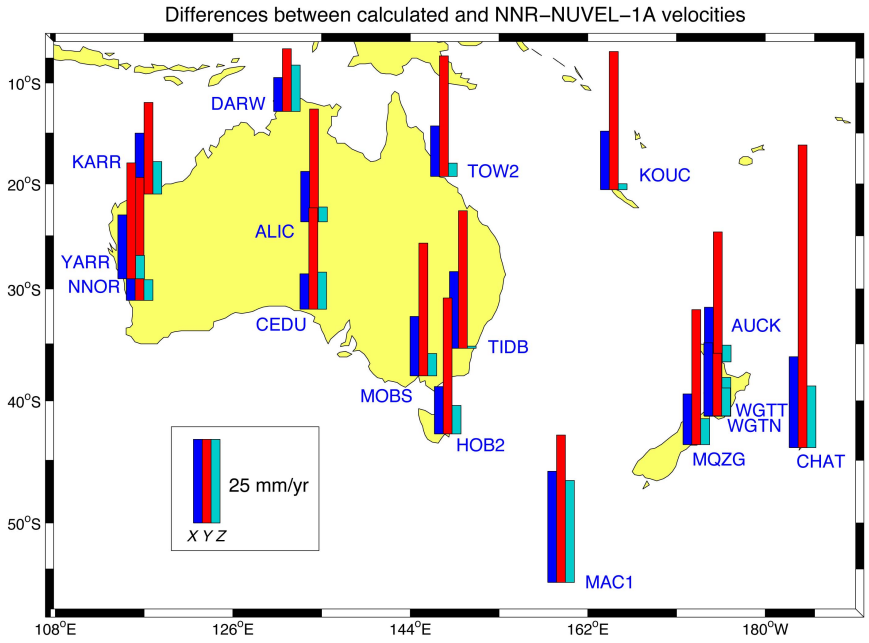

Figure C.2: Absolute velocity differences of 17 IGS/ITRF sites of network NSW with respect to the given NNR-NUVEL-1A plate motion model, secondary approach using a no-net-rotation condition, based on data sets of nine months from January 1st, 2012 until September 29th, 2012

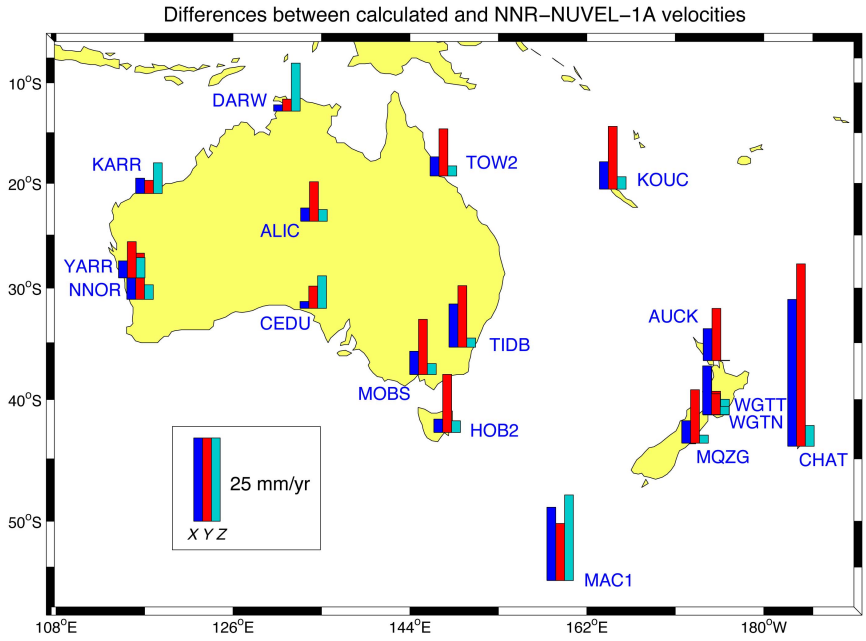

Figure C.3: Absolute velocity differences of 17 IGS/ITRF sites of network NSW with respect to the given NNR-NUVEL-1A plate motion model, tertiary approach using coordinate constraints, based on data sets of nine months from January 1st, 2012 until September 29th, 2012

List of Figures

List of Tables

Acronyms

AIUB	Astronomical Institute of the University of Bern
APREF	Asia-Pacific Reference Frame
AS	Anti-Spoofing
BIH	Bureau International de l'Heure
BPE	Bernese Processing Engine
C/A Code	Coarse/Acquisition Code
CDDIS	Crustal Dynamics Data Information System
CEP	Celestial Ephemeris Pole
CORS	Continuously Operating Reference Station
CRF	Celestial Reference Frame
CRS	Celestial Reference System
DGPS	Differential GPS
DOP	Dilution of Precision
DORIS	Doppler Orbitography and Radiopositioning Integrated by Satellite
ECMWF	European Centre for Medium-Range Weather Forecast
EOP	Earth Orientation Parameter
ERP	Earth Rotation Parameter
EUREF	Reference Frame Sub-Commission for Europe
GA	Geoscience Australia
GDA94	Geocentric Datum of Australia 1994
GGOS	Global Geodetic Observing System
GLONASS	Globalnaja Nawigazionnaja Sputnikowaja Sistema
GNSS	Global Navigation Satellite System
GPS	Global Positioning System
GRS80	Geodetic Reference System 1980
IAU	International Astronomical Union
ICSM	Intergovernmental Committee on Surveying and Mapping
IERS	International Earth Rotation and Reference Frame Service
IGN	National Institute of the Geographic and Forest Information
IGS	International GNSS Service
ITRF	International Terrestrial Reference Frame

ITRS	International Terrestrial Reference System
IUGG	International Union of Geodesy and Geophysics
LAC	Local Analysis Centre
LBS	Location Based Services
MW	Melbourne-Wübbena
NAVSTAR GPS	Navigation System with Time And Ranging Global Positioning System
NNR	No-Net-Rotation
NNS	No-Net-Scale
NNT	No-Net-Translation
NSW	New South Wales
NUVEL	Northwestern University Velocity model
P Code	Precision Code
PCF	Process Control File
PDGPS	Precise Differential GPS
PRN	Pseudo Random Noise
PR	Pseudorange
PZ 90	Parametry Zemli 1990
QIF	Quasi Ionosphere-Free
RINEX	Receiver Independent Exchange Format
RMS	Root Mean Square
RTK	Real-Time Kinematic
SAGE	School of Surveying and Geospatial Engineering
SA	Selective Availability
SINEX	Solution Independent Exchange Format
SIRGAS	Geocentric Reference System for the Americas
SI	International System of Units
SLR	Satellite Laser Ranging
SOPAC	Scripps Orbit and Permanent Array Center
SSIS	School of Surveying and Spatial Information Systems
TEC	Total Electron Content
TRF	Terrestrial Reference Frame
TRS	Terrestrial Reference System
UERE	User Equivalent Range Error
UNAVCO	University Navstar Consortium
UNSW	University of New South Wales
UTC	Coordinated Universal Time
UTM	Universal Transverse Mercator
VLBI	Very Long Baseline Interferometry
VMF1	Vienna Mapping Function 1
WGS 84	World Geodetic System 1984

Bibliography

ALTAMIMI, Z., COLLILIEUX, X. AND MÉTIVIER, L. (2011). *ITRF2008: an improved solution of the international terrestrial reference frame*. Journal of Geodesy, 85(8):457–473, doi:10.1007/s00190-011-0444-4.

ALTAMIMI, Z., MÉTIVIER, L. AND COLLILIEUX, X. (2012). *ITRF2008 plate motion model*. Journal of Geophysical Research, 117(B07402), doi:10.1029/2011JB008930.

BÖHM, J., WERL, B. AND SCHUH, H. (2006). *Troposphere mapping functions for GPS and very long baseline interferometry from European Centre for Medium-Range Weather Forecasts operational analysis data*. Journal of Geophysical Research, 111(B02406), doi: 10.1029/2005JB003629.

BÖHM, S. (2010). *Erdrotation und globale dynamische Prozesse*. Script, Department of Geodesy and Geoinformation, Vienna University of Technology, Vienna.

BOUCHER, C. AND ALTAMIMI, Z. (2001). *ITRS, PZ-90 and WGS 84: current realizations and the related transformation parameters*. Journal of Geodesy, 75(11):613–619, doi:10.1007/s001900100208.

BOUCHER, C., ALTAMIMI, Z. AND DUHEM, L. (1993). *ITRF 92 and its associated velocity field*. In *IERS Technical Note 15*, Institut Géographique National, Terrestrial Frame Section, Central Bureau of IERS - Observatoire de Paris, Paris.

BROWN, A.K. (1989). *A multi-sensor approach to assuring GPS integrity*. In *Proceedings of the annual assembly meeting*, 141–153, Radio Technical Commission for Aeronautics (U.S.), Washington, DC.

DACH, R. (2012). *Bernese GNSS Software*. In *Localisation précise par moyens spatiaux*, Oral presentation, Ecole d'Eté September 3th - 7th 2012, Yverdon-les-Bains.

DACH, R., HUGENTOBLER, U., FRIDEZ, P. AND MEINDL, M., eds. (2007). *Bernese GPS Software Version 5.0*. User manual, Astronomical Institute, University of Bern.

DAWSON, J., ed. (2012). *Reference Frame in Practice, Session 1.2 Regional and National Reference Systems - Asia Pacific*. Oral presentation, IAG/FIG Commission 5/ICG Technical Seminar May 4th - 5th 2012, Rome.

DAWSON, J. AND WOODS, A. (2010). *ITRF to GDA94 coordinate transformations*. Journal of Applied Geodesy, 4(4):189–199, doi:10.1515/JAG.2010.019.

DOW, J.M., NEILAN, R.E. AND RIZOS, C. (2009). *The International GNSS Service (IGS) in a Changing Landscape of Global Navigation Satellite Systems*. Journal of Geodesy, 83(3-4):191–198, doi:10.1007/s00190-008-0300-3.

GA (2011a). *Guidelines for APREF Analysis Centres*. Manual, APREF Central Bureau, Geoscience Australia.

GA (2011b). *Guidelines for APREF Station Operators*. Manual, APREF Central Bureau, Geoscience Australia.

GA (2012). *Asia-Pacific Reference Frame (APREF)*. Geoscience Australia, http://www.ga.gov.au/earth-monitoring/geodesy/asia-pacific-reference-frame.html (February, 2013).

GPS-IS (2011). *Interface Specification - Navstar GPS Space Segment/Navigation User Segment Interfaces, Revision F (IS-GPS-200F)*. Global Positioning Systems Directorate.

GROTZINGER, J., JORDAN, T., PRESS, F. AND SIEVER, R. (2008). *Allgemeine Geologie*. Springer-Spektrum Akademischer Verlag, 5th edn.

HAASDYK, J. (2009). *Automatic Bernese Processing of CORSnet-NSW GPS data for deformation monitoring*. Bachelor's Thesis, School of Surveying and Spatial Information Systems, University of New South Wales.

HOFMANN-WELLENHOF, B., LICHTENEGGER, H. AND WASLE, E. (2008). *GNSS - Global Navigation Satellite Systems*. Springer-Verlag, Wien–New York.

HUISMAN, L., DAWSON, J. AND TEUNISSEN, P. (2011). *The APREF Project*. Coordinates, 7(5):14–18.

ICSM (2006). *Geocenctric Datum of Australia Technical Manual*. Intergovernmental Committee on Surveying and Mapping, Version 2.3.

IGS (2012). *International GNSS Service*. http://igscb.jpl.nasa.gov/ (February, 2013).

JIN, S. AND ZHU, W. (2004). *A revision of the parameters of the NNR-NUVEL-1A plate velocity model*. Journal of Geodynamics, 38(1):85–92, doi:10.1016/j.jog.2004.03.004.

KAPLAN, G. (2005). *The IAU Resolutions on Astronomical Reference Systems, Time Scales, and Earth Rotation Models*. U.S. Naval Observatory, Circular 179.

MARTIN, H., ed. (2008). *GPS Status and Modernization*. Oral presentation, Munich Satellite Navigation Summit February 20th 2008, Munich.

MELBOURNE, W. (1985). *The case for ranging in GPS based systems*. In *Proceedings of the first symposium on precise positioning with the global positioning system, positioning with GPS-1985*, 373–386, U.S. Department of Commerce, Rockville.

OSO (2012). *Free ocean tide loading provider*. Onsala Space Observatory, http://froste.oso.chalmers.se/loading/ (September, 2012).

PETIT, G. AND LUZUM, B. (2010). *IERS Conventions (2010)*. In *IERS Technical Note No. 36*, Verlag des Bundesamts für Kartographie und Geodäsie, Frankfurt am Main.

REBISCHUNG, P., SCHMID, R. AND RAY, J. (2011). *[IGSMAIL-6354] Upcoming switch to IGS08/igs08.atx*. International GNSS Service, http://igscb.jpl.nasa.gov/pipermail/igsmail/2011/006346.html (February, 2013).

RIZOS, C., ed. (2012). *GNSS and Modern Geodesy*. Oral presentation, UNSW Workshop on Geospatial Trends April 13th 2012, Sydney.

RIZOS, C. AND GREJNER-BRZEZINSKA, D.A. (2009). *Geodesy and surveying*, chap. 14 in *GNSS Applications and Methods*. Artech House.

SCHERER, M. (1998). *Vermessungswesen Multimedia 2.0: Grundbegriffe, Meßmethoden, Gerätefunktionen*. CD-ROM, Wichmann Verlag, 2nd edn.

SEEBER, G. (2003). *Satellite Geodesy*. Walter de Gruyter Verlag, Berlin–New York, 2nd edn.

STANAWAY, R., ROBERTS, C., BLICK, G. AND CROOK, C. (2012). *Four Dimensional Deformation Modelling, the link between International, Regional and Local Reference Frames*. In *Knowing to manage the territory, protect the environment, evaluate the cultural heritage*, FIG Working Week May 6th - 10th 2012, Rome.

TEUNISSEN, P. AND KLEUSBERG, A. (1998). *GPS for Geodesy*. Springer-Verlag, Berlin–Heidelberg–New York, 2nd edn.

UNAVCO (2012). *Plate motion calculator*. University Navstar Consortium, http://www.unavco.org/community_science/science-support/crustal_motion/dxdt/model.html (February, 2013).

WELLS, D. (1986). *Guide to GPS Positioning*. Fredericton N.B., Canada.

WÜBBENA, G. (1985). *Software developments for geodetic positions with GPS using TI-4100 code and carrier measurements*. In *Proceedings of the first symposium on precise positioning with the global positioning system, positioning with GPS-1985*, 403–412, U.S. Department of Commerce, Rockville.

WÜBBENA, G. (1989). *The GPS adjustment software package GEONAP, Concepts and models*. In *Proceedings 5th Int. Geod. Symp. Satellite Positioning*, Vol. 1, 452–461, Las Cruces.

ZIEBART, M. AND BAHRAMI, M., eds. (2012). *GNSS geodetic reference frames: consistency, stability and the related transformation parameters*. Oral presentation, iNsight Workshop July 12th 2012, London.